THE UNIVERSITY
of EDINBURGH

New results for two-loop scattering in Quantum Chromodynamics

Christian Brønnum-Hansen

Doctor of Philosophy
The University of Edinburgh
March 2019

Abstract

Decreasing statistical and systematic uncertainties for particle collisions experiments at the Large Hadron Collider (LHC) put increasing demands on precision in theoretical predictions. At the LHC protons are collided at high energy in order to study fundamental interactions. The scattering processes are dominated by strong interactions which are modelled by Quantum Chromodynamics (QCD). In this energy regime theoretical predictions can be calculated using perturbation theory in the coupling constant and hence higher precision is achieved by including higher orders. The higher orders include both processes of additional unresolved external states (higher multiplicity) or internal states (more loops). Currently, calculations at next-to-next-to-leading order (NNLO) precision are in demand for current and future analyses. These calculations require the development of new techniques to handle the growth in complexity. The topic of this thesis is loop calculations in QCD using modern on-shell techniques.

We present new results for planar $2 \to 3$ gluon scattering at two loops. The amplitudes are obtained by employing generalised unitarity and finite field reconstruction methods. The universality of the pole structure is used for verification of the results, but also allows us to reconstruct only a finite remainder. Strategies to obtain compact analytic expressions both at the level of the integrand and after integration are discussed. Integrals are dealt with using a variety of approaches including sector decomposition, integration-by-parts identities, and dimensional shifting and recurrence relations.

We also describe a new unitarity compatible method for dealing with massive fermions at one loop. This method involves an explicit construction of six-dimensional spinors and a discussion of the renormalisation of effective field theories.

Lay summary

At particle physics experiments fundamental particles are collided at high energy in order to probe the fundamental interactions governing the universe. Fundamental particles are indivisible and hence the smallest building blocks of matter. The nuclei of atoms consist of protons and neutrons, which are built out of fundamental particles known as quarks and gluons. At the Large Hadron Collider (LHC), protons are collided at near light speed in order to study the interactions between the quarks and gluons.

These interactions are dominated by the strong nuclear force, which is modelled by a theory known as Quantum Chromodynamics (QCD). The theoretical predictions for high energy collisions are given by scattering amplitudes, which give us information on the probability of the collision outcomes. The calculation of scattering amplitudes in QCD is the main topic of this research. Scattering amplitudes can be calculated as sums of Feynman diagrams, where each diagram is associated with a mathematical expression. Examples of Feynman diagrams are given in the figure below. Including diagrams with loops increases the complexity but also the precision of the calculation. A high level of theoretical precision is necessary to match the precision of the vast amount of experimental data collected by the detectors at the LHC.

This thesis explores modern methods for amplitude calculations within QCD. These mathematical methods are implemented on computers to handle the complexity. In particular, we present a new method for one-loop calculations involving massive quarks and new results for two-loop five-point scattering.

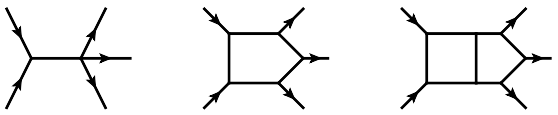

Declaration

I declare that this thesis was composed by myself, that the work contained herein is my own except where explicitly stated otherwise in the text, and that this work has not been submitted for any other degree or professional qualification except as specified.

Parts of this work have been published in [1–4].

(*Christian Brønnum-Hansen, March 2019*)

Acknowledgements

I owe my deepest gratitude to my advisor Simon Badger for everything he has taught me over the last years. His extensive knowledge of scattering amplitudes and high energy physics has been a great inspiration to me. I am thankful for his comprehensive answers to my many questions and his contagious enthusiasm in our work. Without his guidance and encouragement this thesis would not have been possible.

I am also deeply grateful to my advisor Donal O'Connell for his patience and motivation throughout my studies. I am honoured to have collaborated with Donal and thankful for his interest in my work. His advice and feedback have been invaluable for my education.

I would like to express my greatest appreciation to my collaborators Francesco Buciuni, Bayu Hartanto, and Tiziano Peraro. I have greatly benefited from your inspiring work and our numerous discussions. Special thanks also to Gianluca Filaci, Joël Mabillard, Calum Milloy, Einan Gardi, Roman Zwicky, Jennifer Smillie, Hjalte Frellesvig, and Alexander Karlberg for many useful discussions. I would also like to extend my thanks to Poul Henrik Damgaard and Ciaran Williams for suggesting Edinburgh for my studies.

I want to thank Johannes Henn and the Johannes Gutenberg University of Mainz for hosting me during Spring 2018. My appreciation goes to the Augustinus Foundation and the Oticon Foundation for generous financial support. I am indebted to the Institute for Particle Physics Phenomenology for funding visits to Durham University and conference activities.

Finally, I would like to express my heartfelt appreciation to my family and friends for their support and encouragement. Shout-out to MB! for always having my back. I am eternally grateful to Irene for her love.

Contents

List of Figures

List of Tables

Chapter 1

Introduction

For the last decade the world's largest particle accelerator, the Large Hadron Collider (LHC), has tested theory predictions within particle physics. The 27 kilometres long collider ring is placed in a tunnel 100 metres underground. Strong, superconducting magnets curve particles around vacuum tubes and bring them to collide inside detectors at near light speed. Physics in this energy regime is described by Quantum Field Theories (QFTs) which unite quantum mechanics and special relativity.

Theory predictions are provided by the Standard Model and have been confirmed to an impressive accuracy. In particular, with the discovery of the Higgs boson in 2012 all particles within the model have been observed and their masses accounted for through the Higgs mechanism. With the predictions of the Standard Model verified experimentally to very high precision, the programme has entered a precision measurement phase.

The mathematical formulation of the Standard Model is based on invariance under local gauge transformations of the group $SU(3) \times SU(2) \times U_Y(1)$. The electro-magnetic and weak nuclear forces are associated with $SU(2) \times U_Y(1)$ sector, while the strong force is described by the $SU(3)$ sector. Notably, the Standard Model does not account for the gravitational force nor does it include interactions of dark matter and neutrino oscillations. New physics beyond the Standard Model could become evident with higher precision in both measurement and prediction of Standard Model processes.

This thesis concerns high precision predictions within the $SU(3)$ sector. In particular the calculation of the amplitude, a mathematical object ubiquitous in particle physics and a central ingredient in predictions for particle scattering experiments. The amplitude is defined in the next section and its efficient calculation is the continual topic of this work. In section 1.2 we briefly review Quantum Chromodynamics (QCD), the theory modelling the strong interactions of the $SU(3)$ sector of the Standard Model. Section 1.3, the last of this chapter, ties the amplitude to the experimentally observable cross section.

Chapter 2 introduces modern on-shell techniques for the calculation of scattering amplitudes at tree level while Chapter 3 introduces unitarity methods for massless one-loop calculations. In Chapter 4 we present a unitarity compatible approach for calculations of one-loop amplitudes with massive fermions. We extend the unitarity method to two loops in Chapter 5 and present our results for $2 \to 3$ scattering. In the final chapter we present our conclusions.

1.1 Scattering amplitudes in Quantum Field Theory

At scattering experiments like the Large Hadron Collider beams of relativistic particles are collided and experimentalists measure the properties of particles appearing in the final state. The probabilistic nature of interactions at the quantum level means that the outcome of a collision between wavepackets from beam A and beam B is expressed as a probability [5],

$$\mathcal{P} = |\langle \underbrace{\phi_1 \phi_2 \cdots}_{\text{final}} | \underbrace{\phi_A \phi_B}_{\text{initial}} \rangle|^2. \tag{1.1}$$

Considering the initial and final states as linear superpositions of states with definite momentum and taking into account the transverse displacement of the wavepackets in position space, the probability can be expressed in terms of a transition amplitude with definite momenta,

$$\begin{aligned} {}_{\text{out}}\langle p_1 p_2 \cdots | p_A p_B \rangle_{\text{in}} &\equiv \langle p_1 p_2 \cdots | S | p_A p_B \rangle \\ &= \langle p_1 p_2 \cdots | 1 + iT | p_A p_B \rangle. \end{aligned} \tag{1.2}$$

This defines the unitary scattering matrix, S, as well as the T-matrix. The latter in turn defines the scattering amplitude,

$$\mathcal{A}(p_A\ p_B \to p_1\ p_2 \cdots) = \langle p_1 p_2 \cdots | T | p_A p_B \rangle. \tag{1.3}$$

The scattering amplitude satisfies momentum conservation, $p_A + p_B - \sum p_i = 0$ and depends only on the on-shell momenta of the particles. The on-shell condition is $p_i^2 = m_i^2,\ i = A, B, 1, 2, \ldots$. This thesis concerns the calculation of the scattering amplitude for processes within the theory of Quantum Chromodynamics (QCD), which will be briefly reviewed in the following section.

1.2 Quantum Chromodynamics

Quantum Chromodynamics (QCD) is part of the Standard Model and describes the so-called strong interaction between particles, specifically the elementary particles that carry colour charge. The particle content of QCD is presented in Table 1.1. These particles are known as quarks and gluons and together they form bound, colour-neutral states known as mesons and baryons. The proton is a baryon consisting of three valence quarks, two up-quarks and one down-quark bound together by gluons.

QCD is a $SU(N_C)$ gauge theory described perturbatively by the Lagrangian,

$$\mathcal{L} = -\frac{1}{4} F^{a,\mu\nu} F^a_{\mu\nu} + \sum_f^{n_f} \bar{\psi}_{f,j} \left(i\gamma_\mu D^\mu_{jk} - m_f \delta_{jk} \right) \psi_{f,k} + \mathcal{L}_{\text{gauge-fixing}}, \tag{1.4}$$

gauge boson		quarks	
	electric charge	$+\frac{2}{3}$	$-\frac{1}{3}$
	1st generation	up ~ 4 MeV	down ~ 7 MeV
gluon massless	2nd generation	charm ~ 1,500 MeV	strange ~ 135 MeV
	3rd generation	top ~ 175,000 MeV	bottom ~ 5,000 MeV

Table 1.1 *Particle contents of Quantum Chromodynamics. The masses are approximate and given in natural units where the speed of light is set to unity.*

where Greek indices are for space-time and spinor indices have been suppressed. The colour indices a and j, k are in the adjoint and fundamental representations of $SU(N_C)$ respectively. Summation over the colour indices in (1.4) is implied. There is strong experimental evidence for the number of colours to be $N_C = 3$ [6], but for the sake of generality we will mostly keep N_C unfixed throughout this work. The explicit sum is over the number of different quark flavours, n_f, with masses m_f. In the Standard Model there are a total of 6 flavours listed in Table 1.1. γ^μ are the Dirac matrices.

The gluon field strength tensor, $F^{a,\mu\nu}$, and the covariant derivative, D^μ_{ij}, are,

$$F^a_{\mu\nu} = \partial_\mu A^a_\nu - \partial_\nu A^a_\mu - g f^{abc} A^b_\mu A^c_\nu, \tag{1.5a}$$

$$D^\mu_{ij} = \delta_{ij}\partial^\mu + igT^c_{ij}A^{c,\mu}, \tag{1.5b}$$

where g is the coupling constant and T^c_{ij} are the SU(N_C) generators in the fundamental representation. Following [7, 8] we use the normalisation,

$$\mathrm{tr}\left(T^a T^b\right) = T_R \delta^{ab} = \delta^{ab}. \tag{1.6}$$

This choice of normalisation is convenient for the colour ordering that will be discussed in the next sections. The generators are traceless and satisfy the algebra,

$$[T^a, T^b]_{ik} = i\sqrt{2} f^{abc} T^c_{ik}, \tag{1.7}$$

where f^{abc} are the structure constants[1]. In the above, upper colour indices are in the adjoint representation taking the values $1, ..., N_C^2 - 1$, while lower indices are in the fundamental taking the values $1, ..., N_C$. This implies that,

$$\delta_{ii} = N_C, \qquad \delta^{aa} = N_C^2 - 1. \tag{1.8}$$

The two first terms of the Lagrangian (1.4) exhibit local gauge invariance. This means that they are invariant under the following space-time dependent redefinitions of the fields, parametrised by $\alpha^c(x)$,

$$\psi_i(x) \to V_{ij}(x)\psi_j(x) = \left(e^{i\alpha^c(x)T^c}\right)_{ij}\psi_j(x), \tag{1.9a}$$

$$T^c_{ij}A^{c,\mu}(x) \to V(x)\left(\frac{i}{g}\delta_{ij}\partial^\mu + T^c_{ij}A^{c,\mu}(x)\right)V^\dagger(x). \tag{1.9b}$$

[1]The additional factor of $\sqrt{2}$ is a choice related to our choice of T_R.

Gauge invariance permits a mass term for the fermions but forbids a mass term for the gluon. Physical observables must be gauge invariant, while intermediate steps in the calculations may depend on the gauge choice. The methods applied throughout this thesis seek to use gauge-invariant ingredients in all calculations to avoid gauge redundancies in intermediate steps.

1.2.1 Feynman rules

The standard way to compute scattering amplitudes perturbatively is to use Feynman rules and diagrams. The rules and their derivations can be found in textbooks on quantum field theory (see for example [5, 6, 9, 10]). In order to obtain a propagator for the gluon it is necessary to introduce the gauge-fixing term of (1.4). In this thesis we choose the axial gauge where,

$$\mathcal{L}_{\text{gauge-fixing}} = -\frac{1}{2\lambda}\left(n^\mu A^a_\mu\right)^2, \tag{1.10}$$

with gauge parameter, λ, and n is a reference vector. The axial gauge is known as a physical gauge, since it does not require introduction of unphysical internal states known as ghosts in order to counter contributions from longitudinal polarisations of the gauge boson. We further specialise to the light-cone gauge where $n^2 = 0$.

The Feynman rules for calculating colour-ordered amplitudes are given in Figure 1.1. The rules associated with external states are the spinors and polarisation vectors given in section 2.1, equation (2.5) and (2.9) respectively. The propagators include the Feynman $i\delta$-prescription to ensure well-defined vacuum two-point functions.

1.2.2 Tree-level amplitudes and colour ordering

Since $SU(3)$ is non-Abelian, the gauge bosons are self-interacting through three- and four-point vertices. These vertices arise from the last term of the gluon field strength tensor (1.5a) and would be absent in an Abelian theory where the structure constants vanish. The three-gluon vertex comes with a factor of f^{abc} and the four-gluon vertices come with a factor of $f^{abe}f^{cde}$. To study the colour structure of an amplitude we use (1.7) to rewrite the structure constants into

traces over the generators,

$$f^{abc} = -\frac{i}{\sqrt{2}}\mathrm{tr}\left(T^a T^b T^c - T^b T^a T^c\right). \tag{1.11}$$

The quark-quark-gluon vertex comes with a single T^a_{ij}. The quark propagator contracts fundamental colour indices while the gluon propagator contracts adjoint indices. For the latter, the Fierz identity is useful,

$$T^a_{ij} T^a_{kl} = \delta_{il}\delta_{jk} - \frac{1}{N_C}\delta_{ij}\delta_{kl}. \tag{1.12}$$

Using the above properties we can decompose tree-level QCD amplitudes into overall colour factors and partial amplitudes only depending on the kinematics. For pure gluon amplitudes this colour decomposition reads [8, 11, 12],

$$\mathcal{A}_n^{(0)}(1,2,\ldots,n) = g^{n-2} \sum_{\sigma \in S_n/Z_n} \mathrm{tr}\left(T^{a_{\sigma(1)}} T^{a_{\sigma(2)}} \ldots T^{a_{\sigma(n)}}\right) A_n^{(0)}(\sigma(1),\sigma(2),\ldots,\sigma(n)), \tag{1.13}$$

where the sum is over all non-cyclic permutations of the external legs. The amplitude $A_n^{(0)}(1,2,\ldots,n)$ is known as a colour-ordered or partial amplitude. Due to its fixed ordering of the external legs it exhibits singular behaviour only when invariants, $s_{i_1\ldots i_n} = (p_{i_1} + \cdots + p_{i_n})^2$, of adjacent momenta vanish. From the trace basis for the colour decomposition it is clear that the amplitudes are invariant under cyclic permutations of the external legs. This reduces the number of independent colour-ordered amplitudes that it is necessary to calculate.

In the presence of a quark pair the trace is replaced by a string of colour generators carrying fundamental indices,

$$\mathcal{A}_n^{(0)}(1_q,2,\ldots,n_{\bar{q}}) = g^{n-2} \sum_{\sigma \in S_{n-2}} (T^{a_{\sigma(2)}} \ldots T^{a_{\sigma(n-1)}})_{a_1 a_n} A_n^{(0)}(1_q,\sigma(2),\ldots,n_{\bar{q}}). \tag{1.14}$$

The sum runs over all permutation of the gluons, while the positions of the quarks are fixed.

The anti-symmetry of the Feynman rules, Figure 1.1, reveals the reflection symmetry of the colour-ordered amplitudes,

$$A_n^{(0)}(1,2,\ldots,n) = (-1)^n A_n^{(0)}(n,\ldots,2,1). \tag{1.15}$$

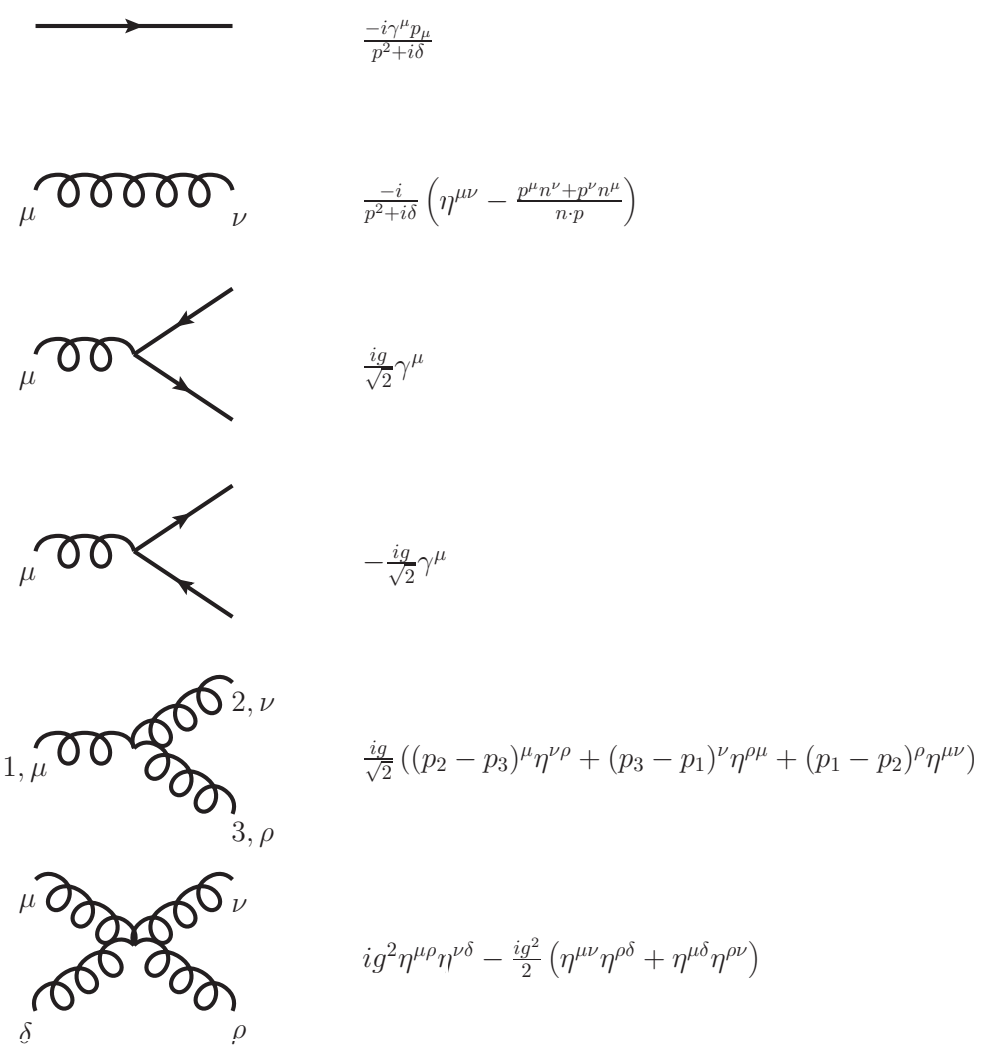

Figure 1.1 *Colour-ordered, momentum-space Feynman rules in massless QCD in the light-cone gauge. Solid lines represent quarks, curly lines represent gluons. All momenta are considered outgoing.*

The colour decomposition for loop amplitudes is less straight-forward, and will in general contain several different colour structures. The loop-level colour decompositions relevant in this thesis will be presented in section 4.2 and 5.1. From colour decomposition it follows that the colour-ordered amplitudes must be gauge-invariant in order for the full amplitude to be gauge-invariant.

1.2.3 Loop amplitudes and dimensional regularisation

Momentum conservation is implied in all the Feynman rules presented in Figure 1.1 and as a consequence all internal momenta at tree level are constrained by the external momenta. However, each closed loop in a diagram has an unconstrained

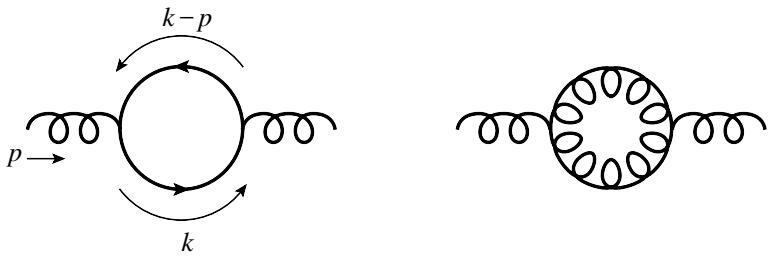

Figure 1.2 *Feynman diagrams contributing to the two-point gluon function at one loop. External momentum, p, is flowing through the diagram, and internal momentum, k, is running in the loop.*

momentum that needs to be integrated over. The two-point gluon function has two contributing diagrams at one-loop level, one with a quark loop and one with a gluon loop, as shown in Figure 1.2.

The calculation of this one-loop contribution involves evaluation of the bubble integral,

$$I_2^{(4)}(p^2) = \int \frac{d^4k}{i\pi^2} \frac{1}{k^2(k-p)^2}, \tag{1.16}$$

where we ignore quark masses and omit the Feynman $i\delta$-prescription. Working in four dimensions, this integral is logarithmically divergent in the ultraviolet, $k \to \infty$, and a regularisation procedure is necessary. We follow the method of dimensional regularisation, where a small excursion from four dimensions is taken and parametrised by the regularisation parameter ϵ,

$$d = 4 - 2\epsilon. \tag{1.17}$$

To keep the mass dimension of the integral fixed we introduce a mass scale, μ. This regularises the integral and the divergence appears as a pole in ϵ [13],

$$\begin{aligned} I_2^{(4-2\epsilon)}(p^2) &= \mu^{2\epsilon} \int \frac{d^dk}{i\pi^{d/2}} \frac{1}{k^2(k-p)^2} \\ &= r_\Gamma \left(\frac{\mu^2}{-p^2}\right)^\epsilon \left(\frac{1}{\epsilon} + 2\right) + \mathcal{O}(\epsilon), \end{aligned} \tag{1.18}$$

$$r_\Gamma = \frac{\Gamma^2(1-\epsilon)\Gamma(1+\epsilon)}{\Gamma(1-2\epsilon)}. \tag{1.19}$$

Within dimensional regularisation the bubble integral vanishes in the absence of an external mass scale, p^2.

The poles in ϵ must cancel for physical quantities such that the limit $\epsilon \to 0$

can be taken safely. The cancellation of ultraviolet poles is accomplished by the procedure of renormalisation discussed in the next section.

Infrared divergences can occur in loop integrals when an internal, massless propagator goes soft, $k \to 0$. Dimensional regularisation works equally well for these integrals. However, infrared divergences are not dealt with by renormalisation but cancel against singular behaviour coming from diagrams with fewer loops but more legs. Consider a diagram where a massless, internal particle splits into two massless external particles, p_1 and p_2. The invariant appearing in the propagator is,

$$s_{12} = (p_1 + p_2)^2 = 2p_1 \cdot p_2 = 2E_1E_2(1 - \cos\theta_{12}), \tag{1.20}$$

where θ_{12} is the angle between the three-momenta of the external particles. We see that the propagator blows up in the limit where

- either of the external particles goes soft, $E_i \to 0,\ i = 1, 2$, or
- they go collinear, $\theta_{12} \to 0$.

In these limits no physical detector is able to resolve both particles, so when calculating physical observables including quantum corrections, the contributions from the loop process (virtual contribution) and from the emission of an additional soft or collinear particle (real radiation contribution) should be combined. Generally, the infrared divergences from an L-loop, n-point amplitude is cancelled by real radiation from an $(L-1)$-loop, $(n+1)$-point amplitude, an $(L-2)$-loop, $(n+2)$-point amplitude and so on. The cancellation is ensured to all orders in perturbation theory by the KLN theorem [14–16].

1.2.4 Renormalisation and the beta function

Renormalisation is the procedure of absorbing ultraviolet divergences from loop contributions to propagators and vertices in the parameters and fields of the Lagrangian (1.4). This can be done by introducing counter-terms, effectively redefining the parameters and fields using renormalisation constants [9, 10],

$$m = Z_m m_r, \qquad g = \mu^\epsilon \frac{Z_1}{Z_2\sqrt{Z_3}} g_r, \qquad \psi = \sqrt{Z_2}\psi_r, \qquad A^\mu = \sqrt{Z_3}A^\mu_r. \tag{1.21}$$

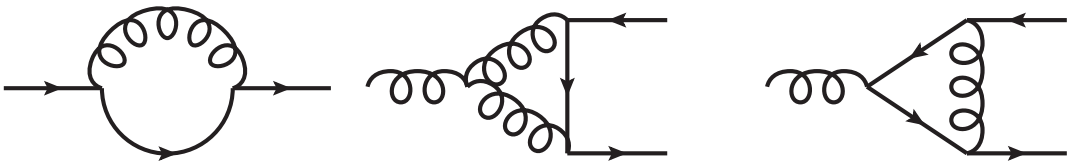

(a) *Fermion self-energy.* **(b)** *Vertex corrections.*

Figure 1.3 *One-loop corrections to fermion self-energy and gluon-quark-quark vertex.*

The renormalisation constant, Z_1, is the overall scaling of the quark-quark-gluon vertex and therefore picks up factors of the renormalisation constants from the fields. The scale, μ, keeps the coupling dimensionless for $d = 4-2\epsilon$. The constants are calculated at each order in perturbation theory.

To establish the validity of perturbation theory in QCD we shall be especially interested in the renormalisation of the coupling constant, g_r, which at one loop receives contributions from the gluon self-energy diagrams in Figure 1.2 through Z_3 as well as the fermion self-energy for Z_2 and vertex corrections for Z_1 shown in Figure 1.3. The renormalisation constants in the one-loop approximation are[2],

$$Z_1 = 1 - \frac{1}{\epsilon}\frac{g_r^2}{16\pi^2}\frac{3N_C^2 - 1}{2N_C}, \tag{1.22a}$$

$$Z_2 = 1 - \frac{1}{\epsilon}\frac{g_r^2}{16\pi^2}\frac{N_C^2 - 1}{2N_C}, \tag{1.22b}$$

$$Z_3 = 1 + \frac{1}{\epsilon}\frac{g_r^2}{16\pi^2}\frac{5N_C - 2n_f}{3}. \tag{1.22c}$$

The scaling behaviour of the coupling constant is then given by the beta function,

$$\beta(g_r) = \left.\frac{\partial g_r}{\partial \ln \mu}\right|_{\epsilon\to 0} = -\frac{g_r^3}{16\pi^2}\left(\frac{11N_C - 2n_f}{3}\right), \tag{1.23}$$

which remains negative for $n_f < \frac{11N_C}{2}$. This is realised in QCD where $n_f = 6$ and $N_C = 3$. This means that the coupling decreases when the scale increases. This behaviour is known as asymptotic freedom and justifies treating partons as free particles at high energy. However, this also tells us that the perturbative expansion is ill-defined at low energies, where the partons form bound, colour-neutral states.

[2]The renormalisation constants are calculated in the Feynman gauge and the $\overline{\text{MS}}$ subtraction scheme for $T_R = \frac{1}{2}$. This calculation involves graphs involving ghosts not shown in the figures.

Introducing $g_r^2 = 4\pi\alpha_S(\mu)$ and solving (1.23) we get,

$$\alpha_S(Q) = \frac{\alpha_S(\mu)}{1 + \alpha_S(\mu)\frac{\beta_0}{2\pi}\ln\left(\frac{Q}{\mu}\right)}, \tag{1.24}$$
$$\beta_0 = \frac{11N_C - 2n_f}{3}.$$

Knowing the strong coupling, α_S, at one scale, μ, allows us to calculate it at a different scale, Q, provided both scales are in the perturbative regime. Currently, the world average measurement of the strong coupling is [17],

$$\alpha_S(m_Z) = 0.1181(11), \tag{1.25}$$

where $m_Z = 91.1876(21)$ GeV. The numbers in parentheses are the uncertainty on the last two digits. β_0 is only the one-loop approximation of the β-function, which has recently been calculated up to 5 loops [18, 19].

1.3 The cross section

While this thesis concerns the calculation of the amplitude (1.3), this is not an observable at experiments. At the Large Hadron Collider (LHC) beams of protons are collided and the primary physical observable is the cross section denoted σ. A proton is a bound state of quarks and gluons, collectively known as partons. The distribution of partons within the proton is described in the non-perturbative regime of QCD by experimentally determined parton distribution functions (PDFs). The information contained in the PDF is therefore intrinsic to the proton (or generally hadron) and is not process-dependent. The interaction between the colliding relativistic partons is on the other hand described perturbatively due to asymptotic freedom and gives the process-dependent information. The cross section for two colliding hadrons with momenta P_1 and P_2 producing a final state X is given by [6, 20],

$$\sigma(P_1P_2 \to X) = \sum_{a,b}\int dx_1 dx_2 f_a(x_1,\mu_F^2) f_b(x_2,\mu_F^2)\hat{\sigma}(p_1p_2 \to X;\mu_F^2,\mu^2,Q^2) + \mathcal{O}\left(\frac{\Lambda_{\text{QCD}}}{Q}\right). \tag{1.26}$$

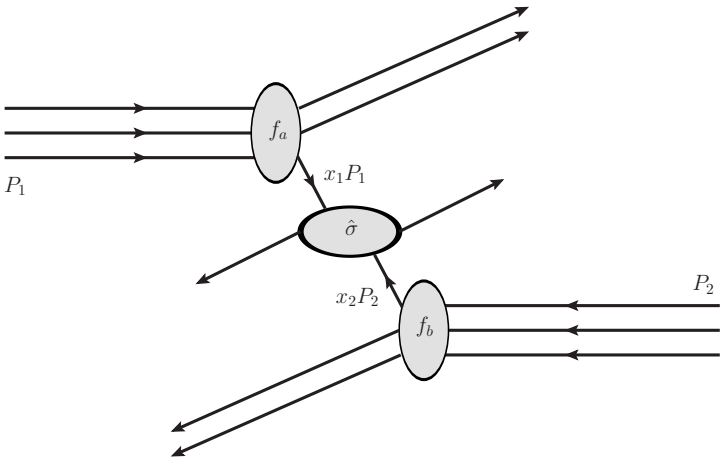

Figure 1.4 *Factorisation of the cross section into parton distribution functions and a perturbatively calculable partonic cross section. The interacting partons carry fractions x_i of the parent proton momenta, P_i.*

The sum is over the partons a and b and the integration is over the fraction of momentum carried by them, $p_i = x_i P_i$. The factorisation scale, μ_F, separates physics described by the PDFs, f_a, and the partonic cross section, $\hat{\sigma}$. The renormalisation scale, μ, was introduced in the previous section. Q is the characteristic scale of the interaction which, for example, can be the mass of an intermediate heavy state or the invariant mass of final state particles. This factorisation structure is illustrated in Figure 1.4. We do not consider the subsequent parton shower, jet clustering, or hadronisation of the final state particles.

The partonic cross-section is expanded as a perturbation series in the strong coupling, $\alpha_S(\mu)$,

$$\hat{\sigma} = \sum_{l=0}^{m} \alpha_S^{k+l} \hat{\sigma}^{(N^l LO)}, \tag{1.27}$$

where k is the order where the process first occurs. For $k = 1$, this contribution is related to a squared tree-level n-point amplitude integrated over the $n-2$ final state phase space,

$$\hat{\sigma}^{(LO)}(p_1 p_2 \to p_3 \dots p_n) = \int_{\Phi_{n-2}} |\mathcal{A}_n^{(0)}|^2. \tag{1.28}$$

The coupling has been extracted from the amplitude and appears in (1.27). As mentioned in the previous section, quantum corrections to physical observables

receive virtual and real radiation contributions. The partonic cross section at next-to-leading order (NLO) is,

$$\hat{\sigma}^{(NLO)}(p_1 p_2 \to p_3 \dots p_n) = \int_{\Phi_{n-2}} 2\mathrm{Re}\left(\mathcal{A}_n^{(1)\star}\mathcal{A}_n^{(0)}\right) + \int_{\Phi_{n-1}} |\mathcal{A}_{n+1}^{(0)}|^2, \tag{1.29}$$

where the infrared divergences cancel between the two terms. Several techniques exist to achieve this cancellation (see for example [21, 22]), but will not be discussed further in this thesis. Figure 1.5 illustrates the amplitudes contributing to the perturbative expansion of the partonic cross section. The amplitudes are colour coded according to the order that they first contribute to. For example, the tree-level five-point amplitude contributes at leading order and all higher orders. Note also that the squared one-loop five-point amplitude contributes at NNLO.

Summed to all orders the cross section is independent of the unphysical scales,

$$\frac{\partial\sigma}{\partial\mu_F} = \frac{\partial\sigma}{\partial\mu} = 0. \tag{1.30}$$

Hence, the dependence on the scales of a fixed-order calculation indicate the magnitude of higher-order corrections and gives an estimate for the theoretical uncertainty of a cross section calculation.

Currently, the state-of-the-art in theoretical predictions is next-to-next-to-leading order for $2 \to 2$, while $2 \to 3$ predictions are limited in part because of unknown two-loop amplitudes [23]. However, there has recently been remarkable development to this end and many new results have emerged for the reduction and evaluation of the necessary loop integrals. In this thesis we will discuss modern methods for the calculation of scattering amplitudes focusing especially on the integrand reduction. We introduce a novel approach to one-loop amplitudes involving massive fermions [1] and present new results for two-loop $2 \to 3$ scattering in QCD [2–4].

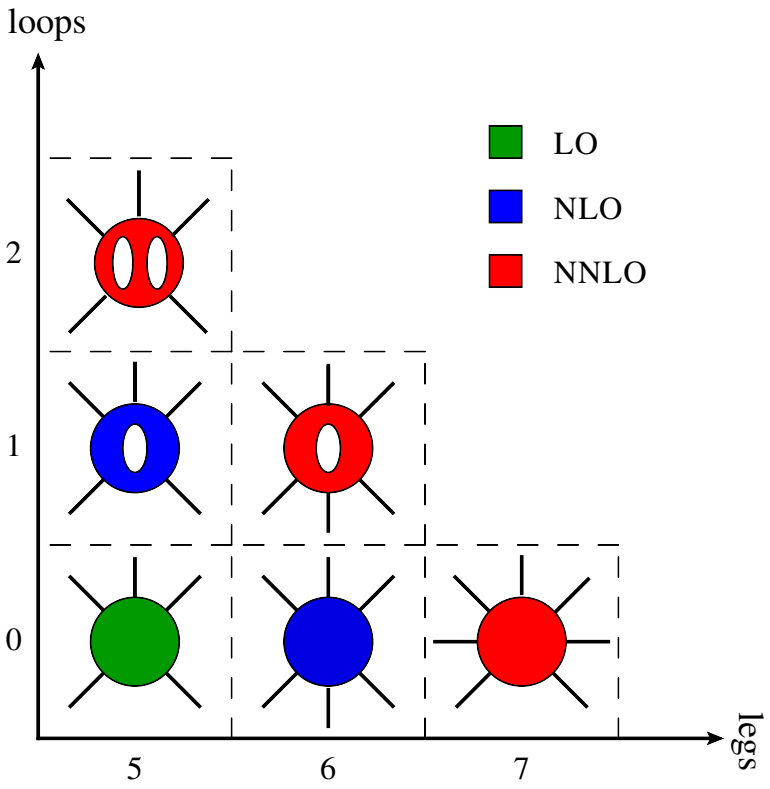

Figure 1.5 *The amplitudes contributing to the* $2 \to 3$ *NNLO partonic cross section. The amplitudes are colour coded according to the order that they first contribute to.*

Chapter 2

Scattering amplitudes at tree level

Traditional Feynman diagrammatic methods rapidly increase in calculational complexity and become unmanageable due to large intermediate expressions. Non-Abelian gauge theories, like QCD, suffer in particular from this due to self-interactions and gauge redundancies. Modern techniques use manifestly on-shell variables and gauge-invariant quantities to avoid unphysical degrees of freedom. This greatly reduces the complexity of calculations. On-shell techniques are applied in this thesis through spinor-helicity formalism and tree-level recursion relations which will be introduced in this chapter. Integrand reduction and generalised unitarity are loop-level techniques which will be introduced in Chapter 3.

2.1 Spinor-helicity formalism

In this section we give a brief introduction to the spinor-helicity formalism following standard references [8, 24]. We take fermions to be massless which, for the lighter quarks, is a reasonable approximation at high energy when particle energy is dominated by the three-momentum. Furthermore, we adopt the convention that all external particles are outgoing. For massless, outgoing fermions with four-momentum $p^\mu = (p^0, p^1, p^2, p^3)$ the Dirac equation reads,

$$\not{p} v_\pm(p) = 0, \quad \bar{u}_\pm(p) \not{p} = 0, \tag{2.1}$$

where we use Feynman slash notation and the Weyl basis,

$$\not{p} = \gamma^\mu p_\mu = \begin{pmatrix} 0 & \tilde{\sigma}^{\mu\dot{a}a} \\ \sigma^\mu_{a\dot{a}} & 0 \end{pmatrix} p_\mu, \tag{2.2}$$

with $\sigma^\mu_{a\dot{a}} = (1, \sigma^i)_{a\dot{a}}$ and $\tilde{\sigma}^{\mu\dot{a}a} = (1, -\sigma^i)^{\dot{a}a}$. The Pauli matrices, σ^i, are given in Appendix A.

The on-shell condition, $p^2 = 0$, translates into vanishing of the determinant, $\det \not{p} = 0$, and motivates a bi-spinor representation,

$$p \cdot \sigma_{a\dot{a}} = \lambda_a \tilde{\lambda}_{\dot{a}}, \quad p \cdot \tilde{\sigma}^{\dot{a}a} = \tilde{\lambda}^{\dot{a}} \lambda^a, \tag{2.3}$$

where we suppressed the momentum dependence of the spinors for ease of notation. The Levi-Civita symbol raises, $\lambda^a = \epsilon^{ab}\lambda_b$, and lowers, $\lambda_a = \epsilon_{ab}\lambda^b$, the spinor indices, with $\epsilon^{12} = 1 = \epsilon_{21}$. For real momentum the spinors are related by complex conjugation, $(\lambda^a)^\star = \tilde{\lambda}^{\dot{a}}$. We define the Lorentz invariant spinor products and introduce a bracket notation,

$$\langle ij \rangle = \lambda_i^a \lambda_{ja} \quad [ij] = \tilde{\lambda}_{i\dot{a}} \tilde{\lambda}_j^{\dot{a}}, \tag{2.4}$$

where $\lambda_i = \lambda(p_i)$. The spinor products are antisymmetric and it follows that $\langle ii \rangle = [ii] = 0$. From this observation the independent solutions to the Dirac equation (2.1) follow immediately,

$$v_-(p_i) = v_{i-} = \begin{pmatrix} 0 \\ \lambda_{ia} \end{pmatrix}, \qquad v_{i+} = \begin{pmatrix} \tilde{\lambda}_i^{\dot{a}} \\ 0 \end{pmatrix}, \tag{2.5a}$$

$$\bar{u}_{i-} = (0, \lambda_i^a), \qquad \bar{u}_{i+} = (\tilde{\lambda}_{i\dot{a}}, 0). \tag{2.5b}$$

An explicit representation of the spinors is,

$$\lambda_a = \sqrt{p_+} \begin{pmatrix} 1 \\ \frac{p_-}{p_-^\perp} \end{pmatrix}, \quad \tilde{\lambda}_{\dot{a}} = \sqrt{p_+} \begin{pmatrix} 1 \\ \frac{p_-^\perp}{p_+} \end{pmatrix}, \quad p_\pm = p^0 \pm p^3, \quad p_\pm^\perp = p^1 \pm i p^2. \tag{2.6}$$

The spinor products are related to generalised Mandelstam variables, $s_{ij} = (p_i + p_j)^2$, for massless particles by,

$$\langle ij \rangle [ji] = 2 p_i \cdot p_j = s_{ij}. \tag{2.7}$$

Linear independence of spinors, $|i\rangle = c_1|j\rangle + c_2|k\rangle,\ c_i \in \mathbb{C}$, leads to the Schouten identity,

$$0 = \langle ij\rangle\langle kl\rangle + \langle ik\rangle\langle lj\rangle + \langle il\rangle\langle jk\rangle. \tag{2.8}$$

The polarisation vectors for massless, gauge bosons can be expressed as,

$$\epsilon^+_\mu(p,n) = -\frac{\langle n|\sigma_\mu|p]}{\sqrt{2}\langle np\rangle}, \qquad \epsilon^-_\mu(p,n) = \frac{[n|\tilde{\sigma}_\mu|p\rangle}{\sqrt{2}[np]}, \tag{2.9}$$

where p refers to particle momentum and $n \neq p$ is a light-like reference vector. The existence of a spinor representation for the polarisation vectors is exclusive to the axial gauge, and summing over helicities we obtain the completeness relation,

$$\sum \epsilon^\pm_\mu(p,n)\epsilon^\mp_\nu(p,n) = -\eta_{\mu\nu} + \frac{p_\mu n_\nu + n_\mu p_\nu}{n\cdot p}. \tag{2.10}$$

By virtue of (2.1) the polarisation vectors are orthogonal to the momentum. They are null vectors and normalised such that $\epsilon^+ \cdot \epsilon^- = -1$. A change in reference vector is equivalent to a shift proportional to the momentum and therefore leaves an on-shell amplitude invariant due to the Ward identity. Helicity can be reversed by complex conjugation,

$$(\epsilon^+_\mu)^\star = \epsilon^-_\mu. \tag{2.11}$$

This has the immediate consequence that the number of independent helicity amplitudes we need to calculate drops, as we can flip all helicities in an amplitude by taking its complex conjugate.

2.1.1 Some tree-level helicity amplitudes

A careful choice of the polarisation reference vector, n, in (2.9) can greatly simplify computations. In particular, with specific choices we can demonstrate that a large number of tree-level amplitudes vanish straightforwardly. An n-point gluon diagram has at most $n-2$ vertices which each contributes at most one momentum vector. Each term must therefore have at least one contraction of two polarisation vectors. Observing that products of polarisation vectors with

the same helicity and reference vector vanish,

$$\epsilon^+(p_i, n) \cdot \epsilon^+(p_j, n) = 0, \tag{2.12}$$

we conclude that choosing the same reference vector, n, for all gluons we have,

$$A^{(0)}(1^+, 2^+, 3^+, \ldots, n^+) = 0. \tag{2.13}$$

We can extend the argument above to the situation when a single gluon has negative helicity. By observing that,

$$\epsilon^-(p_i, n) \cdot \epsilon^+(p_j, p_i) = 0, \tag{2.14}$$

we choose all the gluons with positive helicity to have the negative helicity gluon momentum as reference and conclude that for $n > 3$,

$$A^{(0)}(1^-, 2^+, 3^+, \ldots, n^+) = 0. \tag{2.15}$$

The special case for $n = 3$ will be discussed in section 2.2.4. Finally, turning to an n-point amplitude with one quark pair, we use the observation,

$$\langle 1|\sigma \cdot \epsilon^+(p_n, p_1) = 0, \tag{2.16}$$

and choose all gluons to have positive helicity and the momentum of the negative helicity quark, p_1, as reference vector. It follows that either the polarisation vectors annihilate each other as in (2.12) or against the external fermion such that,

$$A^{(0)}(1_q^-, 2_{\bar{q}}^+, 3^+, \ldots, n^+) = 0. \tag{2.17}$$

The above formulas hold only at tree level. From the next-to-leading order cross section in (1.29) it follows that infrared divergences from one-loop amplitudes have to cancel against the divergences from tree-level amplitudes. The vanishing of the tree-level helicity amplitudes above implies that the renormalised one-loop amplitudes with the same helicity configurations are rational functions.

While the spinor-helicity formalism has made the vanishing of whole classes of helicity amplitudes evident, it also provides compact expressions for more complicated helicity configurations. The most well-known is the maximally helicity violating (MHV) amplitude where all but two gluons have positive

helicity,

$$A(1^+, 2^+, ..., i^-, ..., j^-, .., n^+) = i\frac{\langle ij\rangle^4}{\langle 12\rangle\langle 23\rangle ...\langle n1\rangle}, \tag{2.18}$$

where we left the coupling constant out for brevity. An n-point tree-level amplitude has overall coupling g^{n-2}. This formula was originally conjectured in [25] and derived in [26] using the recursion relation described in section 2.2.3. It can be proven by induction using the recursion relation that will be introduced in section 2.2.4.

2.1.2 Spinors in six dimensions

While space-time is normally four-dimensional we will see several calculational advantages of considering six space-time dimensions. To extend the spinor-helicity formalism to six dimensions [27] we introduce antisymmetric 4×4 matrices that play a similar role to the Pauli matrices in four dimensions. In addition to the Lorentz index, $M = 0, .., 5$, they also carry $SU(4)$ indices, $A, B = 1, 2, 3, 4$, Σ^M_{AB} and $\tilde{\Sigma}^{M,AB}$. An explicit form and useful identities are given in Appendix A. In analogy with the previous section we write,

$$p_{AB} = p \cdot \Sigma_{AB}, \qquad p^{AB} = p \cdot \tilde{\Sigma}^{AB}, \tag{2.19}$$

where p is a six-dimensional vector, $p^M = (p^0, p^1, p^2, p^3, p^4, p^5)$. The massless Dirac equation in six dimensions reads,

$$p_{AB}\lambda^B_a = 0, \qquad p^{AB}\tilde{\lambda}_{B\dot{a}} = 0. \tag{2.20}$$

The extra indices $a, \dot{a}$ are little group indices and take values $1, 2$ so the spinors can be regarded as 4×2 matrices. An explicit representation of the spinors is given by,

$$\lambda^A_a = \sqrt{p_+}\begin{pmatrix} 0 & -\frac{p^\perp_-}{p_+} \\ \frac{-i\tilde{p}_+}{p^\perp_-} & 1 \\ 1 & 0 \\ \frac{p_-}{p^\perp_-} & \frac{i\tilde{p}_-}{p_+} \end{pmatrix}, \quad \tilde{\lambda}_{A\dot{a}} = \sqrt{p_+}\begin{pmatrix} \frac{i\tilde{p}_-}{p^\perp_-} & 1 \\ 0 & \frac{p^\perp_-}{p_+} \\ -\frac{p_-}{p^\perp_-} & \frac{i\tilde{p}_+}{p_+} \\ 1 & 0 \end{pmatrix}, \tag{2.21}$$

where, in addition to the variables used in (2.6), we introduced $\tilde{p}_\pm = p^4 \pm ip^5$. In four dimensions, where $\tilde{p}_\pm = 0$, they take the simple form,

$$\lambda^A{}_a = \begin{pmatrix} 0 & \tilde{\lambda}^{\dot{b}} \\ \lambda_b & 0 \end{pmatrix}, \ \tilde{\lambda}_{A\dot{a}} = \begin{pmatrix} 0 & \tilde{\lambda}_{\dot{b}} \\ -\lambda^b & 0 \end{pmatrix}, \tag{2.22}$$

where the four-dimensional spinors are given in (2.6). Just as in four dimensions, we introduce a bracket notation to write down Lorentz invariant objects,

$$\langle i^a | j_{\dot{b}}] = [j_{\dot{b}} | i^a \rangle = \lambda_i^{Aa} \tilde{\lambda}_{jA\dot{b}}, \tag{2.23a}$$

$$\langle i^a j^b k^c l^d \rangle = \epsilon_{ABCD} \lambda_i^{Aa} \lambda_j^{Bb} \lambda_k^{Cc} \lambda_l^{Dd}, \tag{2.23b}$$

$$[i_{\dot{a}} j_{\dot{b}} k_{\dot{c}} l_{\dot{d}}] = \epsilon^{ABCD} \tilde{\lambda}_{iA\dot{a}} \tilde{\lambda}_{jB\dot{b}} \tilde{\lambda}_{kC\dot{c}} \tilde{\lambda}_{lD\dot{d}}, \tag{2.23c}$$

where ϵ_{ABCD} is the four-dimensional Levi-Civita symbol. Spinor product strings have the following expression (for even n),

$$\langle 1_a | 2\, 3 \ldots (n-1) | n^{\dot{b}}] = \lambda_{1a}^A (\Sigma \cdot p_2)_{AB} \, (\tilde{\Sigma} \cdot p_3)^{BC} \ldots (\tilde{\Sigma} \cdot p_{n-1})^{XA} \tilde{\lambda}_{An}^{\dot{b}}. \tag{2.24}$$

Finally, we can write the polarisation vectors in a spinor representation as,

$$\begin{aligned} \epsilon_{a\dot{a}}^M(p,q) &= \frac{1}{\sqrt{2}} \langle p_a | \Sigma^M | q_b \rangle \langle q_b | p^{\dot{a}}]^{-1} \\ &= \frac{1}{\sqrt{2}} \langle p_a | \Sigma^M | q_b \rangle \frac{\langle q^b | p_{\dot{a}}]}{2p \cdot q}. \end{aligned} \tag{2.25}$$

Note that gluons in six dimensions have four helicity states. The normalisation is such that,

$$\epsilon_{a\dot{a}}^M \epsilon_{Mb\dot{b}} = \epsilon_{ab} \epsilon_{\dot{a}\dot{b}}. \tag{2.26}$$

Since the invariants do not rely on contractions of the helicity indices, these are kept free. When calculating an amplitude all helicity configurations are obtained in one object carrying the helicity indices of the external particles.

The six-dimensional tree-level amplitudes will not be derived here. Amplitudes with relevance for this thesis are given in Appendix B. Further discussion of the six-dimensional spinor-helicity formalism can be found in references [28–34].

2.2 Factorisation and recursion relations

In the first chapter two infrared limits were discussed following (1.20). In this section we will discuss the infrared behaviour of tree-level amplitudes. These limits can be used for checking calculations or even in the construction of amplitudes, for example in order to constrain an Ansatz. It is convenient to study these limit at the level of colour-ordered tree-level amplitudes as they can only have poles when sums of adjacent momenta go on-shell. We finish this section by presenting two methods for recursive construction of tree-level amplitudes.

2.2.1 Soft limits

A particle is said to go soft when its momentum vanishes, $p^\mu \to 0$. Only massless particles can go soft and the soft limit does not depend on flavours or helicities of the other present particles. However, it does depend on the kinematics of the neighbouring particles in the colour-ordered amplitude and therefore the colour-dressed amplitude does not factorise. The soft, or eikonal, factor is easily extracted from the 5-gluon MHV amplitude. In the case where $p_3 \to 0$,

$$\begin{aligned} A(1^-, 2^-, 3^+, 4^+, 5^+) &= i\frac{\langle 12\rangle^4}{\langle 12\rangle\langle 23\rangle\langle 34\rangle\langle 45\rangle\langle 51\rangle}, \\ &\to \frac{\langle 24\rangle}{\langle 23\rangle\langle 34\rangle} \times A(1^-, 2^-, 4^+, 5^+), \end{aligned} \tag{2.27}$$

we obtain the eikonal factor,

$$\mathrm{Eik}^+(2,3,4) = \frac{\langle 24\rangle}{\langle 23\rangle\langle 34\rangle}. \tag{2.28}$$

Starting instead with the anti-MHV amplitude, $A(1^+, 2^+, 3^-, 4^-, 5^-)$, we get,

$$\mathrm{Eik}^-(2,3,4) = \frac{[24]}{[23][34]}. \tag{2.29}$$

2.2.2 Collinear limits

We consider the case when particles 1 and 2 in an n-point amplitude go collinear in direction, P, and use the parametrisation [35],

$$p_1^\mu = zP^\mu + \delta T^\mu - \delta^2 \frac{T^2}{2p_1 \cdot \eta}\eta^\mu, \tag{2.30a}$$

$$p_2^\mu = (1-z)P^\mu - \delta T^\mu - \delta^2 \frac{T^2}{2p_2 \cdot \eta}\eta^\mu, \tag{2.30b}$$

where z is the momentum fraction carried by collinear particle 1, T is transverse to the (light-like) collinear direction P, and η is a light-like reference momentum. We observe the following relations,

$$P \cdot T = \eta \cdot T = P^2 = \eta^2 = 0, \tag{2.31a}$$

$$P \cdot \eta = \frac{p_1 \cdot \eta}{z} = \frac{p_2 \cdot \eta}{1-z}, \tag{2.31b}$$

and the collinear limit is obtained by sending $\delta \to 0$ in (2.30). At the level of spinors this parametrisation can be realised by setting,

$$|i\rangle = \frac{\langle i\eta\rangle}{\langle P\eta\rangle}|P\rangle + \frac{\langle iP\rangle}{\langle \eta P\rangle}|\eta\rangle, \tag{2.32a}$$

$$|i] = \frac{[i\eta]}{[P\eta]}|P] + \frac{[iP]}{[\eta P]}|\eta]. \tag{2.32b}$$

Plugging the spinors into (2.30) we find that,

$$\frac{\langle iP\rangle}{\langle \eta P\rangle} = \mathcal{O}(\delta) \quad \text{and} \quad \frac{[iP]}{[\eta P]} = \mathcal{O}(\delta). \tag{2.33}$$

Following [8], we will study the 5-gluon MHV amplitude's factorisation onto the 4-gluon amplitude in collinear limits,

$$A_5(1^-, 2^-, 3^+, 4^+, 5^+) = i\frac{\langle 12\rangle^4}{\langle 12\rangle\langle 23\rangle\langle 34\rangle\langle 45\rangle\langle 51\rangle} \to \text{Split} \times A_4. \tag{2.34}$$

The vanishing of the helicity amplitudes $A_n^{(0)}(1^\pm, 2^+, 3^+, ..., n^+) = 0$ means the only factorisation channels MHV amplitudes can have are two-particle channels, as opposed to multi-particle channels where the sum of more than two momenta go on-shell.

If we start by considering the situation when particle 4 and 5 go collinear, denoted $4 \parallel 5$, and keep only the leading term as $\delta \to 0$,

$$A_5(1^-, 2^-, 3^+, 4^+, 5^+) \overset{4\parallel 5}{\to} \frac{1}{\sqrt{z}\sqrt{1-z}\langle 45\rangle} \times A_4(1^-, 2^-, 3^+, P^+), \tag{2.35}$$

we extract the splitting function,

$$\text{Split}_-(i^+, j^+) = \frac{1}{\sqrt{z}\sqrt{1-z}\langle ij\rangle}. \tag{2.36}$$

Considering instead the limits $2 \parallel 3$ and $5 \parallel 1$ we get the splitting functions,

$$\text{Split}_+(i^-, j^+) = \frac{z^2}{\sqrt{z}\sqrt{1-z}\langle ij\rangle}, \tag{2.37}$$

$$\text{Split}_+(i^+, j^-) = \frac{(1-z)^2}{\sqrt{z}\sqrt{1-z}\langle ij\rangle}. \tag{2.38}$$

Collinear limits in six dimensions

For the six-dimensional spinor-helicity formalism we realise the parametrisation (2.30) using,

$$\begin{aligned} \lambda_{ia}^A &= \langle z_{iax}\rangle \lambda_P^{Ax} + \langle w_{iax}\rangle \lambda_\eta^{Ax}, \\ \langle z_{iax}\rangle &= \frac{\langle i_a|\eta|P_x\rangle}{2\eta\cdot P}, \quad \langle w_{iax}\rangle = \delta \frac{\langle i_a|P|\eta_x\rangle}{2\eta\cdot P}. \end{aligned} \tag{2.39}$$

We again start from the 5-point amplitude,

$$\begin{aligned} A_5(1_{a\dot{a}}, 2_{b\dot{b}}, 3_{c\dot{c}}, 4_{d\dot{d}}, 5_{e\dot{e}}) = {} & \langle 1_a|2345|1_{\dot{a}}]\langle 2_b 3_c 4_d 5_e\rangle [2_{\dot{b}} 3_{\dot{c}} 4_{\dot{d}} 5_{\dot{e}}] + 4 \text{ cyclic terms} \\ & - \langle 3_c|(4512-4215)|4_{\dot{d}}]\langle 1_a 2_b 4_d 5_e\rangle [1_{\dot{a}} 2_{\dot{b}} 3_{\dot{c}} 5_{\dot{e}}] \\ & - \langle 4_d|(5123-5321)|5_{\dot{e}}]\langle 1_a 2_b 3_c 5_e\rangle [1_{\dot{a}} 2_{\dot{b}} 3_{\dot{c}} 4_{\dot{d}}] \\ & - \langle 3_c|(5321-5123)|5_{\dot{e}}]\langle 1_a 2_b 4_d 5_e\rangle [1_{\dot{a}} 2_{\dot{b}} 3_{\dot{c}} 4_{\dot{d}}] \\ & - \langle 2_b|(3452-5432)|1_{\dot{a}}]\langle 1_a 3_c 4_d 5_e\rangle [2_{\dot{b}} 3_{\dot{c}} 4_{\dot{d}} 5_{\dot{e}}]. \end{aligned} \tag{2.40}$$

This compact expression for the five-gluon amplitude in six dimensions is derived from the one appearing in [27].

The algebra involved in the derivation of the splitting function in six dimensions is lengthy, but since the helicity indices are free all information is contained in

one expression,

$$\begin{aligned}\mathrm{Split}_{x\dot{x}}(1^{a\dot{a}},2^{b\dot{b}}) = &-\frac{1}{s_{12}z(1-z)}\frac{1}{(2P\cdot n)^3}\\ &\times\Big(\langle 1^a|Pn|1^{\dot{a}}]\langle 2^b|n|P_x\rangle[2^{\dot{b}}|n|P_{\dot{x}}]\\ &-\langle 2^b|Pn|2^{\dot{b}}]\langle 1^a|n|P_x\rangle[1^{\dot{a}}|n|P_{\dot{x}}]\\ &+\frac{1}{2P\cdot n}\langle P_x|n12n|P_{\dot{x}}]\langle 1^a|n|2^b\rangle[1^{\dot{a}}|n|2^{\dot{b}}]\Big).\end{aligned} \tag{2.41}$$

Equivalence with the expressions obtained in four dimensions can be checked numerically using the spinors in (2.22).

2.2.3 Berends-Giele off-shell currents

In numerical implementations Berends-Giele recursion relations [26] provide a fast method for computing tree-level amplitudes. A good introduction is given in [8].

The Berends-Giele recursion relies on Feynman rules to produce off-shell vector currents. Dressing a current with an external state gives the amplitude. If we are interested in the n-point gluon amplitude we first construct the $n-1$ point off-shell current, $J^{\mu_k}(1,..,k-1,k+1,..,n)$, recursively. Contracted with the polarisation vector, $\epsilon^{\mu_k}(k)$, we obtain the amplitude. The start of the recursion relations are indeed the polarisation vectors,

$$J^{\mu}(k) = \epsilon^{\mu}(k), \tag{2.42}$$

where we have suppressed the helicity label. To build an amplitude we need at least three particles. The off-shell current, $J^{\mu}(k)$, can be contracted with three- and four-point gluon vertices. The n-point off-shell gluon current is therefore,

$$\begin{aligned}J^{\mu}(1,...,n) = &\sum_{i=1}^{n-1} V^{\mu\alpha\beta}(p_{1n},p_{1i},p_{(i+1)n})S_{\alpha\nu}(p_{1i})J^{\nu}(1,...,i)S_{\beta\rho}(p_{(i+1)n})J^{\rho}(i+1,...,n)\\ &+\sum_{i}^{j}\sum_{j=i+1}^{n} V^{\mu\alpha\beta\gamma}S_{\alpha\nu}(p_{1i})J^{\nu}(1,..,i)S_{\beta\rho}(p_{(i+1)j})J^{\nu}(i+1,..,j)\\ &\times S_{\gamma\delta}(p_{(j+1)n})J^{\delta}(j+1,..,n)\end{aligned} \tag{2.43}$$

where $p_{ij} = p_i + \cdots + p_j$ and the propagators are,

$$S_{\alpha\beta}(p_{ij}) = \begin{cases} \eta_{\alpha\beta} & i = j \\ \frac{-i\eta_{\alpha\beta}}{p_{ij}^2} & i \neq j \end{cases}. \tag{2.44}$$

The Feynman vertices, $V^{\mu\alpha\beta}(p_{1n}, p_{1i}, p_{(i+1)n})$ and $V^{\mu\alpha\beta\gamma}$, are given by the Feynman rules for gluon self-interactions in Figure 1.1. Many lower point currents are shared between the terms of the sum and can be reused to increase performance.

The recursion relation is easily extended for additional flavours. For fermions the second sum is omitted as there is no four-point vertex. Furthermore, spinor indices replace the vector indices, and the propagators and external states are changed appropriately. Extending to colour singlets involves summing over all possible positions of the singlet.

2.2.4 Britto-Cachazo-Feng-Witten recursion

While colour-ordering and spinor-helicity formalism simplify calculations a lot, we still rely on Feynman diagrams when calculating amplitudes. The Berends-Giele recursion relation offers some recycling of the off-shell currents, but the calculations have complicated intermediate steps largely due to guage-dependence. Analytic calculations quickly become impractical as the amount of diagrams grows rapidly with the number of external particles.A recursion method due to Britto, Cachazo, Feng, and Witten [36, 37], which uses on-shell, gauge-invariant amplitudes as input, results in compact results as well as intermediate steps. We present this recursion relation in detail following the derivations in [24, 38].

The key idea is to express an n-point amplitude in terms of amplitudes with fewer external legs connected by single on-shell propagators. We are interested in the gluon amplitude $A_n(1, 2, ..., n)$. The first step is to parametrise the singular behaviour of the amplitude by shifting two spinors by a complex parameter. Without loss of generality we choose to shift the first and last leg as follows,

$$|1\rangle \to |\hat{1}\rangle = |1\rangle + z|n\rangle, \qquad |n\rangle \to |\hat{n}\rangle = |n\rangle, \tag{2.45a}$$

$$|1] \to |\hat{1}] = |1], \qquad |n] \to |\hat{n}] = |n] - z|1], \tag{2.45b}$$

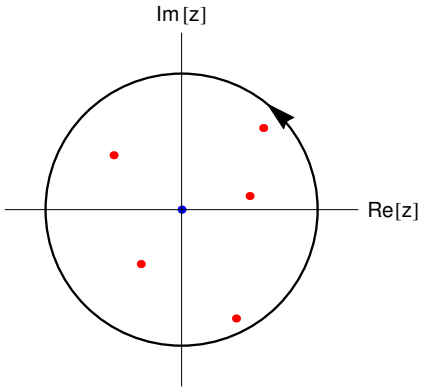

Figure 2.1 *Contour integration for BCFW. The coloured dots represent singularities. The residue at the origin gives the amplitude we are interested in.*

where hatted spinors are shifted and $z \in \mathbb{C}$. In terms of momenta this shift is,

$$\hat{p}_1^\mu = \frac{\langle 1|\sigma^\mu|1]}{2} + z\frac{\langle n|\sigma^\mu|1]}{2}, \tag{2.46a}$$

$$\hat{p}_n^\mu = \frac{\langle n|\sigma^\mu|n]}{2} - z\frac{\langle n|\sigma^\mu|1]}{2}, \tag{2.46b}$$

and the shifted momenta are seen to be on-shell and momentum conservation is retained. The direction of the deformation is proportional to $\epsilon^+(p_1, p_n)$, see (2.9). After the shift the amplitude is a rational function of z, $A_n(z)$. By Cauchy's theorem we have,

$$0 = \frac{1}{2\pi i}\oint_\gamma \frac{A_n(z)}{z} = \sum_k \text{Res}\left[\frac{A_n(z)}{z}\right]\Bigg|_{z=z_k}, \tag{2.47}$$

assuming that $A_n(z) \to 0$ as $|z| \to \infty$ to avoid surface terms as we make the contour, γ, very large. We will justify this assumption later. We denote the poles z_k, illustrated in Figure 2.1. The residue at the origin is the amplitude we are interested in and taking it out of the sum,

$$A_n(0) = -\sum_{\substack{k \\ z_k \neq 0}} \text{Res}\left[\frac{A_n(z)}{z}\right]\Bigg|_{z=z_k}. \tag{2.48}$$

The remaining singularities occur when a propagator in the shifted amplitude goes on-shell, connecting two lower-point amplitudes. From the on-shell condition we

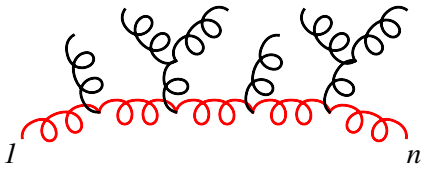

Figure 2.2 *Large z-dependence of a Feynman diagram. Only propagators drawn in red depend on the BCFW shift parameter, z.*

obtain an expression for z_k,

$$\begin{aligned} 0 = \hat{P}_k^2(z_k) = (\hat{p}_1(z_k) + ... + p_k)^2 = (z_k|n\rangle[1| + P_k)^2 \\ \Rightarrow 0 = P_k^2 + z_k[1|P_k|n\rangle. \end{aligned} \tag{2.49}$$

The momenta entering this propagator have to be adjacent, since we are working with colour-ordered amplitudes. With all momenta outgoing this propagator has opposite helicity in the two connected amplitudes as well as opposite sign momentum. We will refer to the connected amplitudes by left and right, $A_L(1, ..., k, -\hat{P}_k^{-h})$ and $A_R(\hat{P}_k^h, k+1, ..., n)$, where h is the helicity of the intermediate state and must be summed over. The poles of $A_n(z)$ are simple and their residues are,

$$\begin{aligned} \text{Res}\left[\frac{A_n(z)}{z}\right]\Bigg|_{z=z_k} =& \frac{1}{z_k}\lim_{z\to z_k}\left[(z-z_k)A_n(z)\right] \\ =& -\frac{[1|P_k|n\rangle}{P_k^2}\lim_{z\to z_k}\left[\frac{z[1|P_k|n\rangle + P_k^2}{[1|P_k|n\rangle}A_n(z)\right] \\ =& -\frac{1}{P_k^2}\lim_{z\to z_k}\left[\hat{P}_k^2(z)A_n(z)\right]. \end{aligned} \tag{2.50}$$

When $z \to z_k$ the amplitude, $A_n(z)$, factorises into a left and a right amplitude as mentioned above. $\hat{P}_k^2$ cancels against the propagator in the amplitude leaving the un-shifted propagator in front. Hence, each pole gives a contribution of $\frac{-1}{P_k^2}$. Note that the un-shifted propagator does not diverge at z_k. Putting everything back into (2.48) we arrive at the BCFW recursion formula,

$$A_n^{(0)}(1, ..., n) = \sum_{k=2}^{n-2}\sum_{h=\pm} A_L^{(0)}(\hat{1}, ..., k, -\hat{P}_k^{-h})\frac{i}{P_k^2}A_R^{(0)}(\hat{P}_k^h, k+1, ..., \hat{n}). \tag{2.51}$$

Note that k is only summed from 2 to $n-2$ since at least three gluons are needed in both lower-point amplitudes. Three-point amplitudes are indeed the starting point of the recursion and we will derive them shortly.

In the derivation of the recursion relation we assumed that the amplitude vanishes for $|z| \to \infty$. We will now justify this assumption for the case of pure gluon amplitudes. Considering the Feynman diagram in Figure 2.2, only internal propagators drawn in red carry z dependence. From the expression for the shifted propagator momentum in (2.49) we find the propagator's large z behaviour,

$$\frac{1}{\hat{P}_k^2(z)} = \frac{1}{(z|n\rangle[1| + P_k)^2} \to 0 \text{ as } z \to \infty. \tag{2.52}$$

Gluon vertices carry up to one power of momentum and hence at most one power of z. Without taking the external states into account and noting that there is one more vertex than there are propagators, the amplitude scales linearly in z for $z \to \infty$. The remedy comes from the scaling of the external states provided that we choose the helicity configuration carefully. Symmetries, such as cyclic permutation, allow us to choose the helicities $1^+, n^-$. For this configuration the polarisation vectors (2.9) have the desired scaling for large z under the shift (2.45),

$$\epsilon^+_{1,\mu}(z) \underset{z\to\infty}{\to} \frac{1}{z}, \qquad\qquad \epsilon^-_{n,\mu}(z) \underset{z\to\infty}{\to} \frac{1}{z}. \tag{2.53}$$

The amplitude therefore scales as $\frac{1}{z}$ in the large z limit. In fact, configurations where the shifted particles have the same helicity work as well, even if the argument above fails. However, the configuration $1^-, n^+$ has bad scaling behaviour and cannot be used for the BCFW shift in (2.45). More generally, it can be shown that choosing the deformation direction in (2.46) to be proportional to the polarisation vector of particle 1, $\epsilon^\pm_\mu(p_1, p_n)$, provides a valid shift [39].

With the recursion relation (2.51) we obtain an amplitude with n external legs by sewing together amplitudes with between 3 and $(n-1)$ external legs. This is a major improvement over the Feynman diagram approach, where we could not recycle lower multiplicity amplitudes. Furthermore, by using only on-shell amplitudes we avoid gauge dependence in intermediate steps. To start the recursion we will need three-point amplitudes.

Three-point kinematics

In the derivation of three-point amplitudes we will allow complex momenta. Indeed, in a BCFW recursion complex momenta are introduced when performing the shift (2.45).

For massless kinematics we have,

$$\langle 12\rangle[21] = (p_1 + p_2)^2 = (-p_3)^2 = 0, \tag{2.54}$$

where we used momentum conservation. For real momenta, angle and square brackets are related by complex conjugation, but working with complex momenta we can conclude that either $\langle 12\rangle = 0$ or $[21] = 0$. Assuming that $\langle 12\rangle$ is non-zero, it follows from momentum conservation that,

$$\langle 12\rangle[23] = 0 \Rightarrow [23] = 0, \tag{2.55a}$$

$$\langle 21\rangle[13] = 0 \Rightarrow [13] = 0, \tag{2.55b}$$

such that all square brackets vanish. Hence three-point amplitudes can be non-vanishing provided that they depend only on the angle brackets or alternatively, only on square brackets. We can now write an Ansatz for the three-point amplitude with arbitrary helicities, h_i,

$$A(1^{h_1}, 2^{h_1}, 3^{h_1}) = c\langle 12\rangle^{x_{12}}\langle 23\rangle^{x_{23}}\langle 31\rangle^{x_{31}}, \tag{2.56}$$

where c is constant. We will determine the exponents, x_{ij}, using arguments based on the little group scaling. A momentum vector, $p^\mu = \frac{1}{2}\langle p|\sigma^\mu|p] = \frac{1}{2}[p|\tilde{\sigma}^\mu|p\rangle$, is left invariant under the little group scaling,

$$\lambda(p) \to \frac{1}{t}\lambda(p), \qquad \tilde{\lambda}(p) \to t\tilde{\lambda}(p). \tag{2.57}$$

From the solutions of the Dirac equation, (2.5), we see that the little group scaling of an external fermion at the amplitude level becomes,

$$A(1_q^{h_1}, 2_{\bar{q}}, 3, \ldots, n) = t^{-2h_1}A(1_q^{h_1}, 2_{\bar{q}}, 3, \ldots, n), \tag{2.58}$$

where $h_1 = \pm\frac{1}{2}$. For a gluon with $h = \pm 1$ the same scaling is found from the polarisation vector expressions in (2.9). Applying the shifts to the Ansatz in (2.56) gives a system of equations that allow for determining the exponents,

$$x_{12} = -h_1 - h_2 + h_3, \tag{2.59a}$$

$$x_{23} = h_1 - h_2 - h_3, \tag{2.59b}$$

$$x_{31} = -h_1 + h_2 - h_3. \tag{2.59c}$$

The Feynman rules, see Figure 1.1, indicate the mass dimension of the three-

point amplitude and this prohibits most helicity configurations. The allowed three-point amplitudes are,

$$A(1^+,2^-,3^-) = -i\frac{\langle 23\rangle^3}{\langle 12\rangle\langle 13\rangle}, \qquad A(1^-,2^+,3^+) = i\frac{[23]^3}{[12][13]}, \tag{2.60a}$$

$$A(1_q^-,2_{\bar{q}}^+,3^-) = -i\frac{\langle 13\rangle^2}{\langle 12\rangle}, \qquad A(1_q^-,2_{\bar{q}}^+,3^+) = i\frac{[23]^2}{[12]}. \tag{2.60b}$$

With these three-point amplitudes we can now construct any higher-multiplicity amplitude using the BCFW recursion relation.

A four-point example

To calculate the four-gluon amplitude, $A_4(1^+,2^+,3^-,4^-)$, we shift particle 1 and 4 according to (2.45) and apply the BCFW recursion relation (2.51) to obtain,

$$\begin{aligned} A_4(1^+,2^+,3^-,4^-) &= A_3(\hat{1}^+,2^+,-\hat{P}_2^-)\frac{i}{P_2^2}A_3(\hat{P}_2^+,3^-,\hat{4}^-) \\ &= \frac{i[\hat{1}2]^3}{[-\hat{P}\hat{1}][-\hat{P}2]}\frac{i}{\langle 12\rangle[21]}\frac{-i\langle 3\hat{4}\rangle^3}{\langle \hat{P}3\rangle\langle \hat{P}\hat{4}\rangle} \\ &= -i\frac{[12]^3\langle 34\rangle^3}{[1\hat{P}][2\hat{P}]\langle 12\rangle[21]\langle \hat{P}3\rangle\langle \hat{P}4\rangle}, \end{aligned} \tag{2.61}$$

where we used the analytic continuation $|-\hat{P}] = i|\hat{P}]$ and that $|\hat{1}] = |1]$ and $|\hat{4}\rangle = |4\rangle$. Hence, we only need to evaluate,

$$\begin{aligned} [1\hat{P}]\langle \hat{P}3\rangle &= [1|\left(\hat{p_1}+p_2\right)|3\rangle \\ &= [1|\left(p_1+z|1]\langle 4|+p_2\right)|3\rangle \\ &= [12]\langle 23\rangle, \end{aligned} \tag{2.62a}$$

$$[2\hat{P}]\langle \hat{P}4\rangle = [21]\langle 14\rangle. \tag{2.62b}$$

Plugging this back in, we arrive at the result expected from (2.18),

$$A_4(1^+,2^+,3^-,4^-) = i\frac{\langle 34\rangle^4}{\langle 12\rangle\langle 23\rangle\langle 34\rangle\langle 43\rangle}. \tag{2.63}$$

In fact, (2.18) can be proved by induction using the BCFW recursion relation. We now turn to the extension of the recursion relation to six dimensions.

BCFW in six dimensions

The BCFW recursion relation was applied to six dimensions in [27]. As mentioned earlier, the helicity indices of spinor-helicity formalism in six dimensions are not fixed and the discussion of valid helicity configurations for BCFW in four dimensions cannot be readily applied to six dimensions. The solution is to introduce a little group matrix carrying the helicity indices, $X^{a\dot{a}}$, to project out appropriate shifts. The shifted six-dimensional vectors are then, cf. (2.46),

$$\hat{p}_1^\mu = p_1^\mu + zX^{a\dot{a}}\epsilon^\mu_{a\dot{a}}(p_1, p_n), \tag{2.64a}$$

$$\hat{p}_n^\mu = p_n^\mu - zX^{a\dot{a}}\epsilon^\mu_{a\dot{a}}(p_1, p_n), \tag{2.64b}$$

where the polarisation vector is defined in (2.25) and due to the on-shell condition, $\det(X) = 0$. Therefore, the matrix can be expressed as an outer product of two little group vectors, $X^{a\dot{a}} = x^a\tilde{x}^{\dot{a}}$. The shift can then be realised using the shifted spinors,

$$|1_a\rangle \to |\hat{1}_a\rangle = |1_a\rangle + zx_a\tilde{x}_{\dot{c}}\langle n_c|1_{\dot{c}}]^{-1}|1_c\rangle, \tag{2.65a}$$

$$|n_b\rangle \to |\hat{n}_b\rangle = |n_b\rangle + zx^c\tilde{x}^{\dot{c}}\langle n^b|1^{\dot{c}}]^{-1}|1_c\rangle, \tag{2.65b}$$

$$|1_{\dot{a}}] \to |\hat{1}_{\dot{a}}] = |1_{\dot{a}}] - z\tilde{x}_{\dot{a}}x^c\langle 1^c|n_{\dot{c}}]^{-1}|1_{\dot{c}}], \tag{2.65c}$$

$$|n_{\dot{b}}] \to |\hat{n}_{\dot{b}}] = |n_{\dot{b}}] - z\tilde{x}^{\dot{c}}x^c\langle 1^c|n^{\dot{b}}]^{-1}|n_{\dot{c}}]. \tag{2.65d}$$

The recursion relation becomes,

$$x^a\tilde{x}^{\dot{a}}A_n^{(0)}(1_{a\dot{a}}, ..., n_{b\dot{b}}) = \sum_{k=2}^{n-2}\sum_{c\dot{c}} x^a\tilde{x}^{\dot{a}}A_L^{(0)}(\hat{1}_{a\dot{a}}, ..., -\hat{P}_{kc\dot{c}})\frac{i}{P_k^2}A_R^{(0)}(\hat{P}_k^{c\dot{c}}, ..., \hat{n}_{b\dot{b}}), \tag{2.66}$$

and the desired amplitude is extracted as the coefficient of $x^a\tilde{x}^{\dot{a}}$. All other helicity indices of the particles are left free and all helicity amplitudes are obtained in one BCFW computation. The relevant three-point amplitude for starting the recursion is computed in [27] and given in Appendix B.

2.3 Momentum twistors

Spinor-helicity makes on-shell conditions for external particles manifest, through the identification,

$$p \cdot \sigma^{\mu}_{a\dot{a}} = \lambda_a \tilde{\lambda}_{\dot{a}}. \tag{2.67}$$

Using momentum twistors [40, 41] momentum conservation can be made manifest and furthermore, we can construct rational phase space points. From the momenta, p_i^{μ}, we define dual momentum coordinates and a spinor,

$$p_i^{\mu} = x_i^{\mu} - x_{i-1}^{\mu}, \quad \mu_i^{\dot{a}} = x_i \cdot \tilde{\sigma}^{\dot{a}a} \lambda_{ia}. \tag{2.68}$$

Using these we define the momentum twistor, Z, and the dual twistor, W,

$$Z_{iA} = \left(\lambda_{ia}, \mu_i^{\dot{a}}\right), \tag{2.69a}$$

$$W_i^A = \frac{\epsilon^{ABCD} Z_{(i-1)B} Z_{iC} Z_{(i+1)D}}{\langle i-1\ i\rangle\langle i\ i+1\rangle} = \left(\tilde{\mu}_{ia}, \tilde{\lambda}_i^{\dot{a}}\right), \tag{2.69b}$$

where the twistor index $A = 1, 2, 3, 4$ and i takes values from 1 to the number of particles, n. It follows that,

$$\tilde{\lambda}_i^{\dot{a}} = \frac{\langle i-1\ i\rangle \mu_{i+1}^{\dot{a}} + \langle i-1\ i+1\rangle \mu_i^{\dot{a}} + \langle i\ i+1\rangle \mu_{i-1}^{\dot{a}}}{\langle i-1\ i\rangle\langle i\ i+1\rangle}, \tag{2.70}$$

and using the Schouten identity (2.8) momentum conservation can be shown to be automatically satisfied,

$$\sum_{i=1}^{n} \lambda_{ia} \tilde{\lambda}_{i\dot{a}} = 0. \tag{2.71}$$

We parametrise the phase space by filling out the $4n$ entries of $\boldsymbol{Z}_n = (Z_{1A}, \ldots, Z_{nA})$. The number of free parameters is deduced from Poincaré invariance in four dimensions; six constraints come from boosts and rotations and another four come from translations. Furthermore, each momentum twistor, Z_{iA}, has a $U(1)$ symmetry. This leaves us with $4n - 6 - 4 - n = 3n - 10$ free parameters. For four-point kinematics we have two free parameters and choose

the following parametrisation,

$$\boldsymbol{Z}_4 = \begin{pmatrix} 1 & 0 & \frac{1}{x_1} & \frac{1}{x_1}+\frac{1}{x_1x_2} \\ 0 & 1 & 1 & 1 \\ 0 & 0 & 0 & 1 \\ 0 & 0 & 1 & 1 \end{pmatrix} \Rightarrow \boldsymbol{W}_4 = \begin{pmatrix} 0 & 0 & -x_1^2x_2 & 0 \\ 0 & 0 & 0 & x_1x_2 \\ -1 & -x_1 & x_1 & 0 \\ 1 & 0 & x_1x_2 & -x_1x_2 \end{pmatrix}, \quad (2.72)$$

where the free parameters are related to the Mandelstam variables, $s = 2p_1 \cdot p_2 = x_1$ and $t = 2p_2 \cdot p_3 = x_1x_2$, and the spinors can be read off. Notice that only x_1 carries mass dimension, so in computations it can be set to a numerical value and reconstructed analytically by dimensional analysis at the end.

For five-point kinematics there are five free parameters. We choose the parametrisation,

$$\boldsymbol{Z}_5 = \begin{pmatrix} 1 & 0 & \frac{1}{x_1} & \frac{1}{x_1}+\frac{1}{x_1x_2} & \frac{1}{x_1}+\frac{1}{x_1x_2}+\frac{1}{x_1x_2x_3} \\ 0 & 1 & 1 & 1 & 1 \\ 0 & 0 & 0 & \frac{x_4}{x_2} & 1 \\ 0 & 0 & 1 & 1 & 1-\frac{x_5}{x_4} \end{pmatrix}. \quad (2.73)$$

With this choice $\boldsymbol{W}_5$ is relatively large and we will not write it explicitly. The free parameters, x_i, have simple relations to the invariants, $s_{ij} = (p_i + p_j)^2$,

$$s_{12} = x_1, \quad (2.74a)$$

$$s_{23} = x_1x_4, \quad (2.74b)$$

$$s_{34} = \frac{x_1}{x_2}\left(-x_2x_3 + x_4 + x_3x_4 + x_2x_3x_5\right), \quad (2.74c)$$

$$s_{45} = x_1x_5, \quad (2.74d)$$

$$s_{51} = x_1x_3\left(x_2 - x_4 + x_5\right). \quad (2.74e)$$

Furthermore, at five point we have the additional Lorentz invariant,

$$\epsilon_{\mu\nu\rho\sigma}p_1^\mu p_2^\nu p_3^\rho p_4^\sigma = \frac{-x_1^2}{4x_2}\big(x_2^2x_3 - x_2x_4 - 2x_2x_3x_4 + x_4^2 + x_3x_4^2 - x_2^2x_3x_5 - x_4x_5 - x_3x_4x_5\big), \quad (2.75)$$

which is related to the Gram determinant, $G = \det p_i \cdot p_j,\ i,j = 1,...,4$, through $G = -\left(\epsilon_{\mu\nu\rho\sigma}p_1^\mu p_2^\nu p_3^\rho p_4^\sigma\right)^2$. This momentum twistor representation of five-point kinematics allows us to write all kinematic variables free of square roots.

Finally, we note that in using the momentum twistor parametrisations the spinor phase has been discarded. Using the parametrisations above, the phase for a gluon amplitude is,

$$\Phi_n(1^{h_1},\ldots,n^{h_n}) = \left(\frac{\langle 13\rangle}{[12]\langle 23\rangle}\right)^{-h_1} \prod_{i=2}^{n} \left(\frac{\langle 1i\rangle^2[12]\langle 23\rangle}{\langle 13\rangle}\right)^{-h_i}, \tag{2.76}$$

where h_i are the helicities. The phase is reintroduced using,

$$A_n(1^{h_1},\ldots,n^{h_n}) = \Phi_n(1^{h_1},\ldots,n^{h_n})\hat{A}_n(\{x_i\}), \tag{2.77}$$

where $\hat{A}_n(\{x_i\})$ is the spinor phase free amplitude.

2.4 Summary

This concludes our discussion of tree-level techniques. The spinor-helicity formalism applied to the gauge-invariant colour-ordered amplitudes, defined in (1.13) and (1.14), provides compact tree-level amplitude expressions with definite helicity configurations. This is achieved through use of the on-shell spinor bracket variables defined in (2.4).

The Berends-Giele recursion relation provides an efficient way of calculating amplitudes of high multiplicity and is especially suitable for numerical implementation. The on-shell recursion relation due to Britto, Cachazo, Feng, and Witten enables us to construct amplitudes without relying on Feynman rules, using only gauge-invariant quantities. Such on-shell methods are central to our discussion on the calculation of loop amplitudes.

We shall rely heavily on the six-dimensional extension of the spinor-helicity formalism throughout this thesis. In the next chapter we use six dimensions for embedding the extra-dimensional loop momentum components from dimensional regularisation that was introduced in section 1.2.3. In Chapter 4 we embed a fermion mass in the sixth dimension to develop a method for calculating amplitudes involving massive fermions. Six dimensions is the minimal embedding dimension at two loops in dimensional regularisation. We shall use this in Chapter 5.

Chapter 3

Techniques for one-loop amplitudes

In the last chapter we introduced several on-shell techniques at tree level. The spinor-helicity formalism makes the on-shell condition on the external kinematics manifest, while momentum twistors ensure momentum conservation throughout our calculations. The BCFW recursion relation (2.51) is an on-shell technique which goes beyond the traditional Feynman diagrammatic methods. By using only physical degrees of freedom, intermediate steps are simplified by avoiding gauge redundancies. As the complexity of Feynman diagrammatic calculations increases rapidly when adding loops, it is desirable to extend these methods beyond tree level. In this chapter we shall apply on-shell principles at the one-loop level. As an example, we will calculate the one-loop four-point gluon amplitude using only on-shell gauge-invariant ingredients.

In dimensional regularisation, with $d = 4 - 2\epsilon$, a general one-loop amplitude can be written schematically as,

$$A^{(1)} = \mu^{2\epsilon} \sum_{\substack{\text{Feynman} \\ \text{diagrams}}} \int \frac{d^d k}{(2\pi)^d} \frac{N(k, \{p\})}{\prod D_i}. \tag{3.1}$$

The sum is over all Feynman diagrams contributing to the one-loop process. The numerator, $N(k, \{p\})$, is a polynomial in scalar products of the loop momentum, independent external momenta, and polarisation vectors. The denominator is a product of the inverse (scalar) propagators, $D_i = (k - q_i)^2$, appearing in the Feynman diagram and q_i is a sum of external momenta p_j. Finally, the factor in front, $\mu^{2\epsilon}$, keeps the mass dimension fixed on excursions away from four

dimensions.

In the first section of this chapter we will discuss integral reduction in order to write one-loop amplitudes solely in terms of Feynman integrals with four or less propagators. The second section introduces integrand reduction and the parametrisation of general gauge theory integrands. The third section describes unitarity methods and generalised unitarity cuts, and also demonstrates an application to the reduction of a four-point, one-loop amplitude. In the last section rational terms and their calculation using d-dimensional unitarity cuts are discussed.

3.1 One-loop integrals

The above representation (3.1) of the amplitude involves n-point tensor integrals of the form,

$$I_n[k^{\mu_1}\cdots k^{\mu_n}] = \mu^{2\epsilon}\int \frac{d^dk}{(2\pi)^d}\frac{k^{\mu_1}\cdots k^{\mu_n}}{\prod_{i=0}^{n-1} D_i}. \tag{3.2}$$

We will limit our discussion to n-point tensor integrals of rank n, since no higher rank appear in a renormalisable gauge theory. Using the technique introduced by Passarino and Veltman [42], tensor integrals can be fully reduced to scalar integrals. We briefly review this method for the case of a massless, four-point integral of rank one,

$$I_{4,0123}[k^\mu] = \int \frac{d^4k}{(2\pi)^4}\frac{k^\mu}{D_0D_1D_2D_3}, \tag{3.3}$$

where we have set $d = 4$. The additional sequence of subscripts on the left hand side specifies the propagators. For outgoing, cyclically ordered momenta the inverse propagators are,

$$D_0 = k^2, \tag{3.4a}$$

$$D_i = (k - q_i)^2, \qquad i = 1, \ldots, n-1, \tag{3.4b}$$

$$q_i = p_{1\ldots i}, \tag{3.4c}$$

where we have used the shorthand notation $p_{i_1 \ldots i_n} = \sum_{j=i_1}^{i_n} p_j$. We will use the fact that the integral can be written in terms of the independent external momenta,

$$I_{4,0123}[k^\mu] = a p_1^\mu + b p_2^\mu + c p_3^\mu. \tag{3.5}$$

The coefficients a, b, c can be projected out by contracting with the external momenta, p_1, p_2, p_3. In these three cases the numerator becomes,

$$k \cdot p_1 = -\frac{1}{2}\left((k-p_1)^2 - k^2\right) = -\frac{1}{2}\left(D_1 - D_0\right), \tag{3.6a}$$

$$k \cdot p_2 = -\frac{1}{2}\left((k-p_{12})^2 - (k-p_1)^2 - s_{12}\right) = -\frac{1}{2}\left(D_2 - D_1 - s_{12}\right), \tag{3.6b}$$

$$k \cdot p_3 = -\frac{1}{2}\left((k-p_{123})^2 - (k-p_{12})^2 + s_{12}\right) = -\frac{1}{2}\left(D_3 - D_2 + s_{12}\right), \tag{3.6c}$$

where $s_{ij} = (p_i + p_j)^2$ and we have used $p_i^2 = 0$. Note the appearance of inverse propagators on the right hand side, which will cancel against the factors in the denominator. Solving for the coefficients, we find,

$$\begin{aligned} 2a = {} & \frac{s_{13} - s_{12}}{s_{13}} I_{4,0123}[1] - \frac{s_{23}}{s_{12}s_{13}} I_{3,123}[1] - \frac{1}{s_{13}} I_{3,023}[1] \\ & + \frac{s_{12} - s_{13}}{s_{12}s_{13}} I_{3,013}[1] - \frac{1}{s_{13}} I_{3,012}[1], \end{aligned} \tag{3.7a}$$

$$\begin{aligned} 2b = {} & -I_{4,0123}[1] + \frac{1}{s_{12}} I_{3,123}[1] + \frac{1}{s_{23}} I_{3,023}[1] \\ & - \frac{1}{s_{12}} I_{3,013} - \frac{1}{s_{23}} I_{3,012}[1], \end{aligned} \tag{3.7b}$$

$$\begin{aligned} 2c = {} & -\frac{s_{12}}{s_{13}} I_{4,0123}[1] + \frac{1}{s_{13}} I_{3,123}[1] - \frac{s_{23} - s_{13}}{s_{23}s_{13}} I_{3,023}[1] \\ & + \frac{1}{s_{13}} I_{3,013}[1] - \frac{s_{12}}{s_{23}s_{13}} I_{3,012}[1], \end{aligned} \tag{3.7c}$$

and the desired reduction is obtained. Note that the reduced expression involves only scalar four- and three-point integrals. The solutions are significantly longer in the massive case, but follow from the same principle. The result from reducing a rank two integral would involve rank one integrals, which can then be further reduced using the result above. This way a chain of reductions is formed and all tensor integrals can be reduced to scalar integrals.

Further, it can be shown that all n-point scalar integrals with $n > 4$ can be reduced to linear combinations of integrals with $n \leq 4$ [43]. To show this we start

by considering the massless pentagon integral in four dimensions,

$$I^{(4)}_{5,01234}[1] = \int \frac{d^4k}{(2\pi)^4} \frac{1}{D_0 D_1 D_2 D_3 D_4}. \tag{3.8}$$

At five points, the four independent momenta sums in the propagators span the four-dimensional space, and therefore the loop momentum can be written as a linear combination of them. This observation leads to a Schouten identity,

$$k^\mu \ \mathrm{tr}_5\,(1234) = \sum_{i=1}^{4} k \cdot q_i \ v_i^\mu, \tag{3.9}$$

where we use the shorthand notation,

$$\mathrm{tr}_5\,(ijkl) = \mathrm{tr}_5\,(q_i q_j q_k q_l) = \mathrm{tr}\,(\gamma_5 \gamma_\mu \gamma_\nu \gamma_\rho \gamma_\sigma)\, q_i^\mu q_j^\nu q_k^\rho q_l^\sigma, \ \ \gamma_5 = -i\gamma^0\gamma^1\gamma^2\gamma^3. \tag{3.10a}$$

$$v_1^\mu = \mathrm{tr}_5\,(\gamma^\mu 234)\,, \ \ v_2^\mu = \mathrm{tr}_5\,(1\gamma^\mu 34)\,, \ \ v_3^\mu = \mathrm{tr}_5\,(12\gamma^\mu 4)\,, \ \ v_4^\mu = \mathrm{tr}_5\,(123\gamma^\mu)\,. \tag{3.10b}$$

Contracting the Schouten identity (3.9) with k^μ leads to a relation between the five-point scalar integral and five four-point scalar integrals through the relations,

$$k \cdot q_i = -\frac{1}{2}\left(D_i - D_0 - q_i^2\right), \qquad i = 1, \ldots, n-1, \tag{3.11}$$

using the definitions in (3.4). We find,

$$k^2 \ \mathrm{tr}_5\,(1234) = -\frac{1}{2}\sum_{i=1}^{4}(D_i - q_i^2) \ v_i \cdot k + \frac{1}{2}\sum_{i=1}^{4} D_0 \ v_i \cdot k. \tag{3.12}$$

Terms proportional to $D_i v_i \cdot k$ are spurious and vanish. Further details on the reduction are worked out in Appendix C and the result is,

$$\begin{aligned} I^{(4)}_{5,01234}[1] = \frac{1}{w^2}\Big(&\left(2\mathrm{tr}_5\,(1234)^2 - \Sigma_{i=1}^4 w \cdot v_i\right) I^{(4)}_{4;1234}\,[1] \\ &+ w \cdot v_1 I^{(4)}_{4;0234}\,[1] + w \cdot v_2 I^{(4)}_{4;0134}\,[1] + w \cdot v_3 I^{(4)}_{4;0124}\,[1] + w \cdot v_4 I^{(4)}_{4;0123}\,[1]\Big), \end{aligned} \tag{3.13}$$

where $w^\mu = \sum_{i=1}^4 q_i^2 \ v_i^\mu$.

This reduction can be extended for $n > 5$-point scalar integrals using the same approach as for the pentagon integral. More details are given in Appendix C and

the result is,

$$I^{(4)}_{n,0\ldots n-1}[1] = \frac{1}{w\cdot q_n - q_n^2\ \mathrm{tr}_5\,(1234)}\Big(\left(\mathrm{tr}_5\,(1234) - \Sigma_{i=1}^4 v_i\cdot q_n\right) I^{(4)}_{n-1;1\ldots n-1}[1] \\ + v_1\cdot q_n I^{(4)}_{n-1;02\ldots n-1}[1] \\ + v_2\cdot q_n I^{(4)}_{n-1;013\ldots n-1}[1] \\ + v_3\cdot q_n I^{(4)}_{n-1;0124\ldots n-1}[1] \\ + v_4\cdot q_n I^{(4)}_{n-1;01235\ldots n-1}[1] \\ - \mathrm{tr}_5\,(1234)\, I^{(4)}_{n-1;0\ldots n-2}[1]\Big). \tag{3.14}$$

The dimensionally regulated generalisations of these integral reduction formulae are derived in [44]. The formula for $n \geq 6$, (3.14), generalises straightforwardly for loop momentum in $d = 4 - 2\epsilon$ dimensions. The formula for the reduction of the pentagon picks up an extra-dimensional contribution,

$$I^{(d)}_{5,01234}[1] = -\frac{1}{2}\sum_{i=0}^{4} a_i I^{(d)}_{5,0\ldots(i-1)(i+1)\ldots 4}[1] + \epsilon a_{-1} I^{(d+2)}_{5,01234}[1], \tag{3.15}$$

where,

$$a_{-1} = \sum_{i=0}^{4} a_i = \sum_{i,j=0}^{4} \left(A^{-1}\right)_{ij}. \tag{3.16}$$

In the massless case the elements of the matrix A are $A_{ij} = -q_i\cdot q_{j-1}$, with $A_{ii} = 0$. The six-dimensional pentagon is finite and hence the last term in (3.15) vanishes in the limit $\epsilon \to 0$.

Reducing the integrals we can write any n-point, one-loop amplitude in dimensional regularisation, where $d = 4 - 2\epsilon$, as,

$$A_n^{(1),4-2\epsilon} = \sum_a c_a I^{4-2\epsilon}_{4,a} + \sum_a c_a I^{4-2\epsilon}_{3,a} + \sum_a c_a I^{4-2\epsilon}_{2,a} + \sum_a c_a I^{4-2\epsilon}_{1,a} + \mathcal{R}_n + \mathcal{O}(\epsilon), \tag{3.17}$$

where the integral coefficients and the rational term, $\mathcal{R}_n$, are rational functions of invariants in external kinematics. The rational term emerges from contributions from the extra-dimensional, -2ϵ, part of the loop momentum and will be discussed in more detail later in this chapter. The indices a are sequences of

length 1 to 4 specifying the relevant propagators. The integrals are defined as,

$$I_{n,a}^{4-2\epsilon}[N(k,\{p_i\})] = \mu^{2\epsilon} \int \frac{d^d k}{(2\pi)^d} \frac{N(k,\{p_i\})}{\prod_{i\in a} D_i}. \tag{3.18}$$

In (3.17) we used the shorthand $I_{n,a}^{4-2\epsilon}[1] = I_{n,a}^{4-2\epsilon}$ for scalar integrals. We will refer to integrals with $n = 4$ as boxes, $n = 3$ as triangles, $n = 2$ as bubbles, and $n = 1$ as tadpoles. Up to an overall normalisation, the results for these integrals are available in the literature [13, 45, 46]. The integrals are expressible in terms of logarithms and dilogarithms and each integral comes with unique discontinuities due to these functions. This fact is central to the unitarity methods presented later in this chapter.

3.2 Integrand reduction

The previous section established how one-loop amplitudes can be written solely in terms of four- and lower-point integrals. This section describes a method for reducing a d-dimensional one-loop integrand into terms with at most d propagators. For example, boxes are the highest appearing topology in four dimensions.

Before reduction, the integrand is a rational function in scalar products of the loop momentum and external momenta. In cases where the external momenta do not span four-dimensional space, scalar products between the loop momentum and spurious directions, transverse to all external momenta, may also be present. These spurious terms are non-vanishing at the level of the integrand, but the associated spurious integrals vanish, explaining why only scalar integrals appeared in (3.17).

Scalar products between loop momenta and external momenta appearing in the numerator can be written in terms of propagators and external kinematics. These are known as reducible scalar products (RSPs) and were used in the integrals reductions of the previous section in (3.6) and (3.11). In later chapters we will see that, starting from two loops, some scalar products between loop momenta and external momenta cannot be expressed in terms of propagators. These are known as irreducible scalar products (ISPs). Scalar products between loop momenta and spurious directions are known as spurious ISPs.

A dimensionally regulated, $d = 4 - 2\epsilon$, n-point one-loop amplitude with four-dimensional external momenta can be written as [47–49],

$$\begin{aligned} A_n^{(1),d} &= \int \frac{d^d k}{(2\pi)^d} B_n^{(1)}, \\ B_n^{(1)} &= \sum_{1\le i<j<k<l<m}^{n} \frac{\Delta_{ijklm}\left(k,\{p\}\right)}{D_{ii}D_{ij}D_{ik}D_{il}D_{im}} + \sum_{1\le i<j<k<l}^{n} \frac{\Delta_{ijkl}\left(k,\{p\}\right)}{D_{ii}D_{ij}D_{ik}D_{il}} \\ &\quad + \sum_{1\le i<j<k}^{n} \frac{\Delta_{ijk}\left(k,\{p\}\right)}{D_{ii}D_{ij}D_{ik}} + \sum_{1\le i<j}^{n} \frac{\Delta_{ij}\left(k,\{p\}\right)}{D_{ii}D_{ij}} + \sum_{1\le i}^{n} \frac{\Delta_{i}\left(k,\{p\}\right)}{D_{ii}}. \end{aligned} \tag{3.19}$$

The irreducible numerators, Δ, are functions of the loop momentum, k, and the set of independent external momenta, $\{p\}$. The numerator subscripts denote the first particle on each leg such that the first leg has momentum $p_{i(j-1)} = p_i + ... + p_{j-1}$. For example, for an 8-point amplitude the box numerator Δ_{1347} has external legs $p_{12}, p_3, p_{456}, p_{78}$. Using this notation, the denominators are,

$$D_{ij} = \left(k - p_{i(j-1)}\right)^2, \tag{3.20}$$

so $D_{ii} = k^2$. This labelling is different to the one used for denominators in the previous section.

Note that bubble and tadpole integrals without an external mass scale vanish in dimensional regularisation. In massless QCD this happens for the bubble terms where $j = i + 1$ in (3.19). Likewise, in dimensional regularisation the tadpole contribution is relevant only in the presence of massive external particles. We will deal with its determination using a new approach in section 4.2.1.

The pentagon has no spurious ISPs in four dimensions. Equation (3.13) and (3.15) allow for the absorption of the four-dimensional part of the pentagon in the box numerators. The extra-dimensional contribution is $\mathcal{O}(\epsilon)$ [44]. Using this we see the equivalence of (3.17) and (3.19) for $d = 4 - 2\epsilon$. We now turn to the parametrisation of the numerators, Δ.

3.2.1 Parametrising the numerators

To parametrise the numerators it is useful to start by expanding the loop momenta around a basis of external momenta and transverse directions (similarly to the

methods of Van Neerven and Vermaseren [43]),

$$k_i = k_{\parallel,i} + k_{\perp,i}, \tag{3.21}$$

where, for generality, the index i runs from 1 to the number of loop momenta.

The parallel part is spanned by independent external momenta, q_j, and we write the expansion, $k_\parallel = \sum_i^{d_\parallel} a_{ij} q_j$, where the dimension of parallel space $d_\parallel \leq 4$. The coefficients a_{ij} are functions of scalar products between the loop momentum and external momenta. The transverse space is further decomposed into a four-dimensional part, $k_\perp^{[4]}$, and an extra-dimensional part, $k^{[-2\epsilon]}$,

$$k_\perp = k_\perp^{[4]} + k_\perp^{[-2\epsilon]}. \tag{3.22}$$

$k_\perp^{[4]}$ is expanded around spurious directions, ω_j, such that $k_\perp^{[4]} = \sum_i^{d_\perp} b_{ij}\omega_j$. The spurious directions satisfy $q_i \cdot \omega_j = 0$ and the dimension of transverse space $d_\perp \leq 3$ for four-dimensional external momenta. The coefficients, b_{ij}, are functions of the spurious ISPs only. Finally, the extra-dimensional part satisfies the relation,

$$\begin{aligned} \mu_{ij} &= -k_{\perp,i}^{[-2\epsilon]} \cdot k_{\perp,j}^{[-2\epsilon]} \\ &= k_i \cdot k_j - k_{\parallel,i} \cdot k_{\parallel,j} - k_{\perp,i}^{[4]} \cdot k_{\perp,j}^{[4]}. \end{aligned} \tag{3.23}$$

The first term on the right hand side can be expressed in terms of denominators and external kinematics while the remaining two are in general functions of the ISPs. To summarise, we have three categories of ISPs,

- physical ISPs, expressed as scalar products between loop momenta and external momenta, $k_i \cdot q_j$,
- spurious ISPs, written as scalar products between loop momenta and spurious directions, $k_i \cdot \omega_j$,
- extra-dimensional ISPs, μ_{ij}, defined in (3.23) and related to the ISPs of the above categories.

As previously mentioned, physical ISPs are absent at one-loop level and we will return to the challenge of parametrising the numerator in their presence in the next chapter. Below, we present d-dimensional parametrisations for the numerators at one loop.

The pentagon numerator is simple since the external momenta fully span four-dimensional space. This means that there are no spurious directions. With the absence of physical ISPs at one loop, we choose the numerator to be,

$$\Delta_{ijklm} = c^{(0)}_{ijklm}\ \mu_{11}. \tag{3.24}$$

For the box numerator we have one spurious direction,

$$\omega^\mu = \epsilon^{\mu\nu\rho\sigma} p_{1\nu} p_{2\rho} p_{3\sigma}. \tag{3.25}$$

Notice in particular that the right hand side of (3.5) vanishes upon contraction with ω^μ. Hence $I_{4,0123}[k\cdot\omega] = 0$, while at the level of the integrand $k\cdot\omega$ is non-zero. This is an example of a spurious integral, which play a central role throughout this thesis.

Renormalisability in four dimensions implies that the rank of a tensor integral cannot exceed the number of propagators. Therefore, the box numerator parametrisation will be a polynomial of at most degree four in the ISPs. Equation (3.23) relates monomials in the extra-dimensional ISPs to the spurious ISPs, exposing a choice in the set of monomials appearing in the parametrisation. We choose the parametrisation,

$$\Delta_{ijkl} = c^{(0)}_{ijkl} + c^{(1)}_{ijkl}\ k\cdot\omega + c^{(2)}_{ijkl}\ \mu_{11} + c^{(3)}_{ijkl}\ \mu_{11} k\cdot\omega + c^{(4)}_{ijkl}\ \mu_{11}^2. \tag{3.26}$$

Note that μ_{11} is of rank 2.

The triangle topology has two spurious directions, ω_1^μ and ω_2^μ, satisfying $q_i\cdot\omega_j = 0$ and we choose them to have the same normalisation, $\omega_i\cdot\omega_j = \omega^2\delta_{ij}$. We use the integrand parametrisation,

$$\begin{aligned}\Delta_{ijk} = {} & c^{(0)}_{ijk} + c^{(1)}_{ijk}\ k\cdot\omega_1 + c^{(2)}_{ijk}\ k\cdot\omega_2 + c^{(3)}_{ijk}\ \ k\cdot\omega_1\ k\cdot\omega_2 \\ & + c^{(4)}_{ijk}\ [(k\cdot\omega_1)^2 - (k\cdot\omega_2)^2] + c^{(5)}_{ijk}\ (k\cdot\omega_1)^2\ k\cdot\omega_2 + c^{(6)}_{ijk}\ k\cdot\omega_1\ (k\cdot\omega_2)^2 \\ & + c^{(7)}_{ijk}\ k\cdot\omega_1\ \mu_{11} + c^{(8)}_{ijk}\ k\cdot\omega_2\ \mu_{11} + c^{(9)}_{ijk}\ \mu_{11}.\end{aligned} \tag{3.27}$$

Finally, the bubble parametrisation, where three spurious directions appear, is,

$$\begin{aligned}\Delta_{ij} = c_{ij}^{(0)} &+ c_{ij}^{(1)}\ k\cdot\omega_1 + c_{ij}^{(2)}\ k\cdot\omega_2 + c_{ij}^{(3)}\ \ k\cdot\omega_3 \\ &+ c_{ij}^{(4)}\ \ k\cdot\omega_1\ k\cdot\omega_2 + c_{ij}^{(5)}\ \ k\cdot\omega_1\ k\cdot\omega_3 + c_{ij}^{(6)}\ \ k\cdot\omega_2\ k\cdot\omega_3 \\ &+ c_{ij}^{(7)}\ [(k\cdot\omega_1)^2 - (k\cdot\omega_2)^2] + c_{ij}^{(8)}\ [(k\cdot\omega_1)^2 - (k\cdot\omega_3)^2] \\ &+ c_{ij}^{(9)}\ \mu_{11}. \end{aligned} \tag{3.28}$$

In the next section we describe a method to obtain the coefficients of the above parametrisations using only on-shell, gauge-invariant tree-level amplitudes.

3.3 Unitarity methods

The traditional unitarity method [38, 50, 51] is derived from the unitarity of the S-matrix, introduced in section 1.1. We start with a short discussion of unitarity before commenting on its use for calculating amplitudes. The method applied for amplitude calculations in this thesis is based on unitarity and discussed in detail in section 3.3.1. Unitarity states that,

$$\begin{aligned} 1 &= S^\dagger S \\ &= (1 - iT^\dagger)(1 + iT) \\ &= 1 - i(T^\dagger - T) + T^\dagger T. \end{aligned} \tag{3.29}$$

Rearranging, we arrive at a representation of the Optical Theorem,

$$i(T^\dagger - T) = T^\dagger T. \tag{3.30}$$

Expanding the transition matrix, T, perturbatively in the coupling constant for four- and five-point amplitudes we have,

$$T_4 = g^2 T_4^{(0)} + g^4 T_4^{(1)} + g^6 T_4^{(2)} + ... \tag{3.31a}$$

$$T_5 = g^3 T_5^{(0)} + g^5 T_5^{(1)} + g^7 T_5^{(2)} + ... \tag{3.31b}$$

Solving (3.29) in powers of the coupling constant, g, we obtain,

$$g^2: \quad i\left(T_4^{(0)^\dagger} - T_4^{(0)}\right) = 0, \tag{3.32a}$$

$$g^4: \quad i\left(T_4^{(1)^\dagger} - T_4^{(1)}\right) = T_4^{(0)^\dagger} T_4^{(0)}, \tag{3.32b}$$

$$g^6: \quad i\left(T_4^{(2)^\dagger} - T_4^{(2)}\right) = T_4^{(1)^\dagger} T_4^{(0)} + T_4^{(0)^\dagger} T_4^{(1)} + T_5^{(0)^\dagger} T_5^{(0)}, \tag{3.32c}$$

where the superscripts denote the number of loops. The first equation implies that tree-level amplitudes are real. The two remaining equations imply that the discontinuities of loop level amplitudes can be related to amplitudes with fewer loops.

We can turn expression (3.29) into a relation between scattering amplitudes by dressing it with an initial state, $|i\rangle$, and a final state, $\langle f|$. In between the T-matrices on the right-hand side we furthermore put a complete set of on-shell states,

$$\langle f|T^\dagger T|i\rangle = \sum_{f,n} \int \prod_{i=1}^{n} \frac{d^d q_i}{(2\pi)^d} \delta^{(+)}(q_i^2) \langle f|T^\dagger|\{q_i\}\rangle\langle\{q_i\}|T|i\rangle, \tag{3.33}$$

where the delta function $\delta^{(+)}(q^2) = \Theta(q^0)\delta(q^2)$ enforces positive energy and real momentum for the intermediate states. The sum runs over flavour configurations, f, and number of intermediate particles, n. Including momentum-conserving delta functions we have,

$$A_{i\to f} - A^\star_{f\to i} = i \sum_{f,n} \int \prod_{i=1}^{n} \frac{d^d q_i}{(2\pi)^d} \delta^{(+)}(q_i^2) A_{i\to\{q_i\}} A^\star_{f\to\{q_i\}}. \tag{3.34}$$

The left-hand side will only be non-zero if the amplitude has a branch cut. In analogue with the observations following (3.32) we see that branch cuts are absent in tree-level amplitudes. At loop level however, discontinuities appear from logarithms.

The discontinuities of loop diagrams and integrals can be calculated using Cutkosky rules [5, 52]. Putting intermediate states on-shell is known as *cutting* and is achieved by replacing propagators,

$$\frac{1}{k^2 - m^2 + i\delta} \to -2\pi i \delta^{(+)}(k^2 - m^2). \tag{3.35}$$

The calculation of the physical discontinuity of a loop diagram follows three steps

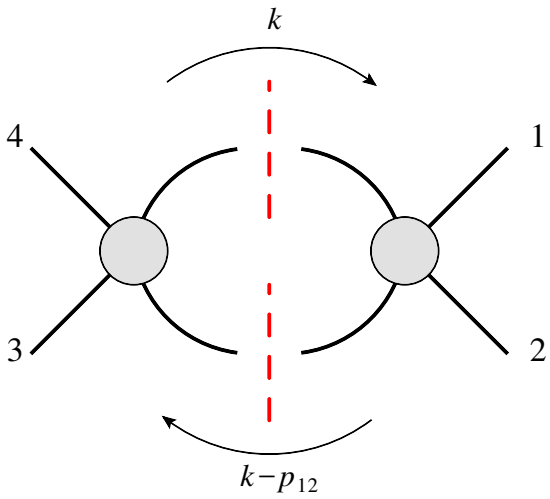

Figure 3.1 *Unitarity cut of a one-loop four-point amplitude. External momenta are outgoing. Grey blobs denote tree-level amplitudes.*

constituting the Cutkosky rules. First step is to systematically apply all cuts that can be satisfied simultaneously, followed by an integration over the remaining degrees of freedom. Finally, summing over the contributions from all the cuts gives the discontinuity. These rules can be used to prove (3.34) order by order in perturbation theory.

Turning to amplitudes, the discontinuity in the s_{12}-channel of the four-point one-loop amplitude can be calculated using,

$$\begin{aligned}\text{Disc}_{s_{12}} A_4^{(1)} = (-2\pi i)^2 i \sum_f \int \frac{d^d k}{(2\pi)^d}\, \delta^{(+)}\left(k^2 - m_1^2\right) \delta^{(+)}\left((k-p_{12})^2 - m_2^2\right) \\ \times A_4^{(0)}(-k, p_1, p_2, k-p_{12}) A_4^{(0)}(-k+p_{12}, p_3, p_4, k),\end{aligned} \tag{3.36}$$

where all momenta are considered to be outgoing. This cut is illustrated in Figure 3.1. In QCD the sum over flavours, f, will be over quarks and gluons as well as their helicity states. Comparing the discontinuities of the amplitude to those of the parametrisation of the amplitude in terms of scalar integrals (3.17), we obtain a system of equations for determining the coefficients.

3.3.1 Generalised unitarity

A weakness of the unitarity method is the complication in disentangling the information when a branch cut is shared by several integrals. In the previous

section we saw an example of a double cut (3.36) where the momenta of the intermediate states are real. In section 2.2.4 the power of working with complex momenta in intermediate states in the context of BCFW was demonstrated. If we allow the cut momenta to take complex values, we can perform more general cuts than the double cut discussed above. These cuts are known as generalised unitarity cuts [47, 53, 54]. The real delta function in (3.35) does not allow complex solutions so we reinterpret the cut as an integral contour deformation. Performing cuts we pick up the residues of the amplitude. Cutting m internal states we get,

$$\mathrm{Cut}_{i_1\dots i_m} A_n^{(1)} = \sum_f \int \frac{d^d k}{(2\pi)^d} \prod_{j=1}^{m} (-2\pi i)\delta(l_{i_j}^2) A^{(0)}(-l_{i_j}, i_j, \dots, i_{j+1}-1, l_{i_{j+1}}), \tag{3.37}$$

where we ignore masses and $l_{i_j} = k - p_{i_j(i_{j+1}-1)} = k - \sum_{l=i_j}^{i_{j+1}-1} p_l$. The indices should be considered cyclic such that $i_{m+1} = i_1$. Using generalised unitarity cuts we can systematically disentangle and extract the contributions from each integral topology. This procedure is most easily shown through an example calculation. The algorithm used in the following is commonly known as OPP after the authors of [47]. We demonstrate the application to a four-point one-loop amplitude.

Quadruple cut

In the context of the four-point amplitude in four dimensions the maximal cut we can perform is quadruple. This quadruple cut is illustrated in Figure 3.2. On this cut the amplitude factorises into four three-point tree-level amplitudes,

$$\begin{aligned} \mathrm{Cut}_{1234} A_4^{(1)} = \sum_f \int \frac{d^4 k}{(2\pi)^4} & (-2\pi i)\delta(l_1^2) A_3^{(0)}(-l_1, 1, l_2) \\ & \times (-2\pi i)\delta(l_2^2) A_3^{(0)}(-l_2, 2, l_3) \\ & \times (-2\pi i)\delta(l_3^2) A_3^{(0)}(-l_3, 3, l_4) \\ & \times (-2\pi i)\delta(l_4^2) A_3^{(0)}(-l_4, 4, l_1). \end{aligned} \tag{3.38}$$

Only one box integral in (3.17) has this singularity and its coefficient can therefore be extracted directly. For intermediate states in four dimensions we choose the

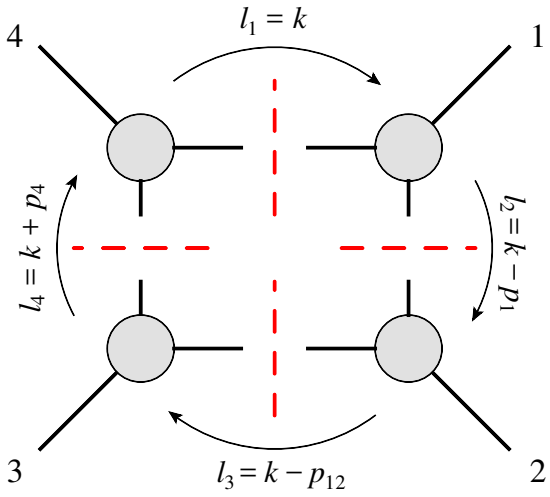

Figure 3.2 *Quadruple cut of a one-loop four-point amplitude. External momenta are outgoing. Grey blobs denote tree-level amplitudes.*

following parametrisation of the loop momentum,

$$\begin{aligned} k^\mu &= \vec{\chi} \cdot \vec{v}^\mu = (\chi_1, \chi_2, \chi_3, \chi_4) \cdot \vec{v}^\mu \\ &= \chi_1 p_1^\mu + \chi_2 p_2^\mu + \chi_3 \frac{\langle 1|\sigma^\mu|2]}{2} + \chi_4 \frac{\langle 2|\sigma^\mu|1]}{2}, \end{aligned} \tag{3.39}$$

and solve the cut constraints. A quadruple cut in four dimensions gives four constraints and therefore localises the internal momentum completely. We get two solutions, a and b, for the parameters,

$$\vec{\chi}_a = \left(1, 0, -\tfrac{[41]}{[42]}, 0\right), \qquad \vec{\chi}_b = \left(1, 0, 0, -\tfrac{\langle 14\rangle}{\langle 24\rangle}\right). \tag{3.40}$$

Applying this cut to the integrand parametrisation in (3.19) we pick out the box numerator, Δ_{1234}. The pentagon is absent in this four-point amplitude and topologies without all four cut propagators are set to zero. Working in four dimensions the numerator parametrisation, (3.26), reduces to,

$$\Delta_{1234} = c_{1234}^{(0)} + c_{1234}^{(1)} k \cdot \omega, \tag{3.41}$$

and evaluating on the two cut solutions yields,

$$\Delta_{1234}|_a = c_{1234}^{(0)} + c_{1234}^{(1)} i s_{12} s_{23}, \tag{3.42a}$$

$$\Delta_{1234}|_b = c_{1234}^{(0)} - c_{1234}^{(1)} i s_{12} s_{23}. \tag{3.42b}$$

So far we have not specified the theory we are working in, except for the

requirement of renormalisability. In this thesis massless QCD is the obvious choice, allowing gluons and fermions to run in the loop. In both cases we need to sum over the helicities of the internal states and we choose the non-adjacent MHV configuration for the external states, $1^-, 2^+, 3^-, 4^+$. For the gluon loop in four dimensions we need four three-point amplitudes from (2.60a) and get,

$$\begin{aligned}
\text{Cut}\left(\quad\right)\Big|_a &= i^4 \sum_{h_i=\pm} A_3^{(0)}(-l_1^{-h_1}, 1^-, l_2^{h_2}) A_3^{(0)}(-l_2^{-h_2}, 2^+, l_3^{h_3}) \\
&\qquad \times A_3^{(0)}(-l_3^{-h_3}, 3^-, l_4^{h_4}) A_3^{(0)}(-l_4^{-h_4}, 4^+, l_1^{h_1}) \\
&= \frac{[l_2 l_1]^3}{[1 l_2][1 l_1]} \frac{\langle l_3 l_2\rangle^3}{\langle 2 l_3\rangle\langle 2 l_2\rangle} \frac{[l_4 l_3]^3}{[3 l_4][3 l_3]} \frac{\langle l_1 l_4\rangle^3}{\langle 4 l_1\rangle\langle 4 l_4\rangle} \\
&= \frac{\langle k|421|k]^3}{\langle 2|k|1]\langle 4|k|1]\langle 2|(k-p_1)|3]\langle 4|k|3]} \\
&= -s_{12} s_{23} A^{(0)}(1^-, 2^+, 3^-, 4^+), \qquad (3.43a)
\end{aligned}$$

$$\text{Cut}\left(\quad\right)\Big|_b = -\frac{s_{12}^5 s_{23} + s_{12} s_{23}^5}{(s_{12}+s_{23})^4} A^{(0)}(1^-, 2^+, 3^-, 4^+), \qquad (3.43b)$$

where the left-hand side subscript refers to the cut solution. In this notation we omit factors of 2π and any other factors from the integral measures as they will appear on both sides of the equation when comparing the cut to the integrand parametrisation (3.19). Equating the numerator parametrisations (3.42) to the cuts (3.43), we obtain the coefficients,

$$c_{1234}^{(0)} = i \frac{s_{12} s_{23} (s_{12}^2 + s_{12} s_{23} + s_{23}^2)^2}{(s_{12}+s_{23})^4} A^{(0)}(1^-, 2^+, 3^-, 4^+), \qquad (3.44)$$

$$c_{1234}^{(1)} = -4 \frac{s_{12} s_{23} (2 s_{12}^2 + 3 s_{12} s_{23} + 2 s_{23}^2)}{(s_{12}+s_{23})^4} A^{(0)}(1^-, 2^+, 3^-, 4^+). \qquad (3.45)$$

For the fermion loop we use the three-point amplitudes in (2.60b) and obtain,

$$c_{1234}^{(0),\text{fermion}} = \frac{1}{2} \frac{s_{12}^2 s_{23}^2 (s_{12}^2 + s_{23}^2)}{(s_{12}+s_{23})^4} A^{(0)}(1^-, 2^+, 3^-, 4^+) = -c_{1234}^{(1),\text{fermion}}. \qquad (3.46)$$

For the rest of this example we will ignore the fermion loop.

Triple cut

At this point we know all relevant box coefficients (in this case one) of the one-loop amplitude parametrisation in four dimensions (3.17). The algorithm proceeds by

determining the triangle coefficients using triple cuts. We have four topologies,

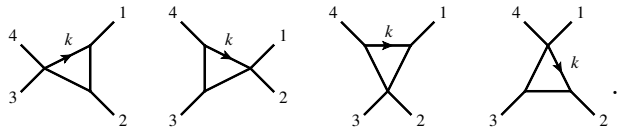

Δ_{123} Δ_{134} Δ_{124} Δ_{234} .

Focusing on the topology associated with numerator Δ_{123} and using the momentum parametrisation (3.39) the cut solutions are,

$$\vec{\chi}_a = (1, 0, \tau, 0)\,, \qquad \vec{\chi}_b = (1, 0, 0, \tau)\,, \tag{3.47}$$

where τ is a free parameter. The corresponding cuts are,

$$\begin{aligned}\text{Cut}\left(\raisebox{-0.5em}{  }\right)\Big|_a &= i^3 \sum_{h_i=\pm} A_3^{(0)}(-k^{-h_3}, 1^-, k_1^{h_1}) A_3^{(0)}(-k_1^{-h_1}, 2^+, k_2^{h_2}) \\ &\qquad \times A_4^{(0)}(-k_2^{-h_2}, 3^-, 4^+, k^{h_3}) \\ &= \frac{i s_{12}}{1+\tau s_{12}} A^{(0)}(1^-, 2^+, 3^-, 4^+), \end{aligned} \tag{3.48a}$$

$$\text{Cut}\left(\raisebox{-0.5em}{  }\right)\Big|_b = \frac{i s_{23}}{2 s_{12}^2} \frac{2\tau^4 - 4\tau^3 s_{12} + 12\tau^2 s_{12}^2 - 16\tau s_{12}^3 + 8 s_{12}^4}{\tau s_{12} + \tau s_{23} - 2 s_{12} s_{23}} A^{(0)}(1^-, 2^+, 3^-, 4^+) \tag{3.48b}$$

In the four-dimensional limit the integrand basis (3.27) is,

$$\begin{aligned}\Delta_{123} = {} & c_{123}^{(0)} + c_{123}^{(1)}\; k\cdot\omega_1 + c_{123}^{(2)}\; k\cdot\omega_2 + c_{123}^{(3)}\;\; k\cdot\omega_1\; k\cdot\omega_2 \\ & + c_{123}^{(4)}\; [(k\cdot\omega_1)^2 - (k\cdot\omega_2)^2] + c_{123}^{(5)}\; (k\cdot\omega_1)^2\; k\cdot\omega_2 + c_{123}^{(6)}\; k\cdot\omega_1\; (k\cdot\omega_2)^2, \end{aligned} \tag{3.49}$$

and we use the two massless legs to construct the spurious directions,

$$\omega_1^\mu = \frac{\langle 1|\sigma^\mu|2]}{\langle 132]} + \frac{\langle 2|\sigma^\mu|1]}{\langle 231]}, \tag{3.50a}$$

$$\omega_2^\mu = i\left(\frac{\langle 1|\sigma^\mu|2]}{\langle 132]} - \frac{\langle 2|\sigma^\mu|1]}{\langle 231]}\right). \tag{3.50b}$$

The four-point tree amplitude entering the cut has a pole in the free parameter, τ. In order to isolate the triangle numerator coefficients we cancel this pole by subtracting the contribution from the quadruple cut,

$$\Delta_{123}|_a = \left(\text{Cut}\left(\raisebox{-0.5em}{  }\right) - \frac{\Delta_{1234}}{(k-p_{123})^2}\right)\Big|_a, \tag{3.51}$$

and similarly for the second cut solution, b. Knowing the spurious box coefficient is necessary to achieve this cancellation. We obtain the coefficients by numerically sampling over several values of the free parameter, τ,

$$c_{123}^{(0)} = \frac{is_{12}^2 s_{23}(2s_{12}^2 + 3s_{12}s_{23} + 2s_{23}^2)}{(s_{12}+s_{23})^4} A^{(0)}(1^-, 2^+, 3^-, 4^+), \tag{3.52a}$$

$$c_{123}^{(1)} = -\frac{is_{23}^2(3s_{12}^2 + 4s_{12}s_{23} + 2s_{23}^2)}{(s_{12}+s_{23})^3} A^{(0)}(1^-, 2^+, 3^-, 4^+), \tag{3.52b}$$

$$c_{123}^{(2)} = -\frac{s_{23}^2(3s_{12}^2 + 4s_{12}s_{23} + 2s_{23}^2)}{(s_{12}+s_{23})^3} A^{(0)}(1^-, 2^+, 3^-, 4^+), \tag{3.52c}$$

$$c_{123}^{(3)} = \frac{s_{23}^3(2s_{12} + s_{23})}{s_{12}(s_{12}+s_{23})^2} A^{(0)}(1^-, 2^+, 3^-, 4^+), \tag{3.52d}$$

$$c_{123}^{(4)} = \frac{is_{23}^3(2s_{12} + s_{23})}{2s_{12}(s_{12}+s_{23})^2} A^{(0)}(1^-, 2^+, 3^-, 4^+), \tag{3.52e}$$

$$c_{123}^{(5)} = -\frac{s_{23}^4}{s_{12}^2(s_{12}+s_{23})} A^{(0)}(1^-, 2^+, 3^-, 4^+), \tag{3.52f}$$

$$c_{123}^{(6)} = \frac{is_{23}^4}{s_{12}^2(s_{12}+s_{23})} A^{(0)}(1^-, 2^+, 3^-, 4^+). \tag{3.52g}$$

For the remainder of the reduction we will only write the non-spurious terms explicitly. The relevant coefficients for the three remaining triangle topologies are,

$$c_{124}^{(0)} = \frac{is_{12}s_{23}^2(2s_{12}^2 + 3s_{12}s_{23} + 2s_{23}^2)}{(s_{12}+s_{23})^4} A^{(0)}(1^-, 2^+, 3^-, 4^+), \tag{3.53}$$

$$c_{134}^{(0)} = c_{123}^{(0)}, \tag{3.54}$$

$$c_{234}^{(0)} = c_{124}^{(0)}. \tag{3.55}$$

Double cut

There are two non-vanishing bubble topologies,

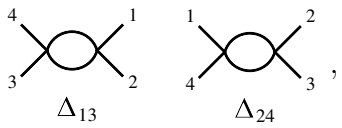

with only one cut solution each. In the case of Δ_{13} the subtraction of higher-lying topologies is performed as follows,

$$\Delta_{13}|_{\text{cut}} = \Bigg(\text{Cut}\Bigg($$
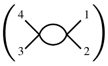
$$\Bigg) - \frac{\Delta_{1234}}{(k-p_1)^2(k-p_{123})^2} - \frac{\Delta_{123}}{(k-p_1)^2} - \frac{\Delta_{134}}{(k-p_{123})^2}\Bigg)\Bigg|_{\text{cut}}, \tag{3.56}$$

and the only non-spurious coefficient in four dimensions in the integrand parametrisation (3.28) is,

$$c_{13}^{(0)} = \frac{i(14s_{12}^2 s_{23} + 19 s_{12} s_{23}^2 + 11 s_{23}^3)}{3(s_{12}+s_{23})^3} A^{(0)}(1^-,2^+,3^-,4^+). \tag{3.57}$$

For the other bubble topology, Δ_{24}, we have,

$$c_{24}^{(0)} = \frac{i(11s_{12}^3 + 19 s_{12}^2 s_{23} + 14 s_{12} s_{23}^2)}{3(s_{12}+s_{23})^3} A^{(0)}(1^-,2^+,3^-,4^+). \tag{3.58}$$

We used the spurious directions,

$$\omega_1 = \frac{\langle 1|\sigma^\mu|2]}{2} + \frac{\langle 2|\sigma^\mu|1]}{2}, \; \omega_2 = i\left(\frac{\langle 1|\sigma^\mu|2]}{2} - \frac{\langle 2|\sigma^\mu|1]}{2}\right), \; \omega_3 = p_1 - p_2, \tag{3.59}$$

for Δ_{13} and a similar construction for Δ_{24}.

This concludes the reduction of the one-loop four-point gluon amplitude in four dimensions.

3.4 Rational terms and d-dimensional cuts

In the previous sections the external particles have been restricted to four dimensions, which is also the spin dimension of the internal particles. This is in accordance with the four-dimensional helicity scheme (FDH) [55, 56]. Using dimensional regularisation, where the loop momentum lives in $d = 4 - 2\epsilon$ dimensions, the numerator acquires dependence on d from contractions of the loop momentum with itself. These contributions to the massless amplitude give rise to the rational term in (3.17), which are overlooked in the four-dimensional treatment. The terms obtained through the four-dimensional integrand reduction are historically known as cut-constructible [54] and several methods have been developed for a subsequent calculation of the rational term, see for example [49, 57–60]. In this section we will demonstrate how to extract the cut-

constructible part as well as the rational terms by using d-dimensional generalised unitarity cuts [33, 48, 49, 61–63].

At this point it is helpful to summarise the different dimensions that appear in our calculations. Using dimensional regularisation, integrals are evaluated in $d = 4 - 2\epsilon$ dimensions. The spin dimension, where polarisation vectors live, is denoted d_s for internal particles and fixed to four for external particles. This leaves us with a choice of two schemes; four-dimensional helicity (FDH) which has $d_s = 4$ and the 't Hooft-Veltman scheme (HV) [64] where $d_s = 4-2\epsilon$. Finally, we need an integer embedding dimension, D, for the particle momenta. To catch the (-2ϵ) contribution we will embed in six dimensions, $D = 6$, for which we introduced a spinor-helicity formalism in section 2.1.2.

In section 3.2.1 we parametrised the numerator in d dimensions. In order to determine the coefficients, we embed the loop momenta in $D = 6$ dimensions and solve the cut conditions and perform the cuts. Revisiting the box cut from the previous section we choose the loop momentum parametrisation,

$$k^M = \chi_1 p_1^\mu + \chi_2 p_2^\mu + \chi_3 \frac{\langle 1|\sigma^\mu|2]}{2} + \chi_4 \frac{\langle 2|\sigma^\mu|1]}{2} + \chi_5 e_5^\perp + \chi_6 e_6^{\bar{\perp}}. \tag{3.60}$$

For the extra dimensions we have chosen light-cone coordinates $e_5^\perp = (0,0,0,0,1,i)$, $e_6^{\bar{\perp}} = (0,0,0,0,1,-i)$, and $e_5^\perp \cdot e_6^{\bar{\perp}} = 2$. At one loop the numerator can only depend on the magnitude and not the direction of the extra-dimensional loop momentum components. Without loss of generality we set $\chi_5 = \frac{\langle 12\rangle[21]}{4}$. We therefore have one free parameter, which we will choose to be $\chi_4 = -\tau\frac{\langle 14\rangle}{\langle 24\rangle}$. This leaves us with a single, rational solution,

$$\vec{\chi} = \left(1, 0, (\tau-1)\frac{[41]}{[42]}, -\tau\frac{\langle 14\rangle}{\langle 24\rangle}, \frac{\langle 12\rangle[21]}{4}, (\tau-1)\frac{\langle 14\rangle[41]}{\langle 24\rangle[42]}\right). \tag{3.61}$$

The four-dimensional limit is taken by solving $\mu_{11} = 0 \Rightarrow \tau = 0, 1$ and the two solutions from (3.40) are obtained. On the cut the amplitude factorises into a product of trees,

$$\begin{aligned}\mathrm{Cut}^{6d}_{1234} = i^4 A_3^{(0)}\left(-k_{x\dot{x}}, 1_{a\dot{a}}, (k-p_1)_{y\dot{y}}\right) A_3^{(0)}\left(-(k-p_1)^{y\dot{y}}, 2_{b\dot{b}}, (k-p_{12})_{z\dot{z}}\right) \\ \times A_3^{(0)}\left(-(k-p_{12})^{z\dot{z}}, 3_{c\dot{c}}, (k+p_4)_{w\dot{w}}\right) A_3^{(0)}\left(-(k+p_4)^{w\dot{w}}, 4_{d\dot{d}}, k^{x\dot{x}}\right).\end{aligned} \tag{3.62}$$

The coefficients in (3.26) for a six-dimensional gluon running in the loop are,

$$c_{1234}^{(0),6d} = \frac{is_{12}s_{23}(s_{12}^4 + 2s_{12}^3 s_{23} + 4s_{12}^2 s_{23}^2 + 2s_{12}s_{23}^3 + s_{23}^4)}{(s_{12}+s_{23})^4} A^{(0)}(1^-, 2^+, 3^-, 4^+), \tag{3.63a}$$

$$c_{1234}^{(1),6d} = -8\frac{s_{12}s_{23}(s_{12}^2 + s_{12}s_{23} + s_{23}^2)}{(s_{12}+s_{23})^4} A^{(0)}(1^-, 2^+, 3^-, 4^+), \tag{3.63b}$$

$$c_{1234}^{(2),6d} = 4i\frac{s_{12}^3 s_{23} + s_{12}s_{23}^3}{(s_{12}+s_{23})^3} A^{(0)}(1^-, 2^+, 3^-, 4^+), \tag{3.63c}$$

$$c_{1234}^{(3),6d} = -16\frac{s_{12}s_{23}}{(s_{12}+s_{23})^3} A^{(0)}(1^-, 2^+, 3^-, 4^+), \tag{3.63d}$$

$$c_{1234}^{(4),6d} = 4\frac{is_{12}s_{23}}{(s_{12}+s_{23})^2} A^{(0)}(1^-, 2^+, 3^-, 4^+). \tag{3.63e}$$

Even without the extra-dimensional contributions, $c_{1234}^{(2),6d}, c_{1234}^{(3),6d}, c_{1234}^{(4),6d}$, this result does not match the coefficients in four dimensions (3.45). This is due to the additional internal helicity states summed over in (3.62). Our goal in the following is to perform a state-sum reduction in order to match the four-dimensional result. In particular, we will derive a formula for obtaining coefficients with explicit spin dimension dependence.

At one loop, a coefficient can at most be linear in the spin dimension, d_s,

$$c^{(d_s)} = a + d_s b, \tag{3.64}$$

since the dependence stems from contraction of the metric tensor around the loop, $\eta^\mu{}_\mu = d_s$. The coefficients a and b are rational functions of the external kinematics and are independent of d_s. We can project them out by calculating the coefficients for two different values of d_s. If we choose $d_s = D, D+1$ (3.64) becomes,

$$c^{(d_s)} = \left((D+1)c^{(D)} - Dc^{(D+1)}\right) + d_s\left(c^{(D+1)} - c^{(D)}\right). \tag{3.65}$$

In calculating both $c^{(D)}$ and $c^{(D+1)}$ we can set the embedding dimension to D. The difference is then only the additional polarisation state in $c^{(D+1)}$, $\epsilon^\perp$, which is perpendicular to all other momentum vectors. Hence, it only contributes through contractions with itself. Consider the three-gluon vertex Feynman rule in Figure 1.1. Contracted with two gluons, 1 and 2, with polarisation $\epsilon^\perp$, only

one term can survive,

$$\frac{ig}{\sqrt{2}}(p_1 - p_2)^\rho \epsilon^\perp \cdot \epsilon^\perp. \tag{3.66}$$

Up to the normalisation of $\epsilon^\perp$ this is just the Feynman rule for a scalar-scalar-gluon vertex. There are no other contributions involving the additional polarisation state. Hence the difference between $c^{(D)}$ and $c^{(D+1)}$ is that of a scalar loop,

$$c^{(D+1)} = c^{(D)} + c^{\text{scalar}}. \tag{3.67}$$

Putting this back into (3.65) yields,

$$c^{(d_s)} = c^{(D)} + (d_s - D)c^{\text{scalar}}. \tag{3.68}$$

We therefore need to calculate the coefficients, c^{scalar}, where the internal gluon loop is replaced by a scalar loop. After state-sum reduction we obtain,

$$c_{1234}^{(0),d_s} = \left(c_{1234}^{(0),4d} + i\frac{d_s - 4}{2}\frac{s_{12}^3 s_{23}^3}{(s_{12}+s_{23})^4}\right) A^{(0)}(1^-, 2^+, 3^-, 4^+), \tag{3.69a}$$

$$c_{1234}^{(1),d_s} = \left(c_{1234}^{(1),4d} + \frac{d_s - 4}{2}\frac{4s_{12}^2 s_{23}^2}{(s_{12}+s_{23})^4}\right) A^{(0)}(1^-, 2^+, 3^-, 4^+), \tag{3.69b}$$

$$c_{1234}^{(2),d_s} = \left(c_{1234}^{(2),6d} - id_s\frac{2s_{12}^2 s_{23}^2}{(s_{12}+s_{23})^3}\right) A^{(0)}(1^-, 2^+, 3^-, 4^+), \tag{3.69c}$$

$$c_{1234}^{(3),d_s} = -4\,(d_s - 2)\,\frac{s_{12}s_{23}}{(s_{12}+s_{23})^3} A^{(0)}(1^-, 2^+, 3^-, 4^+), \tag{3.69d}$$

$$c_{1234}^{(4),d_s} = i\,(d_s - 2)\,\frac{s_{12}s_{23}}{(s_{12}+s_{23})^2} A^{(0)}(1^-, 2^+, 3^-, 4^+). \tag{3.69e}$$

With the explicit d_s dependence we can now choose between the FDH and the HV schemes mentioned earlier.

Finally, we need to evaluate the additional integrals appearing in d dimensions. The μ_{11}-dependent monomials of the integrand parametrisation can be evaluated in terms of scalar integrals of higher dimension [61–63]. Using the integral definition (3.18), we have,

$$I_n^{(4-2\epsilon)}[\mu_{11}^r] = -\epsilon(1-\epsilon)\cdots(r-1-\epsilon)(4\pi)^r I_n^{(4-2\epsilon+2r)}[1], \tag{3.70}$$

and the integrals evaluate to,

$$I_5^{(4-2\epsilon)}[\mu_{11}] = -\epsilon 4\pi I_5^{(6-2\epsilon)}[1] = \mathcal{O}(\epsilon), \tag{3.71a}$$

$$I_4^{(4-2\epsilon)}[\mu_{11}] = \mathcal{O}(\epsilon), \tag{3.71b}$$

$$I_4^{(4-2\epsilon)}[\mu_{11}^2] = \frac{-i}{(4\pi)^2}\frac{1}{6} + \mathcal{O}(\epsilon), \tag{3.71c}$$

$$I_3^{(4-2\epsilon)}[\mu_{11}] = \frac{i}{(4\pi)^2}\frac{1}{2} + \mathcal{O}(\epsilon), \tag{3.71d}$$

$$I_2^{(4-2\epsilon)}[\mu_{11}] = \frac{-i}{(4\pi)^2}\frac{1}{6}\left(p^2 - 3(m_1^2 + m_2^2)\right) + \mathcal{O}(\epsilon), \tag{3.71e}$$

where the momentum, p, is flowing through the bubble and the masses of the propagators are m_1, m_2. These integrals give rise to the rational term in (3.17),

$$\mathcal{R}_n = \frac{-i}{(4\pi)^2}\left(\frac{1}{6}\sum_{1\leq i<j<k<l}^{n} c_{ijkl}^{(4)} - \frac{1}{2}\sum_{1\leq i<j<k}^{n} c_{ijk}^{(9)} + \frac{1}{6}\sum_{1\leq i<j}^{n} c_{ij}^{(9)}\left(p_{i(j-1)}^2 - 3(m_1^2 + m_2^2)\right)\right). \tag{3.72}$$

3.5 Summary

In this chapter we have demonstrated the use of modern on-shell techniques at the one-loop level. We started with the reduction of integrals and integrands into the parametrisations in equation (3.17) and (3.19). Integration of the integrand parametrisations from section 3.2 using the d-dimensional pentagon (3.15) and the extra-dimensional integrals in (3.71) show the equivalence of these parametrisations.

The rational terms were overlooked in the four-dimensional integrand reduction via generalised unitarity cuts in section 3.3.1. Using this method we calculated the *cut-constructible* part of the one-loop four-gluon amplitude. Direct extraction of the rational terms was achieved in section 3.4 using d-dimensional generalised unitarity.

Using state-sum reduction, equation (3.68), we were able to reconstruct the explicit dependence on the spin dimension of the internal particles, d_s, in the integrand coefficients. In the remaining chapters we will continue to use d-dimensional generalised unitarity and state-sum reduction in the calculation of loop amplitudes.

Chapter 4

Unitarity at one loop with massive fermions

Precise predictions for the production of strongly interacting massive particles are in high demand for current experimental analyses at the LHC. The current precision level of predictions is in relatively good shape, with top quark pair production now known differentially at NNLO in QCD [65, 66] and a full range of off-shell decays known at NLO in QCD with an additional jet [67]. Modern one-loop techniques are also able to explore high multiplicity final states where the current state-of-the-art is top quark pair production in association with three jets [68]. The GoSam collaboration has also been able to produce NLO predictions for the challenging $t\bar{t}H + j$ final state [69]. A more complete overview of the current status can be found in reference [70].

On the other hand, these processes are often overlooked by more formal studies of amplitudes in gauge theory which can uncover hidden simplicity and structure. While it is well known that on-shell techniques like unitarity [61], spinor integration [71, 72] and BCFW recursion apply equally well to massive amplitudes, explicit computations are relatively few [73–75]. Nevertheless some computations using these approaches have produced compact analytic results useful for phenomenological applications [74, 76]. While elements of these computations use unitarity cuts and on-shell trees, Feynman diagram techniques were also employed to compute the UV counterterms necessary for mass and wavefunction renormalisation. To the best of our knowledge the only computations not to do this are those with a massive internal loop where a UV

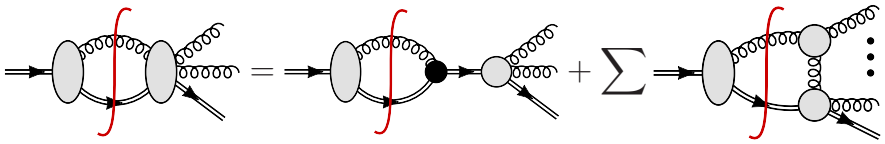

Figure 4.1 *Decomposing the tree amplitude appearing on the left hand side of a wavefunction cut reveals a divergent graph.*

matching prescription was used [61, 73].

The obstacle is that the traditional approach to renormalisation requires the amputation of wavefunction graphs, and the addition of counterterm diagrams. This procedure breaks gauge invariance during intermediate steps and therefore causes problems for methods based on (generalised) unitarity [50, 51, 53], which construct amplitudes from on-shell tree-level building blocks. Naive attempts to amputate wavefunction graphs in generalised unitarity are precluded by the presence of an on-shell propagator, leading to a factor $1/0$: this is depicted explicitly in Figure 4.1, where the on-shell tree amplitude appearing on the right hand side of a two-particle cut is expanded to reveal a divergent propagator inside. Consequently, the favoured method is still to follow an approach based on Feynman diagrams; then the amputation of wavefunction graphs is straightforward.

Two solutions to this problem have been proposed. Ellis, Giele, Kunszt and Melnikov showed that modifying the tree-level input entering the double cuts of the wavefunction graphs allowed a simple implementation of the on-shell renormalisation scheme [77]. All cuts can then be performed but gauge invariance is only restored at the end of the computation. Since the removal of the unwanted graphs is extremely easy to implement within a Berends-Giele construction of the tree-level amplitudes in the cuts this method is quite efficient numerically. A second solution, proposed by Britto and Mirabella [78], is to regulate the divergent tree by introducing a momentum shift. This procedure allows us to preserve gauge invariance but introduces an additional variable into the calculation which will cancel when combined with the mass-renormalisation counterterms. In either case a set of extra two- and single-particle cuts is necessary together with the counterterms to fully determine the amplitude in comparison to the massless case.

Despite both of these solutions there is still an open question: is it possible to compute amplitudes with masses using only on-shell gauge invariant building

blocks and without introducing additional regulators? Both of the approaches mentioned above follow the on-shell renormalisation scheme where divergences can be absorbed into additional terms in the Lagrangian. In this chapter we will seek an alternative way to absorb the divergences by appealing to an effective six dimensional version of QCD.

This procedure relies on first computing a full set of finite d-dimensional unitarity cuts. We show how this can be done efficiently in the six-dimensional spinor-helicity formalism [27] by embedding the additional mass into the higher dimensions and performing cuts in six dimensions. In particular we show how these results can be dimensionally reduced to d-dimensional amplitudes keeping the spin dimension of the gluon d_s arbitrary. This generalises the previous approaches used for massless cuts in six dimensions [30, 33] that were discussed in the previous chapter.

The work in this chapter was also presented in [1]. In section 4.1 we review the spinor-helicity formalisms in four and six dimensions, and show how Dirac spinors for massive fermions can be represented as massless Weyl spinors in six dimensions. We then discuss a simple example of a pair of massive fermions coupling to an off-shell vertex at one-loop. This example allows us to show how computations in six dimensions can be performed, and how they can be dimensionally reduced to results with an arbitrary spin dimension d_s. In section 4.2 we explain some of the key features needed to apply the generalised unitarity method in six dimensions to $gg \to t\bar{t}$ scattering. Section 4.2.1 describes the procedure of fixing the remaining ambiguities using the universal epsilon pole structure in $d = 4 - 2\epsilon$ dimensions and the corresponding epsilon pole structure of the effective theory in $6 - 2\epsilon$ dimensions.

4.1 Massive fermions

In this section we describe how we can use massless six-dimensional momenta to obtain amplitudes in four dimensions with massive particles. Before getting started, we briefly review how massive fermions can be incorporated within the four-dimensional spinor-helicity formalism commonly used for massless amplitudes, see section 2.1. We follow the notation used previously in reference [75] while the formalism itself was established long before that, see for example [79–83].

Starting from a massive 4-momentum, p, with $p^2 = m^2$, we can define a massless projection with respect to a light-like reference vector η,

$$p^\flat = p - \frac{m^2}{2p \cdot \eta}\eta, \tag{4.1}$$

such that $(p^\flat)^2 = 0$. A complete set of solutions of the Dirac equation for the massive momentum p can then be constructed from the Weyl spinors of $p^\flat$ and η,

$$\begin{aligned} \bar{u}_+(p,m) &= \frac{\langle \eta | (\not{p} + m)}{\langle \eta p^\flat \rangle}, & \bar{u}_-(p,m) &= \frac{[\eta | (\not{p} + m)}{[\eta p^\flat]}, \\ v_+(p,m) &= \frac{(\not{p} - m)|\eta\rangle}{\langle p^\flat \eta \rangle}, & v_-(p,m) &= \frac{(\not{p} - m)|\eta]}{[p^\flat \eta]}. \end{aligned} \tag{4.2}$$

These Dirac spinors maintain several of the simplifications which are familiar in the massless case. The tree-level helicity amplitudes for $gg \to t\bar{t}$ scattering, for example, take the relatively simple forms,

$$-i\langle \eta_1 1^\flat \rangle \langle \eta_4 4^\flat \rangle A^{(0)}(1_t^+, 2^+, 3^+, 4_{\bar{t}}^+) = -\frac{m_t^3 s_{23} \langle \eta_1 \eta_4 \rangle}{2p_1 \cdot p_2 \langle 23 \rangle^2}, \tag{4.3}$$

$$-i\langle \eta_1 1^\flat \rangle \langle \eta_4 4^\flat \rangle A^{(0)}(1_t^+, 2^+, 3^-, 4_{\bar{t}}^+) = \frac{m_t \langle \eta_1 3 \rangle \langle \eta_4 3 \rangle \langle 3|1|2]}{2p_1 \cdot p_2 \langle 23 \rangle} + \frac{m_t \langle \eta_1 \eta_4 \rangle \langle 3|1|2]^2}{2p_1 \cdot p_2 s_{23}}. \tag{4.4}$$

We will now show that these results can be rewritten in terms of amplitudes of massless fermions in six dimensions.

4.1.1 Massive fermions from massless six-dimensional spinors

In this section we will use the six-dimensional spinor-helicity formalism [27] introduced in section 2.1.2 to find representations of four-dimensional massive fermion wavefunctions and amplitudes. We begin our discussion by looking at a free massive fermion field in four dimensions,

$$\mathcal{L}^{4d} = \overline{\psi}(x)(i\gamma^\mu \partial_\mu - m)\psi(x). \tag{4.5}$$

For the spinors associated with external fermions we seek solutions to the massive Dirac equation,

$$(\gamma \cdot \bar{p} - m)u_s(\bar{p}) = 0 \text{ and } \bar{u}_s(\bar{p})(\gamma \cdot \bar{p} - m) = 0, \tag{4.6}$$

where the bar on the momentum, $\bar{p}$, denotes a vector in four dimensions.

Alternatively, we can consider a massless fermion field in six dimensions with the Lagrangian,

$$\mathcal{L}^{6d} = \overline{\Psi}(x)(i\Gamma^M \partial_M)\Psi(x). \tag{4.7}$$

Note that for six dimensions we use capital Greek letters and M runs from 0 to 5. In six space-time dimensions the Dirac matrices are 8×8 objects, which we choose to be,

$$\Gamma^M = \begin{pmatrix} 0 & \tilde{\Sigma}^M \\ \Sigma^M & 0 \end{pmatrix}, \tag{4.8}$$

Our representation of the Σ-matrices (A.4) is simply related to the four-dimensional γ-matrices. The relation for the first four Σ-matrices is,

$$-\tilde{\Sigma}^{5,AX}\Sigma^{\mu}_{XB} = (\gamma^{\mu})^{A}{}_{B} = \tilde{\Sigma}^{\mu,AX}\Sigma^{5}_{XB}, \tag{4.9}$$

where we used the Clifford algebra for the last equality. For the remaining two Σ-matrices we have,

$$-\tilde{\Sigma}^{5,AX}\Sigma^{4}_{XB} = (-\gamma^0\gamma^1\gamma^2\gamma^3)^{A}{}_{B} = i(\gamma^5)^{A}{}_{B}, \tag{4.10a}$$

$$-\tilde{\Sigma}^{5,AX}\Sigma^{5}_{XB} = \mathbf{1}^{A}{}_{B}. \tag{4.10b}$$

There is no six-dimensional mass term and in our Weyl basis for the Γ matrices (4.8) we can decompose $\Psi = (\Psi_1, \Psi_2)$. We see that the two fields decouple,

$$\mathcal{L}^{6d} = \overline{\Psi}_1(x)(i\Sigma^M \partial_M)\Psi_1(x) + \overline{\Psi}_2(x)(i\tilde{\Sigma}^M \partial_M)\Psi_2(x). \tag{4.11}$$

Hence the two Ψ_i are essentially copies of each other. Their Dirac equations in momentum space read,

$$(\Sigma \cdot p)_{AB}\lambda^{B}_{a}(p) = 0, \tag{4.12a}$$

$$(\tilde{\Sigma} \cdot p)^{AB}\tilde{\lambda}_{B\dot{a}}(p) = 0. \tag{4.12b}$$

We embed the massive four-dimensional momentum, $\bar{p}$, into a six-dimensional massless momentum by declaring,

$$p = (\bar{p}, 0, m), \text{ so } p^2 = \bar{p}^2 - m^2 = 0. \tag{4.13}$$

Having made this choice, it is consistent to relate the chiral spinor, λ, to the anti-chiral spinor, $\tilde{\lambda}$, by defining,

$$\lambda^A = i\tilde{\Sigma}^{4,AB}\tilde{\lambda}_B. \tag{4.14}$$

It is straightforward to verify that this is a solution to the Dirac equation by inserting equation (4.14) into (4.12a) and using the Clifford algebra,

$$\begin{aligned} 0 &= (\Sigma \cdot p)_{AB}\lambda_a^B(p) \\ &= i(\Sigma \cdot p)_{AB}\tilde{\Sigma}^{4,BC}\tilde{\lambda}_C \\ &= -i\Sigma^4_{AB}(\tilde{\Sigma} \cdot p)^{BC}\tilde{\lambda}_C \\ \Rightarrow 0 &= (\tilde{\Sigma} \cdot p)^{BC}\tilde{\lambda}_C. \end{aligned} \tag{4.15}$$

Having embedded our massive four-dimensional momentum into six dimensions, it is instructive to understand in detail how massless six-dimensional spinors relate to the usual massive four-dimensional Dirac spinors. We begin by writing the massless six-dimensional Dirac equation (4.12a) in detail as,

$$(\Sigma \cdot p)_{AB}\lambda_a^B(p) = \left(\Sigma^\mu p_\mu - \Sigma^5 p^{(5)}\right)_{AB}\lambda_a^B(p) = 0. \tag{4.16}$$

Multiplying from the left by $-\tilde{\Sigma}^{5,XA}$ we obtain,

$$(\gamma \cdot \bar{p} - p_1^{(5)})^X_{\ B}\lambda^B(p) = 0. \tag{4.17}$$

Notice how the sign in the sixth component of the momentum determines whether $\lambda(p)$ should be associated with the four-dimensional spinor for a fermion, $u(p)$, or an anti-fermion, $v(p)$,

$$\lambda(p) = \begin{cases} u(\bar{p}) & , \ p^{(5)} = m \\ v(\bar{p}) & , \ p^{(5)} = -m \end{cases}. \tag{4.18}$$

A similar calculation shows how to identify massless six-dimensional spinors with

the conjugate four-dimensional Dirac spinors,

$$\begin{aligned} 0 &= \lambda^A(p)(\Sigma^\mu p_\mu - \Sigma^5 p^{(5)})_{AB} \\ &= \lambda^A(p)(-\Sigma^5\tilde{\Sigma}^5)_A{}^X(\Sigma^\mu p_\mu - \Sigma^5 p^{(5)})_{XB} \\ &= \lambda^A(p)\Sigma^5_{AX}(\gamma\cdot\bar{p} - p^{(5)})^X{}_B. \end{aligned} \tag{4.19}$$

Again the sixth momentum component determines whether $\lambda(p)\Sigma^5$ should be identified with $\bar{u}(p)$ or $\bar{v}(p)$:

$$\lambda(p)\Sigma^5 = \begin{cases} \bar{u}(\bar{p}) & ,\ p^{(5)} = m \\ \bar{v}(\bar{p}) & ,\ p^{(5)} = -m \end{cases}. \tag{4.20}$$

In the following, we find it useful to write an explicit representation for $\lambda^A(p)$ that allows us to make a direct connection with the four-dimensional Dirac spinors given in (4.2). We use a massless (in the four-dimensional sense) reference vector η, as introduced in (4.1), with Weyl spinors $\kappa_\alpha(\eta), \tilde{\kappa}^{\dot{\alpha}}(\eta)$ and define the six-dimensional spinors,

$$\lambda^{Aa}(\eta,\bar{p}^\flat) = \begin{pmatrix} 0 & \frac{\tilde{\kappa}^{\dot{\alpha}}(\eta)}{[p^\flat\eta]} \\ \frac{\kappa_\alpha(\eta)}{\langle p^\flat\eta\rangle} & 0 \end{pmatrix},\ \tilde{\lambda}_{A\dot{a}}(\eta,\bar{p}^\flat) = \begin{pmatrix} 0 & \frac{\tilde{\kappa}_{\dot{\alpha}}(\eta)}{[p^\flat\eta]} \\ \frac{\kappa^\alpha(\eta)}{\langle p^\flat\eta\rangle} & 0 \end{pmatrix}. \tag{4.21}$$

Using $(\Sigma\cdot p)_{AB}(\tilde{\Sigma}\cdot p)^{BC} = 0$ we see that the Dirac equation (4.12a) is solved by setting,

$$\lambda^A(p) = (\tilde{\Sigma}\cdot p)^{AB}\tilde{\lambda}_B(\eta,\bar{p}^\flat). \tag{4.22}$$

The anti-chiral case is completely analogous,

$$\tilde{\lambda}_A(p) = (\Sigma\cdot p)_{AB}\lambda^B(\eta,\bar{p}^\flat). \tag{4.23}$$

The discussion following (4.16) showed how these six dimensional spinors solve the massive Dirac equation in four dimensions with the appropriate choice of sign for $p^{(5)}$.

4.1.2 Interactions and state-sum reduction

We introduce interactions by replacing the derivative with the covariant derivative. In six dimensions,

$$\partial_M \to D_M = \partial_M - igA^i_M(x)t^i, \tag{4.24}$$

where $A^i_M(x)$ are the gauge fields and t^i are the generators of the gauge group. We dimensionally reduce the six-dimensional gauge field to four dimensions by treating its last two entries as scalar fields,

$$A_M(x) = A^i_M(x)t^i = (A_\mu(x), \phi_1(x), \phi_2(x)), \tag{4.25}$$

leading to the following interaction terms for Ψ_1 (dropping dependence on position for simplicity),

$$\begin{aligned}\mathcal{L}^{6d}_{\text{int},\Psi_1} &= -ig\overline{\Psi}_1\Sigma^M A_M\Psi_1 \\ &= -ig\overline{\Psi}_1\left(\Sigma^\mu A_\mu - \Sigma^4\phi_1 - \Sigma^5\phi_2\right)\Psi_1 \\ &= -ig\overline{\Psi}_1\Sigma^\mu A_\mu\Psi_1 + g\overline{\Psi}_1\phi_1\Psi_2 - ig\overline{\Psi}_1\phi_2\gamma_5\Psi_2.\end{aligned} \tag{4.26}$$

In the last line, we have used the relation between chiral and anti-chiral spinors (4.14), which for the fields reads $\Psi_1 = i\tilde{\Sigma}^4\Psi_2$. The last two terms give rise to the three-point amplitudes given in (B.4) and (B.5). While the first term resembles the four-dimensional interaction term the two last terms are additional contributions arising from the extra momentum components. For internal lines these contributions correspond to additional gluon polarisation states that should be subtracted to obtain the four-dimensional result. This procedure is known as state-sum reduction. This was already discussed in section 3.4, but is revisited here since our specific frame of reference, (4.13), changes the expression slightly.

The contraction of Lorentz indices over internal propagators leads to explicit dependence on the spin dimension d_s. Working explicitly in six dimensions this dependence will be lost but can be recovered through state-sum reduction, as was shown in section 3.4. The general procedure is described in [33, 49]. Gluons in six dimensions have $6 - 2 = 4$ polarisation states, so for each extra dimension introduced we get an additional state. Each of these states correspond to the contribution from replacing gluons in the loop by a scalar. By subtracting these scalars the number of polarisation states can be reduced to $d_s - 2$. In our set-up,

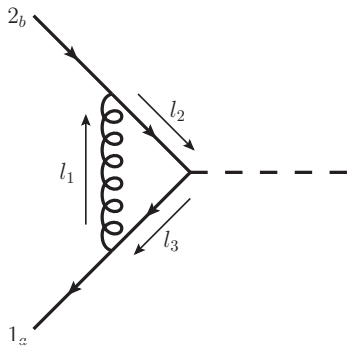

Figure 4.2 *Feynman diagram for one-loop contribution to the coupling between a massive fermion pair and an off-shell scalar. All external momenta are outgoing.*

the scalar associated with the mass direction should be subtracted separately and we arrive at the state-sum reduction prescription,

$$\boldsymbol{c} = \boldsymbol{c}^{6d} - (5 - d_s)\boldsymbol{c}_{\phi_1} - \boldsymbol{c}_{\phi_2}. \tag{4.27}$$

In the massless case $\boldsymbol{c}_{\phi_1} = \boldsymbol{c}_{\phi_2}$ and we recover the expression in (3.68) for embedding dimension $D = 6$.

4.1.3 An example calculation

Let us now illuminate this higher-dimensional formalism with a worked example, the one-loop amplitude for a massive fermion pair coupled to an off-shell scalar, $A^{(1)}$. This calculation involves only one Feynman diagram, Figure 4.2, which is given by,

$$A^{(1),4d} = \int \frac{d^d\ell_1}{(2\pi)^d}\, \bar{u}_1\gamma^\mu \frac{(\gamma\cdot\ell_3 + m)}{\ell_3^2 - m^2}\frac{(\gamma\cdot\ell_2 + m)}{\ell_2^2 - m^2}\gamma^\nu v_2 \frac{\eta_{\mu\nu}}{\ell_1^2} \equiv \int \frac{d^d\ell_1}{(2\pi)^d}\frac{N^{4d}}{D_1 D_2 D_3}, \tag{4.28}$$

where $\ell_2 = \ell_1 - p_2$, $\ell_3 = \ell_1 + p_1$, $D_i = \ell_i^2 - m_i^2$, and N^{4d} is the numerator. We will write the result in terms of the scalar integrals using the notation of [13],

$$\boldsymbol{I} = \left\{ I_3(m^2, s, m^2; 0, m^2, m^2), F_2(s, m^2), I_2(m^2; 0, m^2) \right\}, \tag{4.29}$$

where $F_2(s,m^2) = I_2(s;m^2,m^2) - I_2(m^2;0,m^2)$. The result is $A^{(1),4d} = \boldsymbol{c}^{(d_s)} \cdot \boldsymbol{I} A^{(0),4d}$ where the integral coefficients are given by,

$$\boldsymbol{c}^{(d_s)} = \left\{ -2(s-2m^2), (d_s-4) - \frac{8m^2}{s\beta^2}, d_s \right\}, \tag{4.30}$$

and $\beta^2 = 1 - \frac{4m^2}{s}$ while d_s is the spin dimension.

Using the relation between γ^μ and the Σ- and $\tilde{\Sigma}$-matrices (4.9) we may simplify the numerator by insertion of $\mathbf{1}^A{}_B = -\tilde{\Sigma}^{5,AX}\Sigma^5_{XB}$ in (4.28),

$$\begin{aligned} N^{4d} &= \bar{u}_1\gamma^\mu(\gamma\cdot\bar{\ell}_3 + m)(\gamma\cdot\bar{\ell}_2 + m)\gamma_\mu v_2 \\ &= \bar{u}_1\mathbf{1}\gamma^\mu(\gamma\cdot\bar{\ell}_3 + m)\mathbf{1}(\gamma\cdot\bar{\ell}_2 + m)\mathbf{1}\gamma_\mu v_2 \\ &= -\bar{u}_1\tilde{\Sigma}^5\Sigma^\mu(\tilde{\Sigma}^\nu\bar{\ell}_{3\nu} - \tilde{\Sigma}^5 m)\Sigma^5(\tilde{\Sigma}^\rho\bar{\ell}_{2\rho} - \tilde{\Sigma}^5 m)\Sigma_\mu v_2 \\ &= \lambda_1\Sigma^\mu(\tilde{\Sigma}\cdot\ell_3)\Sigma^5(\tilde{\Sigma}\cdot\ell_2)\Sigma_\mu\lambda_2. \end{aligned} \tag{4.31}$$

Note the leftover Σ^5 which is associated with the scalar interaction. Hence the tree-level amplitude in six dimensions is given by,

$$A^{(0),6d} = \lambda_1\Sigma^5\lambda_2. \tag{4.32}$$

As discussed in section 4.1.2, the contraction of the six-dimensional Lorentz indices of internal gluon lines includes contributions from the extra dimensions. The procedure of reducing the sum over internal states allows us to obtain the explicit dependence on space-time dimensionality. In the case at hand, the numerator in the six-dimensional calculation is,

$$N^{6d} = \lambda_1\Sigma^M(\tilde{\Sigma}\cdot\ell_3)\Sigma^5(\tilde{\Sigma}\cdot\ell_2)\Sigma_M\lambda_2. \tag{4.33}$$

Comparing with N^{4d} in equation (4.31), the extra contributions in six dimensions are evidently,

$$N^{6d}_{\phi_1} = -\lambda_1\Sigma^4(\tilde{\Sigma}\cdot\ell_3)\Sigma^5(\tilde{\Sigma}\cdot\ell_2)\Sigma^4\lambda_2, \tag{4.34a}$$

$$N^{6d}_{\phi_2} = -\lambda_1\Sigma^5(\tilde{\Sigma}\cdot\ell_3)\Sigma^5(\tilde{\Sigma}\cdot\ell_2)\Sigma^5\lambda_2. \tag{4.34b}$$

It follows from (4.26) that contributions from the scalars can equivalently be

obtained with,

$$N_{\phi_1}^{6d} = -\lambda_1(\Sigma\cdot\ell_3)\tilde{\Sigma}^5(\Sigma\cdot\ell_2)\lambda_2, \tag{4.35a}$$

$$N_{\phi_2}^{6d} = \lambda_1\gamma_5(\Sigma\cdot\ell_3)\tilde{\Sigma}^5(\Sigma\cdot\ell_2)\tilde{\gamma}_5\lambda_2, \tag{4.35b}$$

where $(\tilde{\gamma}_5)^A{}_B = -i\tilde{\Sigma}^{4,AX}\Sigma^5_{XB}$. Using the integral basis in (4.29) the result is,

$$\begin{aligned} A^{(1),6d} &= \boldsymbol{c}^{6d}\cdot\boldsymbol{I}A^{(0),6d} \\ &= \left\{-2s, -\frac{16m^2}{s\beta^2}, 4\right\}\cdot\boldsymbol{I}A^{(0),6d}, \end{aligned} \tag{4.36}$$

$$\begin{aligned} A_{\phi_1}^{(1)} &= \boldsymbol{c}_{\phi_1}\cdot\boldsymbol{I}A^{(0),6d} \\ &= \{0,1,1\}\cdot\boldsymbol{I}A^{(0),6d}, \end{aligned} \tag{4.37}$$

$$\begin{aligned} A_{\phi_2}^{(1)} &= \boldsymbol{c}_{\phi_2}\cdot\boldsymbol{I}A^{(0),6d} \\ &= \left\{-4m^2, -1-\frac{8m^2}{s\beta^2}, -1\right\}\cdot\boldsymbol{I}A^{(0),6d}. \end{aligned} \tag{4.38}$$

The coefficients above are the ingredients needed to perform the state-sum reduction and reproduce (4.30).

4.2 $gg \to t\bar{t}$ at one loop

We consider two gauge-invariant primitive amplitudes relevant for the $gg \to t\bar{t}$ one-loop scattering amplitude. Helicity amplitudes for this process have been previously presented in reference [75]. Using the usual colour decomposition [84] we define the ordered partial amplitudes $A^{(1)}_{4;1}$ and $A^{(1)}_{4;3}$ by,

$$\begin{aligned} \mathcal{A}^{(1)}\left(1_t,2,3,4_{\bar{t}}\right) = \sum_{P(2,3)} &\left(T^{a_2}T^{a_3}\right)^{\bar{i}_4}_{i_1} A^{(1)}_{4;1}\left(1_t,2,3,4_{\bar{t}}\right) \\ &+ \mathrm{tr}\left(T^{a_2}T^{a_3}\right)\delta^{\bar{i}_4}_{i_1} A^{(1)}_{4;3}\left(1_t,4_{\bar{t}};2,3\right), \end{aligned} \tag{4.39}$$

$A^{[L]}(1_t, 2, 3, 4_{\bar{t}}) =$ 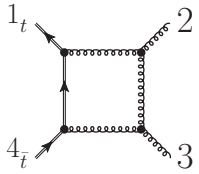 $+\ldots,\ A^{[R]}(1_t, 2, 3, 4_{\bar{t}}) =$ 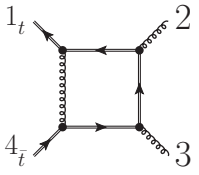 $+\ldots$

Figure 4.3 *Configurations for left- and right-moving primitive amplitudes contributing to $gg \to t\bar{t}$ scattering.*

where $P(2,3)$ is the permutations over the order of gluons. These partial amplitudes can be further decomposed into gauge-invariant primitive amplitudes,

$$\begin{aligned} A^{(1)}_{4;1}(1_t, 2, 3, 4_{\bar{t}}) &= N_c A^{[L]}(1_t, 2, 3, 4_{\bar{t}}) - \frac{1}{N_c} A^{[R]}(1_t, 2, 3, 4_{\bar{t}}) \\ &\quad - N_f A^{[f]}(1_t, 2, 3, 4_{\bar{t}}) - N_H A^{[H]}(1_t, 2, 3, 4_{\bar{t}}), \end{aligned} \tag{4.40}$$

$$A^{(1)}_{4;3}(1_t 4_{\bar{t}}; 2, 3) = \sum_{P(2,3)} \left(A^{[L]}(1_t, 2, 3, 4_{\bar{t}}) + A^{[L]}(1_t, 2, 4_{\bar{t}}, 3) + A^{[R]}(1_t, 2, 3, 4_{\bar{t}}) \right), \tag{4.41}$$

where N_c is the number of colours, while N_f and N_H are the number of light and heavy fermion flavours, respectively. The left-moving $A^{[L]}$ and right-moving $A^{[R]}$ primitive amplitudes are labelled according to the direction of the fermion current as it enters the loop, following the convention of reference [84]. Representative diagrams for these amplitudes are shown in Figure 4.3. We will not consider the fermion loop contributions $A^{[f]}$ and $A^{[H]}$ in this article as they do not present any further technical difficulties.

Each primitive amplitude can be decomposed at the integrand level into the basis of integrals described in section 3.2. In this massive case there are only two possible basis integrals which go beyond those appearing in the massless case,

$$A^{(1)}_n = B^{(1)}_n + c_{2;m^2} I_{2,m^2} + c_1 I_1. \tag{4.42}$$

The amplitude labelled $B^{(1)}_n$ is the part that can be constructed from finite d-dimensional unitarity cuts. The additional basis integrals depend only on the

fermion mass and in dimensional regularisation are,

$$I_{2,m^2} = \mu^{2\epsilon} \int \frac{d^d k}{(2\pi)^d} \frac{1}{k^2((k-p)^2 - m^2)} \overset{d=4-2\epsilon}{=} i c_\Gamma \left(\frac{1}{\epsilon} + \log\left(\frac{\mu^2}{m^2}\right) + 2 \right) + \mathcal{O}(\epsilon), \tag{4.43}$$

$$I_1 = \mu^{2\epsilon} \int \frac{d^d k}{(2\pi)^d} \frac{1}{k^2 - m^2} \overset{d=4-2\epsilon}{=} i c_\Gamma m^2 \left(\frac{1}{\epsilon} + \log\left(\frac{\mu^2}{m^2}\right) + 1 \right) + \mathcal{O}(\epsilon), \tag{4.44}$$

where $c_\Gamma = \frac{\Gamma(1+\epsilon)\Gamma(1-\epsilon)^2}{(4\pi)^{2-\epsilon}\Gamma(1-2\epsilon)}$.

To capture the full d-dimensional dependence, we first compute generalised unitarity cuts in six dimensions using the spinor-helicity formalism described in the previous section. We then compute the two additional scalar loop contributions and perform the state-sum reduction onto a general spin dimension, d_s, according to equation (4.27). The complete set of generalised unitarity cuts needed for the amputated primitives $B^{[L]}$ and $B^{[R]}$, c.f. $B_n^{(1)}$ in equation (4.42), are shown in Figure 4.4 and 4.5, in which the divergent two-particle and one-particle cuts are removed.

Each six-dimensional cut is associated with a set of loop momenta ℓ_i which enter the tree-level amplitudes. These momenta are determined by solving the system of on-shell equations $\{\ell_i^2 = 0, i \in S\}$. The complete set of loop momenta for our ordered amplitudes are labelled as,

$$\begin{aligned} \ell_i^\mu &\equiv \ell_0^\mu - P_i^\mu, \qquad & P_i^\mu &= \sum_{n=1}^{i} p_n^\mu, \\ \ell_0^\mu &\equiv k^\mu, \end{aligned} \tag{4.45}$$

where p_n^μ are the external momenta and k is the loop integration momentum.

The internal particles are embedded into six dimensions by allowing the mass to flow in the sixth component, following our convention in equation (4.13), and the $(d-4)$ part of the loop momentum to flow in the fifth component,

$$\begin{aligned} \text{gluon loop momentum:} \quad & \ell = \{\bar{\ell}, \mu, 0\}, \\ \text{fermion loop momentum:} \quad & \ell = \{\bar{\ell}, \mu, m\}. \end{aligned} \tag{4.46}$$

The gluon and fermion loop propagators can then be expanded into a four-

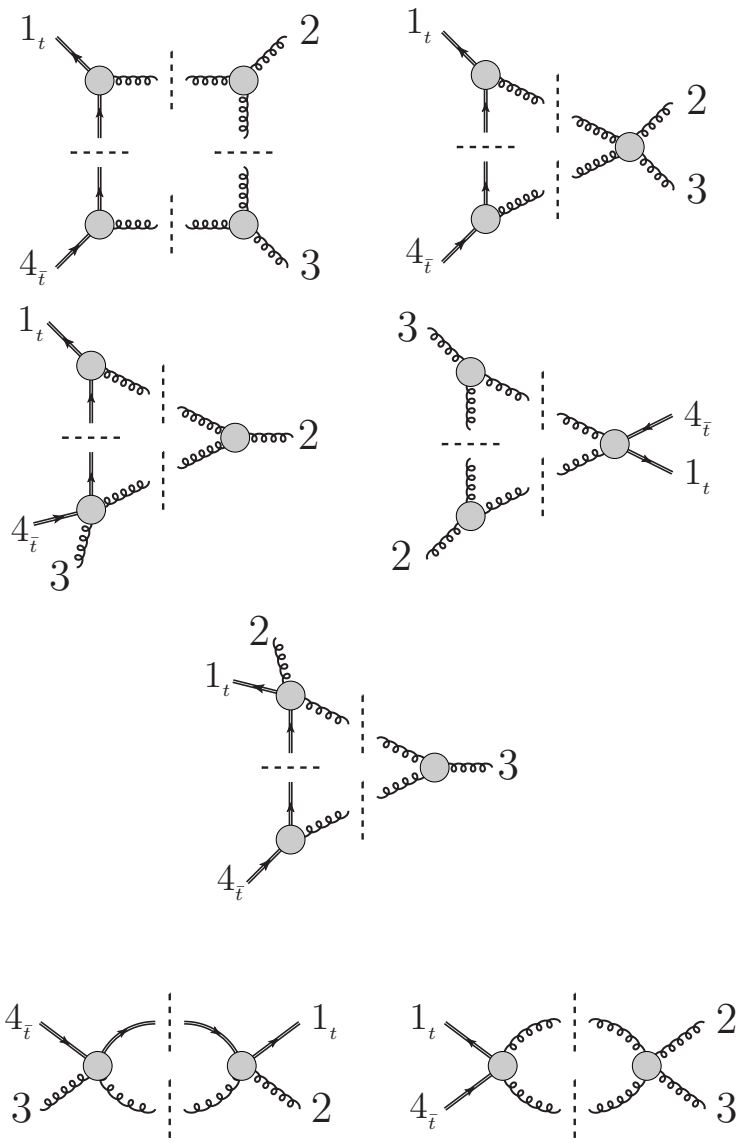

Figure 4.4 *The complete set of cuts for* $B^{[L]}(1_t, 2, 3, 4_{\bar{t}})$. *Double lines represent massive fermions.*

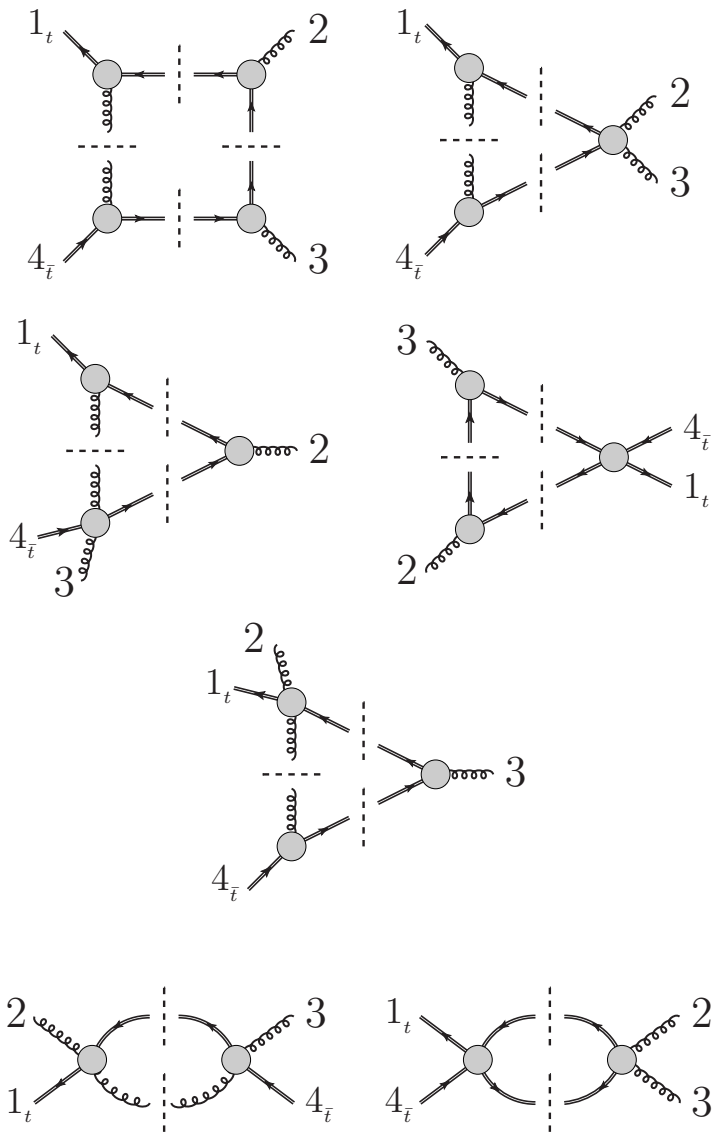

Figure 4.5 *The complete set of cuts for* $B^{[R]}(1_t, 2, 3, 4_{\bar{t}})$. *Double lines represent massive fermions.*

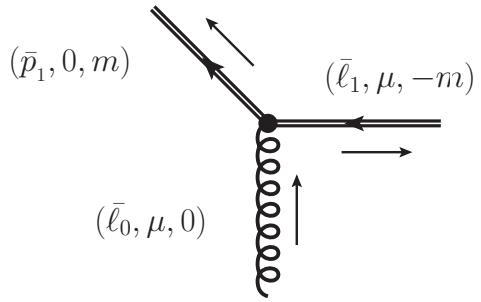

Figure 4.6 *To perform the unitarity cuts of the six dimensional propagators involving internal fermions, we allow the $(d-4)$ part, μ, of the loop momentum to flow in the fifth component and the mass term to flow in the sixth component, in order to easily impose momentum conservation.*

dimensional part and an effective mass term μ^2,

$$\text{gluon propagator:} \quad \ell^2 = \bar{\ell}^2 - \mu^2, \tag{4.47}$$

$$\text{fermion propagator:} \quad \ell^2 = \bar{\ell}^2 - \mu^2 - m^2. \tag{4.48}$$

This choice is particularly convenient when requiring momentum conservation and orthogonality of the -2ϵ component with respect to the external massive fermions momenta expressed in the six-dimensional representation, as shown in Figure 4.6.

As an explicit example we will describe the computation of the quadruple cuts. The on-shell equations for these cuts in the left- and right-moving configurations are,

$$S^L_{4;1234} = \begin{cases} \ell_0^2 = \ell_1^2 = \ell_2^2 = \ell_3^2 = 0 \\ \ell_0^{(5)} = m \end{cases} \quad , \quad S^R_{4;1234} = \begin{cases} \ell_0^2 = \ell_1^2 = \ell_2^2 = \ell_3^2 = 0 \\ \ell_0^{(5)} = 0 \end{cases} \quad . \tag{4.49}$$

The constraint on the sixth component of the loop momentum ℓ_0 distinguishes between the two different configurations.

We construct explicit solutions for the six-dimensional spinors of ℓ_i by introducing arbitrary two-component reference spinors x_a and $\tilde{x}_{\dot{a}}$. These solutions, which have

a similar form to those presented in [85, 86], take a simple form,

$$\ell_0^M = \frac{\langle x.4|\Sigma^M\, 1\, 2\, 3|4.\tilde{x}]}{\langle x.4|2\, 3|4.\tilde{x}]}, \qquad \ell_1^M = \frac{\langle x.4|1\, \tilde{\Sigma}^M\, 2\, 3|4.\tilde{x}]}{\langle x.4|2\, 3|4.\tilde{x}]},$$
$$\ell_2^M = \frac{\langle x.4|1\, 2\, \Sigma^M\, 3|4.\tilde{x}]}{\langle x.4|2\, 3|4.\tilde{x}]}, \qquad \ell_3^M = \frac{\langle x.4|1\, 2\, 3\, \tilde{\Sigma}^M|4.\tilde{x}]}{\langle x.4|2\, 3|4.\tilde{x}]}, \tag{4.50}$$

where $\langle x.4| = x^a\langle 4_a|$, $|4.\tilde{x}] = |4^{\dot{a}}]\tilde{x}_{\dot{a}}$. The expressions for the two reference spinors can be chosen to be,

$$x_a = (1, \tau_1), \qquad \tilde{x}_{\dot{a}} = (1, y), \tag{4.51}$$

where y is fixed, for left and right, by the mass constraint for $\ell_0^{(5)}$ specified in (4.49). Because we have a system of 5 equations for 6 dimensional momenta, the parameter τ_1 is left unconstrained.

On the quadruple cut the amplitudes factorise into products of four tree-level amplitudes,

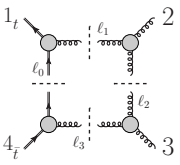

$$C^L_{4;1234} = A(-\ell_{0a}, 1_t^\alpha, \ell_1^{b\dot{b}})A(-\ell_{1\dot{b}b}, 2^{\beta\dot{\beta}}, \ell_2^{c\dot{c}}) \times A(-\ell_{2c\dot{c}}, 3^{\gamma\dot{\gamma}}, \ell_3^{d\dot{d}})A(-\ell_{3d\dot{d}}, 4_t^\delta, \ell_0^a), \tag{4.52}$$

and

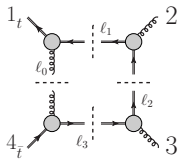

$$C^R_{4;1234} = A(-\ell_{0a\dot{a}}, 1_t^\alpha, \ell_1^b)A(-\ell_{1b}, 2^{\beta\dot{\beta}}, \ell_2^c) \times A(-\ell_{2c}, 3^{\gamma\dot{\gamma}}, \ell_3^d)A(-\ell_{3d}, 4_t^\delta, \ell_0^{a\dot{a}}), \tag{4.53}$$

where in both cases the repeated $SU(2)$ spinor indices are summed over the six-dimensional polarisation states.

The integrand reduction method then proceeds to extract the five independent coefficients in the integrand parametrisation from (3.26) by evaluating both the product of trees and the irreducible scalar products $\mu^2 = \mu_{11}$ and $k \cdot \omega$ using the on-shell solution in (4.50) and comparing the resulting rational functions in τ_1. We encounter an interesting subtlety when following this procedure since the six-dimensional cut contains additional terms which are linear in the extra-dimensional component of the loop momentum μ. These terms are spurious and integrate to zero, but require additional coefficients to be added at the integrand

level if this direct approach is taken. A slightly simpler approach is to cancel the linear part of the cut by averaging over the two different flows of the momentum in the fifth component,

$$\Delta_{1234}\big|_{S_{4;1234}} = \frac{1}{2}\left(C_{4;1234}\big|_{S^+_{4;1234}} + C_{4;1234}\big|_{S^-_{4;1234}}\right), \tag{4.54}$$

where,

$$S^+ = \left\{\ell_i^2 = 0, \ell_i = \{\dots, \mu, \dots\}\right\}, \quad S^- = \left\{\ell_i^2 = 0, \ell_i = \{\dots, -\mu, \dots\}\right\}. \tag{4.55}$$

The triangle and bubble coefficients follow using the OPP method to systematically remove all singularities from the cut amplitude using the previously computed irreducible numerators. The mass dependence of the propagators is now dictated by six-dimensional momentum conservation applied to the loop momenta, so all propagators are simply ℓ_i^2. To remove the terms linear in μ, we average over the two directions for the extra-dimensional component, as described above. Thus,

$$\Delta_{1234}\big|_{S_{4;1234}} = \frac{1}{2}\sum_{\sigma=\pm} C_{4;1234}\big|_{S^\sigma_{4;1234}}, \tag{4.56a}$$

$$\Delta_{123}\big|_{S_{3;123}} = \frac{1}{2}\sum_{\sigma=\pm} C_{3;123}\bigg|_{S^\sigma_{3;123}} - \frac{\Delta_{1234}}{\ell_3^2}\bigg|_{S_{3;123}}, \tag{4.56b}$$

$$\Delta_{13}\big|_{S_{2;13}} = \frac{1}{2}\sum_{\sigma=\pm} C_{2;13}\bigg|_{S^\sigma_{2;13}} - \left(\frac{\Delta_{123}}{\ell_1^2} + \frac{\Delta_{134}}{\ell_3^2} + \frac{\Delta_{1234}}{\ell_1^2\ell_3^2}\right)\bigg|_{S_{2;13}}, \tag{4.56c}$$

where the parametrisations for each irreducible numerator are those of section 3.2. The remaining triple and double cuts follow by permuting the equations (4.56). Further details on the on-shell cut solutions are given in Appendix B.3 and a full set of numerical results for the six-dimensional cuts are listed in the MATHEMATICA notebook accompanying our paper [1].

The final step to dimensionally reduce the coefficients from 6 to a general spin dimension, d_s, is to remove the extra degrees of freedom contained in the six-dimensional loop momentum according to (4.27). The computation of these extra cuts is done using the same procedure as above, but the internal gluon lines in Figure 4.4 and 4.5 are replaced with scalars. For example, the quadruple cuts are

given by the following expressions,

$$C^{L,\phi_{(1,2)}}_{4;1234} = A(-\ell_{0\dot{a}}, 1^{\alpha}_{t}, \ell_1)A(-\ell_1, 2^{\beta\dot{\beta}}, \ell_2)A(-\ell_2, 3^{\gamma\dot{\gamma}}, \ell_3)A(-\ell_3, 4^{\delta}_{\bar{t}}, \ell^{\dot{a}}_0), \tag{4.57}$$

$$C^{R,\phi_{(1,2)}}_{4;1234} = A(-\ell_0, 1^{\alpha}_{t}, \ell^{\dot{b}}_1)A(-\ell_{1\dot{b}}, 2^{\beta\dot{\beta}}, \ell^{\dot{c}}_2)A(-\ell_{2\dot{c}}, 3^{\gamma\dot{\gamma}}, \ell^{\dot{d}}_3)A(-\ell_{3\dot{d}}, 4^{\delta}_{\bar{t}}, \ell_0). \tag{4.58}$$

A complete set of fermion and scalar integrand coefficients are presented in the attached notebook of [1].

4.2.1 Determining the remaining integral coefficients

At this point, let us pause to take stock of what has been achieved, and what remains to be done. To do so, we return to equation (4.42), the standard expression for a one-loop amplitude, expanded in a basis of scalar integrals,

$$A^{(1)}_n = B^{(1)}_n + c_{2;m^2} I_{2,m^2} + c_1 I_1. \tag{4.59}$$

By definition, $B^{(1)}_n$ is the part of the amplitude which can be computed using finite d-dimensional unitarity cuts; its expansion in terms of an integral basis was explicitly given in equation (3.19), ignoring the bubble and tadpole topologies with divergent cuts. We have therefore computed $B^{(1)}_n$ explicitly in section 4.2. A complete construction of the amplitude requires us to find the integral coefficients $c_{2;m^2}$ and c_1. This is the task of the present section.

Fixing c_{2,m^2} by matching the poles in $4-2\epsilon$ dimensions

Our first source of additional information is the universal pole structure of four-dimensional amplitudes. The poles of general one-loop QCD amplitudes in four dimensions were inferred from the corresponding real-radiation contributions to the NLO cross-section in full generality by Catani, Dittmaier and Trocsanyi [87],

$$A^{(1),4-2\epsilon} = c_\Gamma \, I^{(1)}(\epsilon) A^{(0)} + \text{finite}. \tag{4.60}$$

The integrals I_{2,m^2} and I_1 appearing in equation (4.59) are divergent, and therefore the coefficients $c_{2;m^2}$ and c_1 contribute to the pole structure of our amplitude. This will allow us to constrain them.

For the simplified case of $t\bar{t} + n(g)$ with n_f light quark flavours and one heavy

flavour of mass m, the function $I^{(1)}(\epsilon)$ appearing in the univeral pole formula is, explicitly,

$$I^{(1)}(\epsilon) = \frac{n_g \beta_0(n_f+1)}{2\epsilon} + \sum_{i,j} \left(\frac{\mu_R^2}{s_{ij}}\right)^{\epsilon} \mathcal{V}_{ij} - n_g \Gamma_g - 2\Gamma_t + \text{finite}. \tag{4.61}$$

Following Catani et al. [87], this formula corresponds to partially renormalised amplitudes. The first term contains UV poles related to charge renormalisation, the second term corresponds to soft-collinear poles and takes the familiar dipole form in colour space. The last terms contain poles given by the anomalous dimensions,

$$\Gamma_g = \frac{\beta_0(n_f)}{2\epsilon} + \frac{2T_R}{3} \log\left(\frac{\mu_R^2}{m_t^2}\right), \tag{4.62}$$

$$\Gamma_t = C_F \left(\frac{1}{\epsilon} - \frac{1}{2}\log\left(\frac{\mu_R^2}{m_t^2}\right) - 2\right). \tag{4.63}$$

The QCD β function appears as a function of the active fermion flavours $\beta_0(n_f) = (11C_A - 4T_R n_f)/3$. For the purposes of this chapter we will not require the finite parts of $I^{(1)}$ which depend on the dimensional regularisation scheme. The exact form of the function $\mathcal{V}$ is a little more complicated and not of direct relevance here. Clearly there is an enormous amount of information contained in this result and further details can be found by consulting the original reference [87].

The simple observation relevant for our approach is that this universal information can be compared to the integral basis in equation (4.59), enabling a partial determination of the unknown coefficients of wavefunction bubble and tadpole integrals. These integrals give rise to single poles in ϵ and single logarithms in the mass m. This comparison is however insufficient to constrain both c_{2,m^2} and c_1.

It is convenient to modify the integral basis slightly, introducing finite bubble and tadpole functions defined by,

$$F_{2;i_1,i_2} = I_{2,i_1,i_2} - I_{2,m^2}, \tag{4.64}$$

$$F_1 = I_1 - m^2 I_{2,m^2}. \tag{4.65}$$

The result of this modification is that only the finite bubble integrals and the wavefunction integral contribute to the $\log(\mu_R^2/m_t^2)$ dependence of the universal pole structure (4.61). Upon matching the amplitude with the universal pole

structure, we find that the amplitude takes the explicit expression

$$A^{(1)} = A^{6D,(1)}\Big|_{I_2 \to F_2} + \frac{d_s - 2}{4} A^{(0)} I_{2,m^2} + c_1 F_1, \tag{4.66}$$

where the only missing information now lies in the tadpole coefficient c_1.

Counterterms for QCD in six dimensions

Because of our exploitation of the universal four-dimensional pole structure, the one-loop amplitude, in the form given in equation (4.66), has the property that its infrared and ultraviolet poles have been correctly determined. In addition, all logs in the mass m_t are correctly reproduced. Indeed, the unknown coefficient c_1 now multiplies an integral F_1 which we may explicitly compute,

$$F_1 \overset{d=4-2\epsilon}{=} -ic_\Gamma m^2 + \mathcal{O}(\epsilon) = -\frac{im^2}{(4\pi)^2} + \mathcal{O}(\epsilon). \tag{4.67}$$

Since c_1 is also a rational function, the part of the amplitude which remains to be determined is simply a rational function of the external momenta and masses.

Having made heavy use of higher dimensional methods so far in our computation, it is natural to regard the four-dimensional result we wish to determine as a specialisation of an amplitude that exists in higher dimensions. Indeed, a quantum field theory which is an analogue of QCD exists in six dimensions. Moreover, in six dimensions the integral F_1 is no longer simply a finite rational function. It has an epsilon-pole given by,

$$F_1 \overset{d=6-2\epsilon}{=} -\frac{im^4}{(4\pi)^3} \frac{1}{6\epsilon} + \mathcal{O}(\epsilon). \tag{4.68}$$

We may therefore find c_1 by comparison with the universal epsilon-pole structure of the amplitude in six dimensions.

Thus, we are motivated to consider QCD in six dimensions. Above four dimensions QCD ceases to be renormalisable, so to determine the universal epsilon-pole structure in six dimensions we must include higher (mass-)dimension

operators[1] and treat the theory as an effective theory. By power counting, these operators have one or two powers of momentum more than in the usual QCD Lagrangian, so that they have mass-dimension five or six. The point of view we adopt is that the role of the additional operators is simply to provide counterterms, subtracting the infinities from any one-loop amplitude in the theory. Once all the counterterms have been determined, the epsilon-pole structure of any one-loop amplitude is known.

We therefore begin by constructing a basis of the dimension five and six operators which are required for renormalising QCD amplitudes in six dimensions. These operators contain either two quark fields and up to three derivatives, such as $\mathcal{O}_1 \equiv i\bar{\psi}\not{D}\not{D}\not{D}\psi$, or are purely bosonic operators such as $\mathrm{tr}\,(F^{\mu\nu}F_{\nu\rho}F^{\rho}{}_{\mu})$.[2] A full list of potential operators appears in Table 4.1.

Since we are only concerned with poles of on-shell amplitudes, rather than of off-shell correlation functions, we need only study operators which lead to independent contributions to the S matrix. It is a well known fact that operators which are related by the classical equations of motion of the theory lead to the same contribution to the S matrix, to all orders of perturbation theory [88–92]. Thus we may simplify the list of operators in Table 4.1 using the equations of motion,

$$i\not{D}\psi = m\psi, \tag{4.69}$$

$$D^{\mu}F^{a}_{\mu\nu} = -g\bar{\psi}\gamma^{\nu}T^{a}\psi. \tag{4.70}$$

It is straightforward to see that many operators in Table 4.1 are related to other operators in our Lagrangian. For example,

$$\mathcal{O}_1 \equiv i\bar{\psi}\not{D}\not{D}\not{D}\psi = -im^2\bar{\psi}\not{D}\psi, \tag{4.71}$$

so that $\mathcal{O}_1$ does not lead to a new, independent counterterm. It may therefore be omitted.

Our task now is to construct a basis of operators which are independent under the use of the equations of motion, integration by parts etc. To construct such a basis,

[1] It is linguistically unfortunate that we are now dealing with operators of mass-dimension five and six (using the usual four-dimensional classification of operator dimension) in a theory defined in six space-time dimensions. We hope that context will make the meaning of the word "dimension" clear.

[2] Recall that a field strength F counts as two derivatives since $[D_\mu, D_\nu] = -igF_{\mu\nu}$.

Quark fields	Operator	Operator class name
Two quarks	$i\bar{\psi}\not{D}\not{D}\not{D}\psi$ $i\bar{\psi}\not{D}D^2\psi$ $i\bar{\psi}D^\mu\not{D}D_\mu\psi$	$[\bar{\psi}D^3\psi]$
	$\psi\gamma^\mu\gamma^\nu F_{\mu\nu}\not{D}\psi$ $\bar{\psi}D^\mu F_{\mu\nu}\gamma^\nu\psi$ $\bar{\psi}F_{\mu\nu}\gamma^\mu D^\nu\psi$	$[\bar{\psi}DF\psi]$
	$\psi\not{D}\not{D}\psi$ $\bar{\psi}D^2\psi$	$[\bar{\psi}D^2\psi]$
	$i\psi\gamma^\mu\gamma^\nu F_{\mu\nu}\psi$	$[\psi F\psi]$
Zero quarks	$i\mathrm{tr}\,(F^{\mu\nu}F_{\nu\rho}F^\rho{}_\mu)$ $\mathrm{tr}\,(F^{\mu\nu}D^2F_{\mu\nu})$ $\mathrm{tr}\,((D^\mu F_{\mu\nu})(D^\rho F_\rho{}^\nu))$	

Table 4.1 *Table of potential higher-dimension operators in the six-dimensional QCD effective Lagrangian. We have ignored four-quark operators, which are not relevant for $t\bar{t}$ + gluons scattering at this order, and operators related to those in our table by integration-by-parts or Hermitian conjugation. We have also imposed the parity symmetry of QCD.*

we consider several categories of operators. Firstly, we will focus on operators containing two quark fields. We classify these operators further according to the powers of derivatives, or of derivatives and field strength insertions as shown in detail in Table 4.1. We will begin by examining operators containing the largest number of derivatives or field strengths, as the use of the equations of motion may reduce these operators to simpler operators containing fewer derivatives (or field strength tensors).

Each of the derivatives contained in operators of type $[\bar{\psi}D^3\psi]$ has one Lorentz index which we must contract using either metric tensors or gamma matrices. By making use of the equations of motion, we may ignore the options of contracting the left-most or right-most D index against a gamma matrix—such a contraction would reduce to an operator with fewer derivatives which we will analyze below. We are left with the unique possibility $\bar{\psi}D^\mu\not{D}D_\mu\psi$. However, this operator is equivalent to a linear combination of operators of class $[\bar{\psi}DF\psi]$ and $[\bar{\psi}D^2\psi]$ upon use of the equations of motion since,

$$\bar{\psi}D^\mu\not{D}D_\mu\psi = \bar{\psi}\left(-imD^\mu D_\mu - igD^\mu\gamma^\nu F_{\mu\nu}\right)\psi. \tag{4.72}$$

Therefore, the class $[\bar{\psi}D^3\psi]$ can be completely reduced to simpler operators.

Next, consider the class $[\bar{\psi}DF\psi]$. In this case we again have three possible Lorentz indices which must be contracted against gamma matrices or metric tensors. We may ignore the possibility of contracting the Lorentz index of the covariant derivative against a gamma matrix because of the equations of motion. We are left with two potential operator structures: $\bar{\psi}D^\mu F_{\mu\nu}\gamma^\nu\psi$ and $\bar{\psi}F_{\mu\nu}D^\mu\gamma^\nu\psi$. But,

$$\bar{\psi}D^\mu F_{\mu\nu}\gamma^\nu\psi = \bar{\psi}(-g\bar{\psi}\gamma_\nu\psi)\gamma^\nu\psi + \bar{\psi}F_{\mu\nu}D^\mu\gamma^\nu\psi, \tag{4.73}$$

using the Yang-Mills equation. Since we are only interested in processes with two quarks, we will systematically ignore four quark operators. Therefore, we may replace the operator $\bar{\psi}D^\mu F_{\mu\nu}\gamma^\nu\psi$ with $\bar{\psi}F_{\mu\nu}D^\mu\gamma^\nu\psi$. This is the only member of the class $[\bar{\psi}DF\psi]$ which is of interest to us.

We now turn to operator structures containing two quark fields but only one extra power of derivatives or gauge fields. Thus the available operator structures are $[\bar{\psi}DD\psi]$ and $[\bar{\psi}F\psi]$. Up to equations of motion, there is only one operator of the first type: $\bar{\psi}D^\mu D_\mu\psi$. However, this is a reducible operator,

$$\bar{\psi}D^\mu D_\mu\psi = \bar{\psi}\not{D}\not{D}\psi - \frac{ig}{2}\bar{\psi}F_{\mu\nu}\gamma^\nu\gamma^\mu\psi. \tag{4.74}$$

Thus, up to equations of motion, we may reduce the $[\bar{\psi}DD\psi]$ class to the $[\bar{\psi}F\psi]$ class. Because of the antisymmetry of the field strength tensor, there is only one operator in the $[\bar{\psi}F\psi]$ class, namely $\bar{\psi}F_{\mu\nu}\gamma^\nu\gamma^\mu\psi$.

Finally, we must consider operators containing no quark fields. There are three gauge invariant possibilities:

$$\mathrm{tr}\,(F^{\mu\nu}F_{\nu\rho}F^\rho{}_\mu),\ \mathrm{tr}\,(F_{\mu\nu}D^2F^{\mu\nu}),\ \text{and}\ \mathrm{tr}\,((D^\mu F_{\mu\nu})(D^\rho F_\rho{}^\nu)).$$

The last of these three operators is equivalent to a four quark operator using the Yang-Mills equation, and is therefore of no interest to us. Meanwhile, the second of the three is equivalent to the other two,

$$\mathrm{tr}\left(F_{\mu\nu}D^2F^{\mu\nu}\right) = -2\mathrm{tr}\left((D^\mu F_{\mu\nu})D_\alpha F^{\alpha\nu}\right) - 2ig\mathrm{tr}\left(F_{\nu\mu}F^\mu{}_\alpha F^{\alpha\nu}\right). \tag{4.75}$$

As a result, we may also ignore this operator, leaving only $\mathrm{tr}\,(F^{\mu\nu}F_{\nu\rho}F^\rho{}_\mu)$.

In summary, there are only three higher dimension operators that contribute to the on-shell amplitudes. We may therefore take the full QCD Lagrangian in six

dimensions, at one-loop order, to be,

$$\mathcal{L}^6_{QCD} = \bar{\psi}(i\not{D} - m)\psi - \frac{1}{2}\mathrm{tr}\,(F_{\mu\nu}F^{\mu\nu}) + \frac{i}{2}\sigma_1\, g_s^3 m_t\, \bar{\psi}\gamma^\mu\gamma^\nu F_{\mu\nu}\psi \\ + i\sigma_2\, g_s^3\, \bar{\psi}F_{\mu\nu}\gamma^\mu D^\nu\psi + \frac{i}{6}\gamma\, g_s^3\, \mathrm{tr}\left(F^{\mu\nu}[F_{\mu\lambda}, F_\nu{}^\lambda]\right). \quad (4.76)$$

A selection of the resulting Feynman rules are listed in Appendix B.4.

We adopt the point of view that σ_1, σ_2 and γ are couterterms which remove the divergences in loop amplitudes. In addition there are the usual counterterms from the dimension four vertices $t\bar{t}g$ and ggg. We can compute the constants $\delta_{t\bar{t}g}, \delta_{ggg}, \sigma_1, \sigma_2$ and γ from simple one-loop vertex graphs. For example, expanding the $t\bar{t}g$ vertex to $\mathcal{O}(g_s^3)$ leads to,

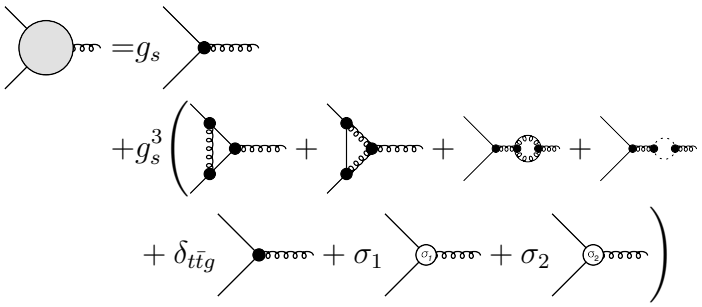

$$+\mathcal{O}(g_s^5). \quad (4.77)$$

Renormalising this correlation function off-shell would require the inclusion of all possible counterterms (before using the equations of motion.) For us, it is simpler to compute the on-shell three-point vertex, in which case all infinities can be absorbed in our effective Lagrangian, equation (4.76). This presents a minor problem since the three-point vertex is not well defined for real momenta. The computation may be performed using complex external kinematics or alternatively performed with the gluon taken off-shell and the constants extracted by taking the on-shell limit $p^2 \to 0$ at the end of the computation. We find this amplitude is UV finite in $6 - 2\epsilon$ dimensions for the values,

$$\delta_{t\bar{t}g} = \frac{m_t^2}{24(4\pi)^3\epsilon} C_F(3d_s + 2), \quad (4.78)$$

$$\sigma_1 = -\frac{1}{12(4\pi)^3\epsilon}\left(C_A(d_s - 5) - \frac{C_F}{2}(3d_s - 14)\right), \quad (4.79)$$

where $C_F = \frac{N_c^2-1}{2N_c}$ and $C_A = N_c$. A similar computation for the three-gluon

vertex,

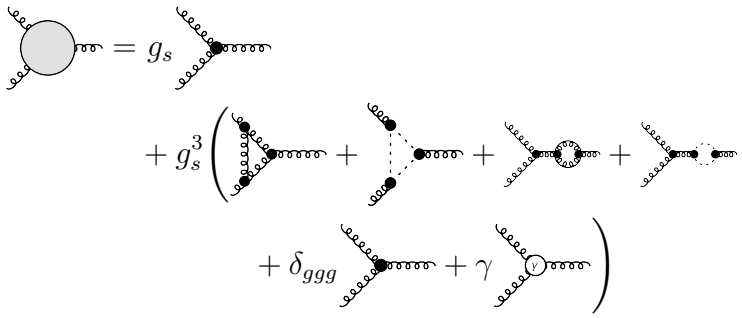

$$+ \mathcal{O}(g_s^5), \tag{4.80}$$

results in

$$\delta_{ggg} = 0, \tag{4.81}$$

$$\gamma = \frac{1}{12(4\pi)^3\epsilon} C_A \frac{(d_s - 2)}{5}. \tag{4.82}$$

Fixing c_1 by matching poles in $6 - 2\epsilon$ dimensions

We finally apply this knowledge of the universal epsilon poles in six dimensions to determine the remaining unknown coefficient, c_1 in equation (4.66). The six-dimensional leading colour partial amplitude, $A_{4;1}^{(1),6-2\epsilon}(1_t, 2, 3, 4_{\bar{t}})$, can be decomposed into gauge invariant primitives,

$$A_{4;1}^{(1),6-2\epsilon}(1_t, 2, 3, 4_{\bar{t}}) = N_c A^{[L],6-2\epsilon}(1_t, 2, 3, 4_{\bar{t}}) - \frac{1}{N_c} A^{[R],6-2\epsilon}(1_t, 2, 3, 4_{\bar{t}}), \tag{4.83}$$

precisely as in four dimensions (we ignore fermion loops as they present no technical difficulties). Because the epsilon-poles are universal, we know that the poles of this amplitude are,

$$A_{4;1}^{(1),6-2\epsilon}(1_t, 2, 3, 4_{\bar{t}}) = g_s^4 \Big(2\delta_{t\bar{t}g} A^{(0)}(1_t, 2, 3, 4_{\bar{t}}) + \sigma_1 A^{[\sigma_1]}(1_t, 2, 3, 4_{\bar{t}}) + \sigma_2 A^{[\sigma_2]}(1_t, 2, 3, 4_{\bar{t}}) + \gamma A^{[\gamma]}(1_t, 2, 3, 4_{\bar{t}}) \Big) + \mathcal{O}(\epsilon^0), \tag{4.84}$$

where the tree-type amplitudes $A^{[\sigma_1]}(1_t, 2, 3, 4_{\bar{t}})$, $A^{[\sigma_2]}(1_t, 2, 3, 4_{\bar{t}})$ and $A^{[\gamma]}(1_t, 2, 3, 4_{\bar{t}})$ are associated with the three higher-dimension operators in the effective six-dimensional QCD Lagrangian, equation (4.76). They are explicitly defined by

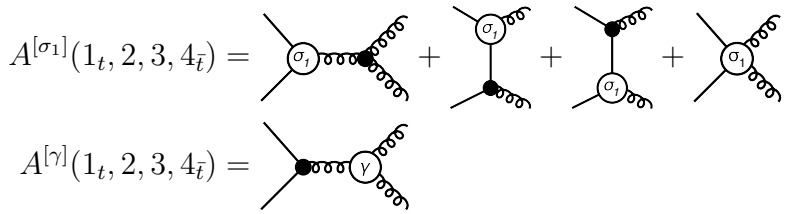

Figure 4.7 *The Feynman diagrams contributing to the tree-level amplitudes appearing in the pole structure of the one-loop $ggt\bar{t}$ amplitudes in $6-2\epsilon$ dimensions. Solid vertices correspond to the usual QCD interactions while the open vertices are those resulting from the corresponding dimension six operators in $\mathcal{L}^6_{QCD}$ of* (4.76).

the diagrams shown in Figure 4.7. In a similar fashion to the vertex computation we find that $A^{[\sigma_2]}(1_t, 2, 3, 4_{\bar{t}}) = 0$. By collecting in powers of N_c, and inserting the known expressions for $\delta_{t\bar{t}g}$, σ_1 and γ given in equations (4.78), (4.79) and (4.82) we find,

$$A^{[L],6-2\epsilon}(1_t, 2, 3, 4_{\bar{t}}) = \frac{g_s^4}{48(4\pi)^3\epsilon}\Bigg(2(3d_s+2)m_t^2 A^{(0)}(1_t, 2, 3, 4_{\bar{t}}) + \frac{4(d_s-2)}{5}A^{[\gamma]}(1_t, 2, 3, 4_{\bar{t}}) - (d_s-6)A^{[\sigma_1]}(1_t, 2, 3, 4_{\bar{t}})\Bigg) + \mathcal{O}(\epsilon^0) \quad (4.85)$$

for the left-moving ordering and

$$A^{[R],6-2\epsilon}(1_t, 2, 3, 4_{\bar{t}}) = \frac{g_s^4}{48(4\pi)^3\epsilon}\Bigg(2(3d_s+2)m_t^2 A^{(0)}(1_t, 2, 3, 4_{\bar{t}}) + (3d_s-14)A^{[\sigma_1]}(1_t, 2, 3, 4_{\bar{t}})\Bigg) + \mathcal{O}(\epsilon^0) \quad (4.86)$$

for the right-moving case.

The tree amplitudes $A^{[\sigma_1]}(1_t, 2, 3, 4_{\bar{t}})$ and $A^{[\gamma]}(1_t, 2, 3, 4_{\bar{t}})$ are easily determined by calculating the diagrams in Figure 4.7. Written in terms of four dimensional

spinor products, the independent helicity amplitudes are,

$$
\begin{aligned}
&-i\langle\eta_1 1^\flat\rangle\langle\eta_4 4^\flat\rangle A^{[\sigma_1]}(1_t^+,2^+,3^+,4_{\bar{t}}^+) = \\
&\quad\frac{-2m_t(2m_t^2-4p_1\cdot p_2-s_{23})s_{23}\langle\eta_1 2\rangle\langle\eta_4 3\rangle}{\langle 23\rangle^3}+\frac{2m_t(m_t^2-2p_1\cdot p_2)s_{23}\langle\eta_1\eta_4\rangle}{m_t\langle 23\rangle^2} \\
&\quad-\frac{m_t(m_t^2-2p_1\cdot p_2)s_{23}\langle\eta_1 3\rangle\langle\eta_4 3\rangle\langle 2|1|3]}{p_1\cdot p_2\langle 23\rangle^3} \\
&\quad+\frac{m_t(m_t^2-2p_1\cdot p_2)s_{23}\langle\eta_1 2\rangle\langle\eta_4 2\rangle\langle 3|1|2]}{p_1\cdot p_2\langle 23\rangle^3},
\end{aligned}
\tag{4.87a}
$$

$$
\begin{aligned}
&-i\langle\eta_1 1^\flat\rangle\langle\eta_4 4^\flat\rangle A^{[\sigma_1]}(1_t^+,2^+,3^-,4_{\bar{t}}^+) = \\
&\quad\frac{(-4m_t(p_1\cdot p_2)^2+m_t^2 s_{23}-2p_1\cdot p_2 s_{23})\langle\eta_1 3\rangle\langle\eta_4 3\rangle\langle 3|1|2]}{p_1\cdot p_2 s_{23}\langle 23\rangle} \\
&\quad-\frac{2m_t\langle\eta_1\eta_4\rangle\langle 3|1|2]^2}{m_t s_{23}}+\frac{m_t(4p_1\cdot p_2+s_{23})\langle\eta_1 2\rangle\langle\eta_4 3\rangle\langle 3|1|2]^2}{p_1\cdot p_2 s_{23}\langle 23\rangle} \\
&\quad-\frac{m_t\langle\eta_1 2\rangle\langle\eta_4 2\rangle\langle 3|1|2]^3}{p_1\cdot p_2 s_{23}\langle 23\rangle},
\end{aligned}
\tag{4.87b}
$$

$$
-i\langle\eta_1 1^\flat\rangle\langle\eta_4 4^\flat\rangle A^{[\gamma]}(1_t^+,2^+,3^+,4_{\bar{t}}^+) = \frac{m_t s_{23}^2\langle\eta_1 2\rangle\langle\eta_4 3\rangle}{2\langle 23\rangle^3}+\frac{m_t p_1\cdot p_2 s_{23}\langle\eta_1\eta_4\rangle}{\langle 23\rangle^2},
\tag{4.87c}
$$

$$
-i\langle\eta_1 1^\flat\rangle\langle\eta_4 4^\flat\rangle A^{[\gamma]}(1_t^+,2^+,3^-,4_{\bar{t}}^+) = 0,
\tag{4.87d}
$$

$$
-i\langle\eta_1 1^\flat\rangle\langle\eta_4 4^\flat\rangle A^{[\sigma_2]}(1_t^+,2^+,3^+,4_{\bar{t}}^+) = 0,
\tag{4.87e}
$$

$$
-i\langle\eta_1 1^\flat\rangle\langle\eta_4 4^\flat\rangle A^{[\sigma_2]}(1_t^+,2^+,3^-,4_{\bar{t}}^+) = 0.
\tag{4.87f}
$$

We note that the amplitudes of the σ_2 operator vanish in the cases we have considered. We still include it in our analysis since the operator remains in the Lagrangian after using the equations of motion despite not playing a role for the amplitudes in this section.

The final step necessary to determine the tadpole coefficient is to evaluate the poles of the basis integrals of the one-loop amplitude in $6-2\epsilon$ dimensions. We find,

$$
I_1^{6-2\epsilon}[1](m^2) = \frac{-im^4}{2(4\pi)^3\epsilon}+\mathcal{O}(\epsilon^0)
\tag{4.88}
$$

$$
I_2^{6-2\epsilon}[1](P^2,m_1^2,m_2^2) = i\frac{P^2-3(m_1^2+m_2^2)}{6(4\pi)^3\epsilon}+\mathcal{O}(\epsilon^0)
\tag{4.89}
$$

$$
\begin{aligned}
I_2^{6-2\epsilon}[\mu^2](P^2,m_1^2,m_2^2) = i&\frac{P^4-5P^2(m_1^2+m_2^2)+10\left((m_1^2+m_2^2)^2-m_1^2m_2^2\right)}{60(4\pi)^3\epsilon} \\
&+\mathcal{O}(\epsilon^0),
\end{aligned}
\tag{4.90}
$$

$$I_3^{6-2\epsilon}[1] = \frac{-i}{2(4\pi)^3\epsilon} + \mathcal{O}(\epsilon^0) \tag{4.91}$$

$$I_3^{6-2\epsilon}[\mu^2](P_1^2, P_2^2, P_3^2, m_1^2, m_2^2, m_3^2) = -i\frac{P_1^2 + P_2^2 + P_3^2 - 4(m_1^2 + m_2^2 + m_3^2)}{24(4\pi)^3\epsilon} + \mathcal{O}(\epsilon^0), \tag{4.92}$$

$$I_4^{6-2\epsilon}[1] = \mathcal{O}(\epsilon^0), \tag{4.93}$$

$$I_4^{6-2\epsilon}[\mu^2] = \frac{i}{6(4\pi)^3\epsilon} + \mathcal{O}(\epsilon^0). \tag{4.94}$$

We do not list the formulae for box integrals in 10 dimensions (μ^4) since they do not appear in amplitudes with a fermion pair and any number of gluons. The formulae are easy to derive using the dimensional recurrence relation implemented in LiteRed [93] in any case.

The only unknowns in equations (4.85) and (4.86) are then the left- and right-moving tadpole coefficients c_1, allowing a direct determination of these rational functions. The results are somewhat lengthy formulae which are explicitly derived in the Mathematica workbook included with the arXiv version of our paper [1]. We have checked that this procedure matches the expected result by comparing with the previous computation of reference [75].

4.3 Summary

In this chapter we have demonstrated a unitarity compatible method for calculating one-loop amplitudes involving massive fermions. In addition to the extra-dimensional component of the loop momentum from dimensional regularisation also the fermion mass was embedded in six dimensions. We demonstrated how the massless six-dimensional spinor-helicity formalism can be applied to this case.

With a massive particle involved, two integrals with divergent cuts appear in the parametrisation of the amplitude (4.42). The coefficients of these integrals were determined from the pole structure of the amplitude in four and six dimensions. The latter involved considering QCD in six dimensions were it ceases to be renormalisable. Higher mass dimension operators, acting as effective counter-terms, were introduced in order to remove divergences from loops.

In section 4.2.1 we discussed how to reduce the possible effective terms to a minimal set and the operator $i\sigma_2\, g_s^3\, \bar{\psi} F_{\mu\nu}\gamma^\mu D^\nu \psi$ was included in the final Lagrangian (4.76). It turned out not to contribute to the process under consideration. It was shown in [94] that this operator can be reduced to four-quark operators and therefore does not contribute in our case.[3]

Finally, the integral basis was evaluated in six dimensions (4.90) - (4.94). These integrals are related to the μ_{11}-dependent integrals of equation (3.71) from the previous chapter through (3.70).

[3]We thank Roman Zwicky for pointing this out to us.

Chapter 5

New results at two loops

In this chapter we turn our attention to the two-loop contribution to five-parton scattering in QCD. While there has been remarkable progress in Standard Model (SM) predictions for multi-particle final states at next-to-leading-order (NLO) and $2 \to 2$ scattering processes at next-to-next-to-leading order (NNLO), the computational complexity of $2 \to 3$ scattering processes at NNLO results in many important measurements being currently (or in the near future) limited by theoretical uncertainties. Pure gluon scattering at two loops in QCD is a key bottleneck in making such predictions which have been known for $gg \to gg$ for more than 15 years [95, 96]. The one-loop five-gluon amplitudes have been known since 1993 [97] and were among the first results from the on-shell methods that led to the modern unitarity method [50, 51] discussed in Chapter 3.

The work in this chapter was also presented in [2–4] and is based chronologically on these papers. The first section is on a benchmark approach, with focus on optimisations of the integrand basis for the gluon amplitude. The integrals are evaluated numerically using a variety of methods and the results verified by comparison to the universal pole structure. We present the numerical results for the amplitude with external fermions in the Euclidean region and for the gluon amplitude in the physical region as well as the Euclidean. The second section presents a different approach where the amplitude is reconstructed at the level of the master integrals expanded in a Laurent series in ϵ and pentagon functions. Pentagon functions and the expanded master integrals are presented in [98].

5.1 A first look at two-loop five-gluon scattering

In this section we demonstrate how new evaluation techniques based on generalised unitarity [53, 99] and integrand reduction [47, 100–105] can offer a solution to the traditional bottlenecks in loop computations and present the first results for a complete set of planar five-gluon helicity amplitudes in QCD. The results extend previous results obtained for 'all-plus' helicity amplitudes [106–113]. These on-shell techniques have also been explored in the context of maximal unitarity [114, 115] and numerical unitarity [116–118] approaches to QCD amplitudes.

We define the unrenormalised leading-colour (planar) five-gluon amplitudes using the simple trace basis:

$$\mathcal{A}^{(L)}(1,2,3,4,5) = n^L g_s^3 \sum_{\sigma\in S_5/Z_5} \mathrm{tr}\left(T^{a_{\sigma(1)}}\cdots T^{a_{\sigma(5)}}\right) \times A^{(L)}\left(\sigma(1),\sigma(2),\sigma(3),\sigma(4),\sigma(5)\right), \qquad (5.1)$$

where T^a are the fundamental generators of $SU(N_c)$ and S_5/Z_5 are all noncyclic permutations of the external particles. The overall normalisation is $n = m_\epsilon N_c \alpha_s/(4\pi)$ where $\alpha_s = g_s^2/(4\pi)$ is the strong coupling constant and $m_\epsilon = i(4\pi)^\epsilon e^{-\epsilon\gamma_E}$ (γ_E is the Euler–Mascheroni constant). The L-loop partial amplitude $A^{(L)}$ can be constructed from colour-ordered Feynman diagrams. Here we will compute the pure gluonic contributions to these amplitudes at two loops including the dependence on the spin dimension, d_s. Results in the 't Hooft-Veltman (HV) and four-dimensional-helicity (FDH) schemes can be obtained by setting $d_s = 4-2\epsilon$ and $d_s = 4$ respectively [56].

The integrand of the ordered partial amplitudes can be parametrised in terms of irreducible numerators, Δ,

$$A^{(2)}\left(1,2,3,4,5\right) = \int [dk_1][dk_2] \sum_T \frac{\Delta_T(\{k\},\{p\})}{\prod_{\alpha\in T} D_\alpha}, \qquad (5.2)$$

where $\{k\} = \{k_1, k_2\}$ are the $(d = 4-2\epsilon)$-dimensional loop momenta, T are the set of independent topologies and $\{p\} = \{1,2,3,4,5\}$ are the ordered external momenta. The measure is $[dk_i] = -i\pi^{-d/2} e^{\epsilon\gamma_E} d^{4-2\epsilon}k_i$ and the index α runs over the set of propagators associated with the topology T.

5.1.1 Two-loop cuts

Our planar five-gluon amplitudes are built from 57 distinct topologies, giving 425 irreducible numerators when including permutations of the external legs. 18 of these 57 topologies can be extracted from the (1-loop)^2 cut configurations as shown in Figure 5.1. For example,

$$\Delta\left(\text{}\right) + \frac{\Delta\left(\text{ 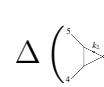 }\right)}{(k_1+k_2)^2} = \text{Cut}\left(\text{}\right), \tag{5.3}$$

where it is understood that the integrand parametrisations are evaluated on the cut. This means that all topologies with an additional propagator including k_1+k_2 are computed simultaneously with the (1-loop)^2 cuts. This is more efficient since the parametrisations of the cut loop momentum solutions are much simpler. The remaining 39 can be extracted from a further 31 configurations shown in Figure 5.2. The 8 topologies shown in Figure 5.3 have divergent maximal cuts and are extracted simultaneously with sub-topologies within the set of 31 2-loop cuts. For example,

$$\Delta\left(\text{ 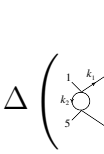 }\right) + \frac{\Delta\left(\text{ 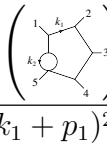 }\right)}{(k_1+p_1)^2} = \text{Cut}\left(\text{ 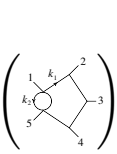 }\right) - \sum_{T\in\text{subtractions}} \frac{\Delta(T)}{\prod D_\alpha}, \tag{5.4}$$

where the product over denominators, D_α, is over the denominators present in subtraction topology, T, that are non-vanishing on the cut. The sum is over the six subtraction topologies,

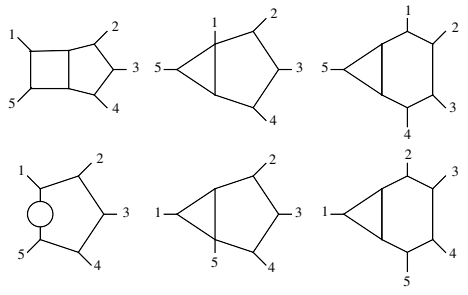

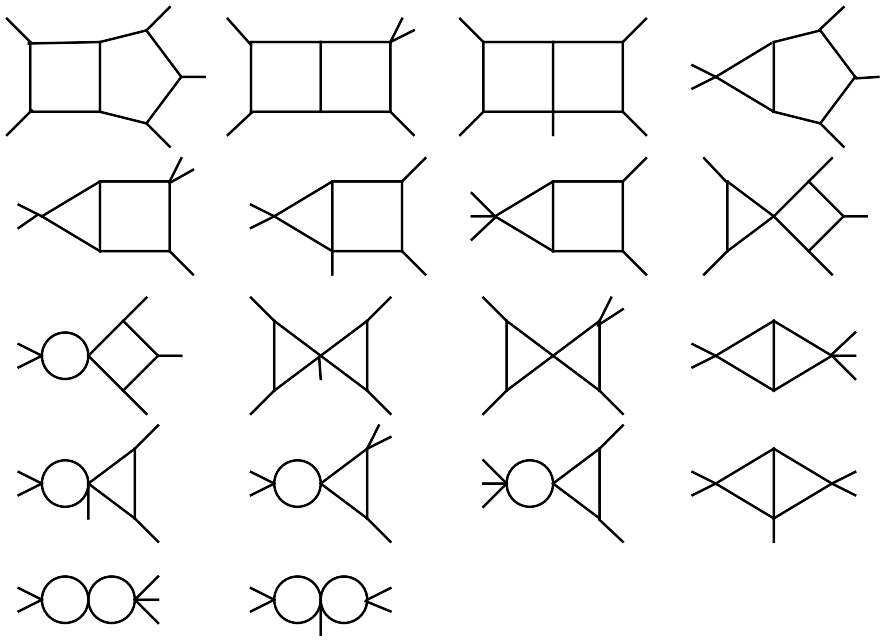

Figure 5.1 *The 18 distinct topologies extractable from (1-loop)^2 cuts.*

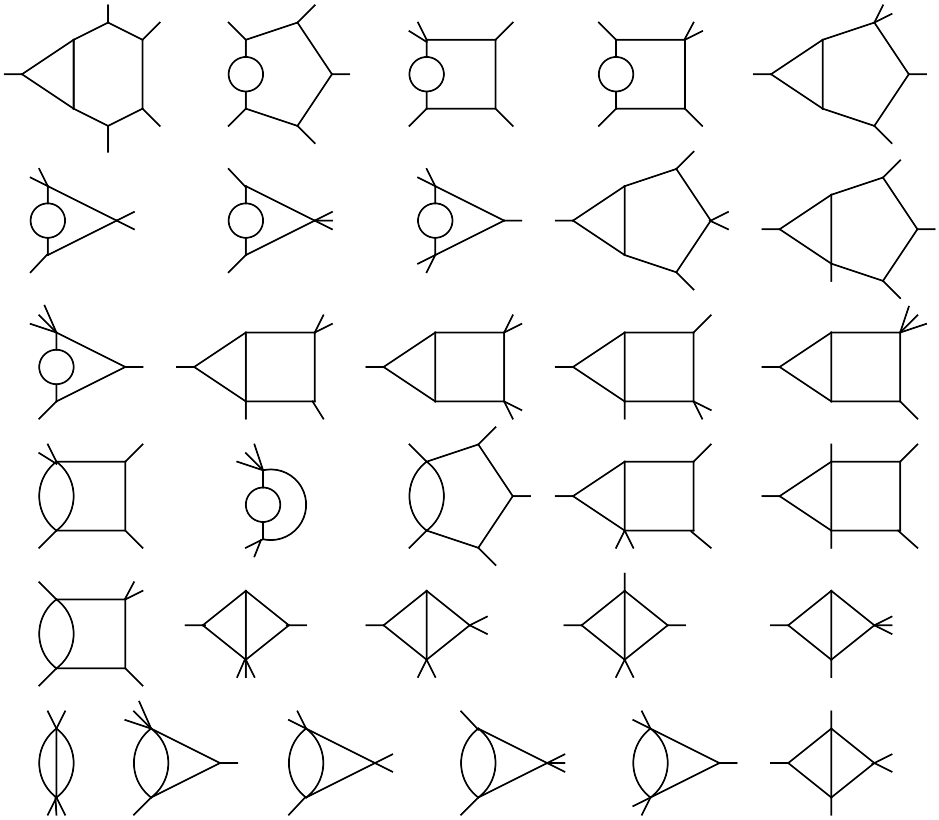

Figure 5.2 *31 distinct topologies extractable from 2-loop cuts.*

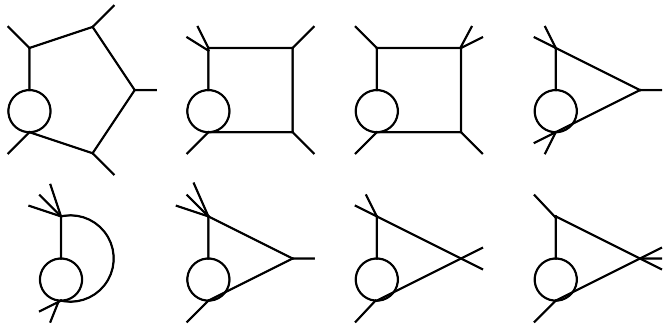

Figure 5.3 *The 8 distinct topologies with divergent cuts that must be computed simultaneously with subtopologies.*

5.1.2 Integrand basis

The construction of an integrand basis has been discussed in the literature using the language of computational algebraic geometry through polynomial division over a Gröbner basis [101, 105]. In this work we took a simpler approach which did not rely on the computation of a Gröbner basis, instead relying on the inversion of a linear system which can be performed efficiently with finite field reconstruction methods. We begin by expanding the loop momenta around a basis of external momenta and transverse directions. This is similar to the methods of Van Neerven and Vermaseren [43] also discussed in section 3.2.1 in the context of one-loop integrand parametrisation,

$$k_i^\mu = k_{\parallel,i}^\mu + k_{\perp,i}^\mu, \tag{5.5}$$

where $k_\parallel$ lives in the physical space spanned by the external momenta of the topology and $k_\perp$ lives in the transverse space. We further decompose the transverse space into four dimensional and (-2ϵ) dimensional spaces,

$$k_{\perp,i} = k_{\perp,i}^{[4]} + k_{\perp,i}^{[-2\epsilon]}. \tag{5.6}$$

The four-dimensional transverse space (which we will call the spurious space) has dimension $d_\perp = 4 - d_\parallel$ where $d_\parallel$ is equal to the number of independent momenta entering the vertices of the topology, up to a maximum value of four. We choose a spanning basis v for the physical space of each topology $k_{\parallel,i}^\mu = \sum_{j=1}^{d_\parallel} a_{ij} v_j^\mu$ and a basis ω for the spurious space $k_{\perp,i}^{\mu,[4]} = \sum_{j=1}^{d_\perp} b_{ij} \omega_j^\mu$, with $v_i \cdot \omega_j = 0$.

The coefficients in the physical space $k_\parallel$ are functions of the $a_{ij}(k_i) \equiv a_{ij}(\{D\}, \{k \cdot q\})$ where D are the inverse propagators and $k_i \cdot q_j$ are the physical space irreducible scalar products (ISPs) for a given topology, where q_j are suitable linear combinations of external momenta. The coefficients in the spurious

and (-2ϵ)-dimensional spaces are functions of the additional ISPs $k_i \cdot \omega_j$ and $\mu_{ij} = -k_{\perp,i}^{[-2\epsilon]} \cdot k_{\perp,j}^{[-2\epsilon]}$ respectively. Having completed this decomposition we find relations between monomials in the ISPs by expanding (5.5), see also (3.23),

$$\mu_{ij} = k_i \cdot k_j - k_{\parallel,i} \cdot k_{\parallel,j} - k_{\perp,i}^{[4]} \cdot k_{\perp,j}^{[4]}. \tag{5.7}$$

From this equation it is easy to obtain a valid basis of monomials for each irreducible numerator of a dimensionally regulated amplitude by using (5.7) to remove dependence on the extra dimensional ISPs. This basis is just the most general polynomial in the ISPs $k_i \cdot q_j$ and $k_i \cdot \omega_j$ where the power counting is restricted by the renormalisability constraints.

This simple basis, without dependence on μ_{ij} monomials, is trivial to obtain without polynomial division but results in high rank tensor integrals with a complicated infrared (IR) pole structure. Instead we prefer to map to a new basis which prefers to keep monomials in μ_{ij} in the numerator and make the $\epsilon \to 0$ limit easier to perform. The map to the new basis is performed in four steps,

1. Write down an over-complete set of monomials in $k_i \cdot q_j$, $k_i \cdot \omega_j$, and μ_{ij} obeying the power counting restrictions.

2. Choose a set of criteria to order the over-complete set of monomials (for example prefer lower rank monomials or prefer monomials proportional to μ_{ij}).

3. Map each monomial containing μ_{ij} from the set of step 1) onto a linear combination of monomials of the simple basis using equation (5.7), to obtain a system of linear relations between monomials in the over-complete set.

4. Solve for the independent monomials of this linear system to find the new basis.

The result of this procedure is a process-independent basis of monomials whose coefficients can be fixed from unitarity cuts in six dimensions. We take a top-down, OPP-like, approach to solving the complete system using information from previously computed cuts to remove known poles from the factorised product of tree amplitudes using the six-dimensional spinor-helicity formalism [27]. The product of tree amplitudes is efficiently evaluated by sewing together Berends-Giele currents [26] as described in [119].

We can improve the integrand basis further by replacing some monomials with spurious integrands. These spurious integrands are constructed by building in integration identities and symmetry relations. For example, the three-propagator sunrise topology in Figure 5.2 is invariant under the exchange $k_1 \leftrightarrow k_2$. Extra-dimensional monomials, μ_{ii}, of rank two are swapped under this symmetry,

$$\mu_{11} \underset{k_1 \leftrightarrow k_2}{\leftrightarrow} \mu_{22}. \tag{5.8}$$

We can use this to obtain a spurious polynomial in place of a non-spurious monomial,

$$\mu_{22} \to \mu_{22} - \mu_{11}, \tag{5.9}$$

for the sunrise topologies. Similarly, the bubble insertion topologies appearing in Figure 5.2 and 5.3 have the symmetry $k_2 \to -k_1 - k_2$. Under this transformation we have for example,

$$\mu_{12} \underset{k_2 \to -k_1 - k_2}{\to} -\mu_{11} - \mu_{12}. \tag{5.10}$$

We therefore obtain a spurious polynomial by replacing the non-spurious monomial,

$$\mu_{12} \to \mu_{11} + 2\mu_{12}, \tag{5.11}$$

for bubble insertion topologies.

For the spurious space we note that integrands with odd powers of spurious monomials vanish. This can be seen from a Passarino-Veltman tensor decomposition argument as there are no physical vectors to expand in. Writing out a quadratic monomial in the spurious ISPs,

$$(k_i \cdot \omega_j)^2 = k_i^\mu k_i^\nu \omega_{j\mu} \omega_{j\nu} \qquad \text{(no sum over } i \text{ and } j\text{)}, \tag{5.12}$$

we get the tensor decomposition,

$$k_i^\mu k_i^\nu = A \eta_{\perp,[4]}^{\mu\nu} \Rightarrow A = \frac{k_{\perp,i}^{[4]} \cdot k_{\perp,i}^{[4]}}{d_\perp}, \tag{5.13}$$

where $\eta_{\perp,[4]}^{\mu\nu} \eta_{\perp,[4]\,\mu\nu} = d_\perp$. This means that we can construct a spurious integrand

helicity	flavour	non-zero coefficients	non-spurious coefficients	contributions @ $\mathcal{O}(\epsilon^0)$
	$(d_s-2)^0$	50	50	0
$+++++$	$(d_s-2)^1$	175	165	50
	$(d_s-2)^2$	320	90	60
	$(d_s-2)^0$	1153	761	405
$-++++$	$(d_s-2)^1$	8745	4020	3436
	$(d_s-2)^2$	1037	100	68
	$(d_s-2)^0$	2234	1267	976
$--+++$	$(d_s-2)^1$	11844	5342	4659
	$(d_s-2)^2$	1641	71	48
	$(d_s-2)^0$	3137	1732	1335
$-+-++$	$(d_s-2)^1$	15282	6654	5734
	$(d_s-2)^2$	3639	47	32

Table 5.1 *The number of non-zero coefficients found at the integrand level both before ('non-zero') and after ('non-spurious') removing monomials which integrate to zero. Last column ('contributions @ $\mathcal{O}(\epsilon^0)$') gives the number of coefficients contributing to the finite part. Each helicity amplitude is split into the components of $d_s - 2$.*

by replacing the monomial in (5.12),

$$(k_i \cdot \omega_j)^2 \to (k_i \cdot \omega_j)^2 - \frac{\omega_j^2}{d_\perp} k_{\perp,i}^{[4]} \cdot k_{\perp,i}^{[4]}. \tag{5.14}$$

For example, rather than fitting the coefficient of $(k_1.\omega_2)^2$ we replace it with the function

$$(k_1 \cdot \omega_2)^2 \longrightarrow (k_1 \cdot \omega_2)^2 - \frac{\omega_2^2}{d_\perp} k_{\perp,1}^{[4]} \cdot k_{\perp,1}^{[4]}, \tag{5.15}$$

which will integrate to zero. In Appendix E we show a selection of our integrand bases. In Table 5.1 we summarise the result of our fit to unitarity cuts listing the number of non-zero coefficients at the integrand level before and after performing the integration over the spurious space.

After completing the integrand level reconstruction, the remaining transverse integration must be performed to obtain a form compatible with traditional integration-by-parts (IBP) relations. Following a recent approach [120], we have two options in order to achieve this: 1) to integrate the full transverse space to remove $k_i \cdot \omega_j$ and μ_{ij} introducing dependence in ϵ into the integral coefficients or, 2) integrate only over the spurious space retaining μ_{ij} dependence which can

subsequently be removed through dimension shifting identities. In this work we have taken the second approach since it turned out to have better numerical stability to use dimension shifted integrals instead of high rank tensor integrals.

Cuts with scalar loops are required for the reduction from 6 to $4-2\epsilon$ dimensions. We perform the fit taking into account the individual contribution of these scalar loops in order to reconstruct the dependence of the numerator on the spin dimension $d_s = g^{\mu}{}_{\mu}$. The relevant scalar loops are discussed in [56]. In [108] the d_s-dependent integrands are decomposed according to their loop flavour content. In six dimensions this decomposition is,

$$\Delta_T^{d_s} = \Delta_T^g + (d_s - 6)\Delta_T^s + (d_s - 6)^2\Delta_T^{s^2}. \tag{5.16}$$

The second term on the right hand side receives contributions from a single closed scalar loop. The last term receives contribution from two closed scalar loops and therefore only get contributions from the (1-loop)^2 topologies in Figure 5.1. We prefer a decomposition around $d_s = 2$,

$$\Delta_T^{d_s} = \Delta_T^{[0]} + (d_s - 2)\Delta_T^{[1]} + (d_s - 2)^2\Delta_T^{[2]}, \tag{5.17}$$

and read off the contributions,

$$\Delta_T^{[0]} = \Delta_T^g - 4\Delta_T^s + 16\Delta_T^{s^2}, \tag{5.18a}$$
$$\Delta_T^{[1]} = \Delta_T^s - 8\Delta_T^{s^2}, \tag{5.18b}$$
$$\Delta_T^{[2]} = \Delta_T^{s^2}. \tag{5.18c}$$

Expanding the amplitudes around $d_s = 2$ yields,

$$A^{(1)}\left(1_g, 2_g, 3_g, 4_g, 5_g\right) = \sum_{i=0}^{1}(d_s - 2)^i A^{(1),[i]}\left(1_g, 2_g, 3_g, 4_g, 5_g\right), \tag{5.19a}$$

$$A^{(2)}\left(1_g, 2_g, 3_g, 4_g, 5_g\right) = \sum_{i=0}^{2}(d_s - 2)^i A^{(2),[i]}\left(1_g, 2_g, 3_g, 4_g, 5_g\right). \tag{5.19b}$$

This is useful since the $d_s = 2$ limit behaves like a supersymmetric amplitude, where additional cancellations and simplifications can be seen. One can show that setting $d_s = 2$ is equivalent to performing a supersymmetric decomposition [97] with $n_f = 0$ adjoint fermions and $n_s = -1$ (complex) adjoint scalars, and that this yields a linear combination of supersymmetric contributions.

The fit can be performed efficiently using rational numerics for each phase space point and in most cases it was possible to obtain completely analytic expressions for the integrands of the helicity amplitudes using modest computing resources.

5.1.3 Numerical evaluation

The unitarity based method outlined above has been complemented by an approach based on numerical evaluation of Feynman diagrams to determine the coefficients of independent monomial bases. Both of these methods use a momentum twistor [40] parametrisation of the external kinematics to obtain a rational numerical phase-space point, as described in section 2.3. This is extremely important since in order to make use of the finite field reconstruction methods our numerical algorithm must be free of all square roots [121–124]. The momentum twistor parametrisation is given in (2.73). These methods have been implemented using a combination of tools including QGRAF [125], FORM [126, 127], MATHEMATICA and a private implementation of the finite field reconstruction method [119]. A short introduction to the techniques of the latter is given in Appendix D.

We have validated our setup on a number of known cases. Firstly, we have reproduced integrand level expressions for the 'all-plus' helicity sector [106] and against the known integrands in $\mathcal{N} = 4$ Super-Yang-Mills theory [128]. The latter check was obtained by computing all fermion and (complex)-scalar loop contributions and subsequently setting $n_f = \mathcal{N}$ and $n_s = \mathcal{N} - 1$. We also have performed gauge invariance checks at the integrand level using the Feynman diagram setup.

To obtain a numerical value for the complete amplitude after integration we perform a sector decomposition of the basis integrals combined with Monte Carlo integration. After applying dimension shifting relations [96, 129, 130] to rewrite the extra-dimensional ISPs as standard integrals we processed the full set of integrals using both FIESTA [131] and PYSECDEC [132] packages. This setup was validated with the four-gluon helicity amplitudes and cross-checked against results in the literature [116]. Simple topologies with $2 \to 2$ kinematics were reduced to the known master integrals (MIs) of [133] using IBPs from FIRE5 [134] and REDUZE2 [135] and dimensional recurrence relations from LITERED [93]. This gave a substantial improvement in the numerical accuracy.

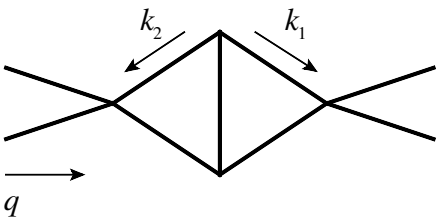

Figure 5.4 *Double-triangle topology with momentum q flowing through.*

We briefly discuss the used techniques in the following sections. An example of an integration-by-parts identity and the Laporta algorithm are presented. Next, two complementary methods for dealing with μ_{ij}-integrals are discussed. The method of dimension shifting was applied in this work, while transverse integration has similarities to the integrand improvements discussed in section 5.1.2 and also applies to monomials quadratic in the spurious ISPs.

Integration-by-parts identities

A large number of the two-loop integrals appearing after integrand reduction are linearly related through integration by parts identities (IBPs) [136–140]. These relations arise from the vanishing integration of total derivatives in dimensional regularisation,

$$0 = \int \prod_{i=1}^{L} \frac{d^d k_i}{(2\pi)^{d/2}} \frac{\partial}{\partial k_j^\mu} \frac{v_j^\mu P}{D_0^{a_0} ... D_k^{a_k}}, \tag{5.20}$$

for L loops and $k+1$ propagators. v^μ is taken to be any independent external momentum or loop momentum. In particular, special linear combinations of momenta can be used to avoid double propagators. The polynomial, P, is a function of the ISPs and denominators, D. The system closes provided a complete set of independent v_j^μ's are used and by considering P of sufficiently high degree.

As a simple demonstration of the linear relations derived from (5.20) we consider the double-triangle topology, shown in Figure 5.4. The associated scalar integral is,

$$I_{\text{double-triangle}} = \int \frac{d^d k_1}{(2\pi)^{d/2}} \frac{d^d k_2}{(2\pi)^{d/2}} \frac{1}{k_1^2 (k_1 - q)^2 k_2^2 (k_2 + q)^2 (k_1 + k_2)^2}. \tag{5.21}$$

For this two-loop, $L = 2$, example we set $j = 1$ in (5.20) and choose $v_1^\mu = k_1^\mu + k_2^\mu$

and $P = 1$ to obtain the identity,

$$0 = \int \frac{d^d k_1}{(2\pi)^{d/2}} \frac{d^d k_2}{(2\pi)^{d/2}} \frac{\partial}{\partial k_1^\mu} \frac{k_1^\mu + k_2^\mu}{k_1^2 (k_1 - q)^2 k_2^2 (k_2 + q)^2 (k_1 + k_2)^2}. \tag{5.22}$$

After differentiation we obtain,

$$\begin{aligned} \epsilon \int \frac{d^d k_1}{(2\pi)^{d/2}} \frac{d^d k_2}{(2\pi)^{d/2}} \frac{1}{k_1^2 (k_1 - q)^2 k_2^2 (k_2 + q)^2 (k_1 + k_2)^2} \\ = \int \frac{d^d k_1}{(2\pi)^{d/2}} \frac{d^d k_2}{(2\pi)^{d/2}} \frac{1}{k_1^2 (k_1 - q)^4 k_2^2} \left(\frac{1}{(k_1 + k_2)^2} - \frac{1}{(k_2 + q)^2} \right), \end{aligned} \tag{5.23}$$

where $\epsilon = \frac{1}{2}(4 - d)$ is the dimensional regularisation parameter. Relations like $k_1 \cdot q = -\frac{1}{2}(D_1 - D_0)$, that were heavily used for one-loop integrals in section 3.1, were applied in this calculation as well. The two integrals on the right hand side turn out to be easier to evaluate than the one we started out with [137]. Notice that each term in an IBP relation (5.20) is at most linear in the space-time dimension, $d = 4 - 2\epsilon$.

Constructing a complete set of linear IBP relations is a challenge as the amount of relations grows rapidly with increasing numbers of loops and legs. A systematic approach to this problem is provided by the Laporta algorithm [138]. The key idea is to divide the Feynman integrals into subsystems defined by the number of propagators and the exponents appearing in the numerator and denominator. Starting from scalar integrals with the lowest number of propagators the algorithm works its way upwards, eliminating integrals according to a predefined ordering. Upper limits on the exponents of propagators and numerators are imposed at each step to bound the system. Since the system is under-determined, not all integrals can be eliminated. The remaining integrals are known as master integrals (MIs). The Laporta algorithm exists in numerous implementations, see for example [141–147].

By applying a complete set of IBP relations we end up with a set of master integrals, $\mathcal{I}(\{x_i\}, \epsilon)$, where x_i are kinematic variables. These master integrals can be evaluated using the differential equation method. Differentiating with respect to the kinematic variables, a system of differential equations is obtained,

$$\frac{\partial}{\partial x_m} \mathcal{I}(\{x_i\}, \epsilon) = A_m(\{x_i\}, \epsilon) \mathcal{I}(\{x_i\}, \epsilon). \tag{5.24}$$

Using appropriate boundary conditions, for example from physical limits, the master integrals can be obtained. The set of master integrals, $\mathcal{I}$, is not unique and choosing a set with specific properties can greatly help in solving the differential equations. In [148] a canonical form of the system (5.24) which has proven very successful at two loops was first presented. In particular this approach led to the results for planar five-point integrals presented in [98] that are used in this chapter.

Dimension shifting

Integrals with numerator dependence on extra-dimensional ISPs, μ_{ij}, can be replaced with higher dimensional scalar integrals at the cost of introducing squared propagators [96]. We show this procedure by again taking the double triangle as example, Figure 5.4. We start by rewriting the scalar integral (5.21),

$$I_{\text{double-triangle}} = \int \frac{d^d k_1}{(2\pi)^{d/2}} \frac{d^d k_2}{(2\pi)^{d/2}} \int_0^\infty \prod_{i=1}^{5} dt_i \exp\big[- t_1 k_1^2 - t_2 (k_1 - q)^2 - t_3 k_2^2 - t_4 (k_2 + q)^2 - t_5 (k_1 + k_2)^2 \big], \tag{5.25}$$

by using the Schwinger parametrisation,

$$\frac{1}{D_i} = \int_0^\infty dt_i \ \exp\left[-t_i D_i\right], \tag{5.26a}$$

$$\frac{1}{D_i^\alpha} = \frac{1}{\Gamma(\alpha)} \int_0^\infty dt_i \ t_i^{\alpha-1} \exp\left[-t_i D_i\right]. \tag{5.26b}$$

The second identity can be verified using integration by parts. We continue by splitting up the loop momentum in a four-dimensional and an extra-dimensional part, $k_i = \bar{k}_i + \tilde{k}_i$, and note that for four-dimensional momentum q,

$$(k_i + q)^2 = \big(\bar{k}_i + q\big)^2 + \tilde{k}_i^2. \tag{5.27}$$

Splitting up the measure, we perform the extra-dimensional part of the integration,

$$\begin{aligned}
&\int d^{-2\epsilon}\tilde{k}_1 d^{-2\epsilon}\tilde{k}_2 \ \exp\left[-(t_1+t_2+t_5)\tilde{k}_1^2-(t_3+t_4+t_5)\tilde{k}_2^2-2(t_5)\tilde{k}_1\cdot\tilde{k}_2\right] \\
&= \int d^{-2\epsilon}\tilde{k}_1 d^{-2\epsilon}\tilde{k}_2 \ \exp\left[-(T_1+T_3)\tilde{k}_1^2-(T_2+T_3)\tilde{k}_2^2-2(T_3)\tilde{k}_1\cdot\tilde{k}_2\right] \\
&= \left(\frac{T_1T_2+T_2T_3+T_3T_1}{\pi}\right)^{\epsilon}, \qquad (5.28)
\end{aligned}$$

where we introduced $T_1 = t_1+t_2$, $T_2 = t_3+t_4$, and $T_3 = t_5$ and did the integration by completing the square. Acting with $\frac{\partial}{\partial T_1}$ on the equation above we derive a replacement rule,

$$\mu_{11} \to \epsilon\frac{T_2+T_3}{T_1T_2+T_2T_3+T_3T_1}, \qquad (5.29)$$

since $\mu_{11} = -\tilde{k}_1^2$. We obtain similar results for the other extra-dimensional IBPs by appropriately chosen differential operators.

Turning back to (5.25) but with numerator insertion μ_{11} we have,

$$\begin{aligned}
I_{\text{double-triangle}}[\mu_{11}] &= \int \frac{d^dk_1}{(2\pi)^{d/2}}\frac{d^dk_2}{(2\pi)^{d/2}}\int_0^\infty \prod_{i=1}^5 dt_i \ \mu_{11}\exp[\dots] \\
&\to \epsilon\int \frac{d^dk_1}{(2\pi)^{d/2}}\frac{d^dk_2}{(2\pi)^{d/2}}\int_0^\infty \prod_{i=1}^5 dt_i \ \frac{T_2+T_3}{T_1T_2+T_2T_3+T_3T_1}\exp[\dots], \qquad (5.30)
\end{aligned}$$

where the exponential is unchanged from the original Schwinger parametrisation expression. Completing the square to perform the integration over the loop momenta we obtain,

$$\begin{aligned}
I_{\text{double-triangle}}[\mu_{11}] &= \epsilon\int_0^\infty \prod_{i=1}^5 dt_i \ \frac{T_2+T_3}{T_1T_2+T_2T_3+T_3T_1}(T_1T_2+T_2T_3+T_3T_1)^{-d/2} \\
&\qquad \times \exp\left[\frac{-Q(q^2,t_i)}{T_1T_2+T_2T_3+T_3T_1}\right] \\
&= \epsilon\int_0^\infty \prod_{i=1}^5 dt_i \ (T_2+T_3)(T_1T_2+T_2T_3+T_3T_1)^{-(d+2)/2} \\
&\qquad \times \exp\left[\frac{-Q(q^2,t_i)}{T_1T_2+T_2T_3+T_3T_1}\right]. \qquad (5.31)
\end{aligned}$$

The exact form of $Q(q^2, t_i)$ is not important for our current purposes. Since the dimension, d, only appears in the exponent this corresponds to a higher dimensional Feynman integral with squared propagators coming from the term $T_2 + T_3$. The dimension can be lowered using dimensional recurrence relations described in [130, 149] and implemented in LiteRed [93].

Transverse integration

For completeness, we introduce a method for transverse integration even though the method of dimension shifting was used in our paper [2]. Integrating out dependence on $k_i \cdot \omega_i$ and μ_{ij} this way, comes at the expense of introducing dependence on space-time dimension, $d = 4 - 2\epsilon$, in the integral coefficients. The idea relies on the decomposition of the loop momenta (5.5) used previously,

$$k_i^\mu = k_{\parallel,i}^\mu + k_{\perp,i}^\mu = k_{\parallel,i}^\mu + k_{\perp,i}^{[4]\mu} + k_{\perp,i}^{[-2\epsilon]\mu}, \tag{5.32}$$

as well as a decomposition of the metric tensor,

$$\eta^{\mu\nu} = \eta_\parallel^{\mu\nu} + \eta_\perp^{\mu\nu} = \eta_\parallel^{\mu\nu} + \eta_\perp^{[4]\mu\nu} + \eta_\perp^{[-2\epsilon]\mu\nu}. \tag{5.33}$$

For extra-dimensional monomials we do the following replacement,

$$\begin{aligned}
\mu_{ij} &= k_{\perp,i}^{[-2\epsilon]} \cdot k_{\perp,j}^{[-2\epsilon]} \\
&= k_{\perp,i\,\rho} k_{\perp,j\,\sigma} \eta_\perp^{[-2\epsilon]\mu\rho} \eta_\perp^{[-2\epsilon]\nu\sigma} \eta_{\mu\nu} \\
&= \frac{k_{\perp,i} \cdot k_{\perp,j}}{d_\perp - 2\epsilon} \eta_{\perp,\rho\sigma} \eta_\perp^{[-2\epsilon]\mu\rho} \eta_\perp^{[-2\epsilon]\nu\sigma} \eta_{\mu\nu} \\
&= \frac{-2\epsilon}{d_\perp - 2\epsilon} k_{\perp,i} \cdot k_{\perp,j} \\
&= \frac{-2\epsilon}{d_\perp - 2\epsilon} \left(k_{\perp,i}^{[4]} \cdot k_{\perp,j}^{[4]} + \mu_{ij} \right),
\end{aligned} \tag{5.34}$$

where we used a Passarino-Veltman like tensor decomposition in the third line and that $k_{\perp,i} = k_{\perp,i}^{[4]} + k_{\perp,i}^{[-2\epsilon]}$. It follows from (5.7) that $k_{\perp,i} \cdot k_{\perp,j}$ is only a function of propagators and physical ISPs. The same method can be applied to higher rank μ_{ij}^n monomials with an appropriate generalisation of the tensor decomposition,

$$k_{\perp,i_1}^{\mu_1} \dots k_{\perp,i_{2n}}^{\mu_{2n}} = \sum_{\sigma \in S} A_{\sigma(1)\dots\sigma(2n)} \eta_\perp^{\mu_{\sigma(1)}\mu_{\sigma(2)}} \dots \eta_\perp^{\mu_{\sigma(2n-1)}\mu_{\sigma(2n)}}, \tag{5.35}$$

where at two loops the indices $i_1, ..., i_{2n} = i, j$. The sum is over non-equivalent permutations, S, of the Lorentz indices.

Following similar steps for the spurious ISPs, $k_i \cdot \omega_j$, we get,

$$(k_i \cdot \omega_j)^2 = \frac{\omega_j^2}{d_\perp - 2\epsilon}\, k_{\perp,i} \cdot k_{\perp,i}. \tag{5.36}$$

We see that expressing spurious and extra-dimensional ISPs in terms of propagators and physical ISPs has come at the cost of introducing dependence on space-time dimensionality via $\epsilon = \frac{1}{2}(4 - d)$.

5.1.4 Benchmark results

	ϵ^{-4}	ϵ^{-3}	ϵ^{-2}	ϵ^{-1}	ϵ^0
$\widehat{A}^{(2),[0]}_{--+++}$	12.5	27.7526	-23.773	-168.117	-175.207±0.004
$P^{(2),[0]}_{--+++}$	12.5	27.7526	-23.773	-168.116	—
$\widehat{A}^{(2),[0]}_{-+-++}$	12.5	27.7526	2.5029	-35.8094	69.661±0.009
$P^{(2),[0]}_{-+-++}$	12.5	27.7526	2.5028	-35.8086	—

Table 5.2 *The numerical evaluation of* $\widehat{A}^{(2),[0]}(1,2,3,4,5)$ *for the Euclidean phase space point in* (5.37)*. The comparison with the universal pole structure,* P*, is shown. The* `+++++` *and* `-++++` *amplitudes vanish to* $\mathcal{O}(\epsilon)$ *for this* $(d_s - 2)^0$ *component.*

We evaluate the obtained irreducible integrands and integrals numerically at a Euclidean phase space point,

$$s_{12} = -1, \quad s_{23} = -\frac{37}{78}, \quad s_{34} = -\frac{2023381}{3194997}, \quad s_{45} = -\frac{83}{102}, \quad s_{15} = -\frac{193672}{606645}, \tag{5.37}$$

which corresponds to the values of our momentum twistor variables in (2.73),

$$x_1 = -1, \quad x_2 = \frac{79}{90}, \quad x_3 = \frac{16}{61}, \quad x_4 = \frac{37}{78}, \quad x_5 = \frac{83}{102}. \tag{5.38}$$

The results for the evaluation are given in Table 5.2 and 5.3 for the amplitudes,

$$\widehat{A}^{(2),[i]}_{\lambda_1\lambda_2\lambda_3\lambda_4\lambda_5} = \frac{A^{(2),[i]}(1^{\lambda_1}, 2^{\lambda_2}, 3^{\lambda_3}, 4^{\lambda_4}, 5^{\lambda_5})}{A^{\text{LO}}(1^{\lambda_1}, 2^{\lambda_2}, 3^{\lambda_3}, 4^{\lambda_4}, 5^{\lambda_5})}, \tag{5.39}$$

with helicities λ_i and $A^{(2)} = \sum_{i=0}^{2}(d_s - 2)^i A^{(2),[i]}$. The leading order amplitudes A^{LO} are the tree-level for the `--+++` and `-+-++` and rational one-loop amplitudes

	ϵ^{-4}	ϵ^{-3}	ϵ^{-2}	ϵ^{-1}	ϵ^{0}
$\widehat{A}^{(2),[1]}_{+++++}$	0	0.0000	-2.5000	-6.4324	-5.311±0.000
$P^{(2),[1]}_{+++++}$	0	0	-2.5000	-6.4324	—
$\widehat{A}^{(2),[1]}_{-++++}$	0	0.0000	-2.5000	-12.749	-22.098±0.030
$P^{(2),[1]}_{-++++}$	0	0	-2.5000	-12.749	—
$\widehat{A}^{(2),[1]}_{--+++}$	0	-0.6250	-1.8175	-0.4871	3.127±0.030
$P^{(2),[1]}_{--+++}$	0	-0.6250	-1.8175	-0.4869	—
$\widehat{A}^{(2),[1]}_{-+-++}$	0	-0.6249	-2.7761	-5.0017	0.172±0.030
$P^{(2),[1]}_{-+-++}$	0	-0.6250	-2.7759	-5.0018	—

Table 5.3 *The numerical evaluation of* $\widehat{A}^{(2),[1]}(1,2,3,4,5)$ *and comparison with the universal pole structure,* P*, at the same kinematic point of Table 5.2.*

for the `+++++` and `-++++`. The finite (1-loop)^2 configuration $A^{(2),[2]}$ is presented in Table 5.4. Numerical accuracy is not an issue here since the integrand level reduction already leads to a basis of one-loop MIs. In addition, we find complete agreement with the finite part of the known integrated 'all-plus' amplitude [109].

In cases where the ϵ pole structure of the amplitudes is non-trivial we compared with the known universal IR structure [150–153] including the dependence on d_s extracted from the FDH scheme results [154]. The leading pole in $1/\epsilon^4$ was verified analytically and is therefore quoted exactly in Table 5.2 and 5.3. By comparing the agreement in the poles between the $(d_s-2)^0$ and $(d_s-2)^1$ we clearly see the effect of the highest rank tensor integrals which only appear in the latter case. We find convincing agreement between the poles and our amplitudes within the numerical integration error [1]. Since the full amplitude is the sum of all three parts we see in this case that the simple $(d_s-2)^0$ part dominates and the complete amplitude is evaluated with sub-percent level accuracy. This feature is probably not generic for the whole phase-space however.

While a lot of effort was taken to find manageable expressions, the final integrand form was still extremely large and significantly more challenging than the previously known 'all-plus' helicity configuration. One obvious next step is to include a full set of integration-by-parts identities and reduce the amplitude onto a basis of analytically computed master integrals.

[1] The uncertainty on the finite terms in Table 5.2 and 5.3 is a rough estimate made by comparing Fiesta evaluations with different numbers of sample points.

	$\widehat{A}^{(2),[2]}_{+++++}$	$\widehat{A}^{(2),[2]}_{-++++}$	$\widehat{A}^{(2),[2]}_{--+++}$	$\widehat{A}^{(2),[2]}_{-+-++}$
ϵ^0	3.6255	-0.0664	0.2056	0.0269

Table 5.4 *The numerical evaluation of finite* $\widehat{A}^{(2),[2]}(1,2,3,4,5)$ *helicity amplitudes at the same kinematic point of Table 5.2. As only one-loop integrals are required for these amplitudes the integration error is negligible.*

5.1.5 Evaluation in a physical region

For numerical evaluation in the physical region, we use a phase space point defined by the invariants

$$s_{12} = \frac{113}{7}, \quad s_{23} = -\frac{152679950}{96934257}, \quad s_{34} = \frac{1023105842}{138882415}, \quad s_{45} = \frac{10392723}{3968069}, \quad s_{15} = -\frac{8362}{32585}, \tag{5.40}$$

which corresponds to the values of our momentum twistor variables in (2.73),

$$x_1 = \frac{113}{7}, \quad x_2 = -\frac{2}{9} - \frac{i}{19}, \quad x_3 = -\frac{1}{7} - \frac{i}{5}, \quad x_4 = -\frac{1351150}{13847751}, \quad x_5 = \frac{91971}{566867}. \tag{5.41}$$

The results in the physical region have been obtained using the analytic expressions of the master integrals in [109], by-passing the time consuming step of integral evaluations with sector decomposition [131, 132] previously.

The master integrals were computed in [109] using first-order differential equations. All functions needed are expressed in terms of iterated integrals, where the integration kernels are taken from a set that was identified in [98]. The boundary conditions for the differential equations were determined by constraints such as the absence of unphysical branch cuts. We determined such boundary points for each of the physical regions, as well as for the Euclidean region.

Up to weight two, all master integrals are expressed in terms of logarithms and dilogarithms. Weight-three contributions are expressed in terms of Li_3 functions and in terms of one-dimensional integrals of logarithms and dilogarithms. At weight four, we use a representation proposed in [155] that allows to write the functions as a one-fold integral of known functions, leading to a fast and reliable numerical evaluation, for all kinematic regions.

As a validation of these formulas, we have performed numerical comparisons with [156] and, for the four-point subtopologies, with [133], finding perfect agreement.

	ϵ^{-4}	ϵ^{-3}	ϵ^{-2}	ϵ^{-1}	ϵ^{0}
$\widehat{A}^{(2),[0]}_{--+++}$	12.5	-9.17716 + 47.12389 i	-107.40046 - 25.96698 i	17.24014 - 221.41370 i	388.44694 - 167.45494 i
$\widehat{A}^{(2),[0]}_{-+-++}$	12.5	-9.17716 + 47.12389 i	-111.02853 - 12.85282 i	-39.80016 - 216.36601 i	342.75366 - 309.25531 i

Table 5.5 *The leading colour primitive two-loop helicity amplitudes for the $d_s = 2$ component of $\widehat{A}^{(2)}(1_g, 2_g, 3_g, 4_g, 5_g)$ at the physical phase space point given in the text.*

	ϵ^{-4}	ϵ^{-3}	ϵ^{-2}	ϵ^{-1}	ϵ^{0}
$\widehat{A}^{(2),[1]}_{+++++}$	0	0	-2.5	0.60532 - 12.48936 i	35.03354 + 9.27449 i
$\widehat{A}^{(2),[1]}_{-++++}$	0	0	-2.5	-7.59409 - 2.99885 i	-0.44360 - 20.85875 i
$\widehat{A}^{(2),[1]}_{--+++}$	0	-0.625	-0.65676 - 0.42849 i	-1.02853 + 0.30760 i	-0.55509 - 6.22641 i
$\widehat{A}^{(2),[1]}_{-+-++}$	0	-0.625	-0.45984 - 0.97559 i	1.44962 + 0.53917 i	-0.62978 + 2.07080 i

Table 5.6 *The leading colour primitive two-loop helicity amplitudes for the d_s-2 component of $\widehat{A}^{(2)}(1_g, 2_g, 3_g, 4_g, 5_g)$ at the physical phase space point given in the text.*

The numerical results in the physical region for the five-gluon partonic channel are shown in Table 5.5 - 5.7.

	$\widehat{A}^{(2),[2]}_{+++++}$	$\widehat{A}^{(2),[2]}_{-++++}$	$\widehat{A}^{(2),[2]}_{--+++}$	$\widehat{A}^{(2),[2]}_{-+-++}$
ϵ^0	0.60217 - 0.01985 i	-0.10910 - 0.01807 i	-0.06306 - 0.01305 i	-0.03481 - 0.00699 i

Table 5.7 *The leading colour primitive two-loop helicity amplitudes for the $(d_s-2)^2$ component of $\widehat{A}^{(2)}(1_g, 2_g, 3_g, 4_g, 5_g)$ at the physical phase space point given in the text.*

	ϵ^{-4}	ϵ^{-3}	ϵ^{-2}	ϵ^{-1}	ϵ^{0}
$\widehat{A}^{(2)}_{++++-}$	0	0	-4	-13.53227	6.04865
$\widehat{A}^{(2)}_{+++--}$	8	7.96829	-52.39270	-140.15637	47.56872
$\widehat{A}^{(2)}_{++-+-}$	8	7.96829	-32.22135	-47.92349	145.97201
$\widehat{A}^{(2)}_{+-++-}$	8	7.96829	-40.88511	-87.02993	101.23299

Table 5.8 *The leading colour primitive two-loop helicity amplitudes for* $\widehat{A}^{(2)}(1_q, 2_g, 3_g, 4_g, 5_{\bar{q}})$ *in the HV scheme at the Euclidean phase space point given in* (5.37)*.*

5.1.6 Quark amplitudes

For the amplitudes involving external quarks the colour decompositions are given by,

$$\mathcal{A}^{(L)}(1_q, 2_g, 3_g, 4_g, 5_{\bar{q}}) = n^L g_s^3 \sum_{\sigma \in S_3} \left(T^{a_{\sigma(2)}} T^{a_{\sigma(3)}} T^{a_{\sigma(4)}}\right)_{i_1}^{\bar{i}_5} \times A^{(L)}(1_q, \sigma(2)_g, \sigma(3)_g, \sigma(4)_g, 5_{\bar{q}}), \tag{5.42}$$

for a quark pair and three gluons channel and,

$$\mathcal{A}^{(L)}(1_q, 2_{\bar{q}}, 3_g, 4_Q, 5_{\bar{Q}}) = n^L g_s^3 \Big[\left(T^{a_3}\right)_{i_4}^{\bar{i}_2} \delta_{i_1}^{\bar{i}_5} A^{(L)}(1_q, 2_{\bar{q}}, 3_g, 4_Q, 5_{\bar{Q}}) + \big(1 \leftrightarrow 4, 2 \leftrightarrow 5\big) \Big], \tag{5.43}$$

for the case of two distinct quark pairs and one gluon. In addition we normalise all amplitudes to the leading order amplitudes which removes any complex phase, using again (5.39).

For the quark amplitudes we use the Feynman diagrammatic setup introduced in the previous section. 't Hooft algebra has been used to evaluate the extra-dimensional spinor strings and we use QGRAF [125] to generate Feynman diagrams and FORM [126, 127] to perform algebraic manipulations.

The numerical results are shown in Table 5.8 and 5.9 for the $qggg\bar{q}$ and $q\bar{q}gQ\bar{Q}$ partonic channels, respectively. We have compared the poles of our results against the known universal IR structure [150–153].

	ϵ^{-4}	ϵ^{-3}	ϵ^{-2}	ϵ^{-1}	ϵ^{0}
$\widehat{A}^{(2)}_{+-++-}$	4.5	2.28315	-32.09848	-41.39350	149.33050
$\widehat{A}^{(2)}_{+--+-}$	4.5	2.28315	-6.32369	-4.61657	-32.03278
$\widehat{A}^{(2)}_{+-+-+}$	4.5	2.28315	-38.29478	-43.52329	-56.71968
$\widehat{A}^{(2)}_{+---+}$	4.5	2.28315	-26.71316	-69.75805	22.23653

Table 5.9 *The leading colour primitive two-loop helicity amplitudes for* $\widehat{A}^{(2)}(1_q, 2_{\bar{q}}, 3_g, 4_Q, 5_{\bar{Q}})$ *in the HV scheme at the Euclidean phase space point given in the text.*

5.2 Reduction to pentagon functions

Analytic results can offer many benefits over numerical algorithms. The one-loop amplitudes for five-gluon scattering, first derived in 1993 by Bern, Dixon and Kosower [97], are strikingly simple. One immediate consequence of this is that amplitudes are fast and stable to evaluate numerically and well suited for Monte Carlo integration. Analytic results also give us more insight into the structure of on-shell amplitudes in gauge theory. Simplicity in maximally super-symmetric Yang-Mills theory has enabled huge leaps into the structure of perturbative amplitudes based on constraints from universal behaviour in physical limits [157–160]. While in QCD these constraints are not quite enough to fix the amplitudes (such techniques have been applied in the computation of the QCD soft anomalous dimension [161]), it would be an extremely powerful tool if the function space of multi-loop amplitudes could be better understood in general gauge theories.

In this section we present new, analytic results for the scattering of five gluons in pure Yang-Mills at two loops in which one gluon has negative helicity and the remaining gluons have positive helicities. We employ finite field numerics to a combined system of integrand reduction, integration-by-parts identities and expansion into a basis of pentagon functions. After multiple evaluations we were able to reconstruct the analytic form of the amplitude.

We use the same expansion of the amplitudes around $d_s = 2$ as used in (5.19b). In the case of the single-minus helicity configuration, it was already observed that $A^{(2),[0]}\left(1_g^-, 2_g^+, 3_g^+, 4_g^+, 5_g^+\right) = \mathcal{O}(\epsilon)$ [2].

Since the tree-level helicity amplitude is zero, the universal infrared (IR) poles

take a very simple form [150–153],

$$A^{(1),[1]}\left(1_g^-,2_g^+,3_g^+,4_g^+,5_g^+\right) = F^{(1),[1]}\left(1_g^-,2_g^+,3_g^+,4_g^+,5_g^+\right) + \mathcal{O}(\epsilon), \tag{5.44a}$$

$$A^{(2),[1]}\left(1_g^-,2_g^+,3_g^+,4_g^+,5_g^+\right) = \left[-\frac{r_\Gamma}{\epsilon^2}\sum_{i=1}^{5}\left(\frac{\mu_R^2 e^{\gamma_E}}{-s_{i,i+1}}\right)^\epsilon\right] A^{(1),[1]}\left(1_g^-,2_g^+,3_g^+,4_g^+,5_g^+\right) + F^{(2),[1]}\left(1_g^-,2_g^+,3_g^+,4_g^+,5_g^+\right) + \mathcal{O}(\epsilon), \tag{5.44b}$$

$$A^{(2),[2]}\left(1_g^-,2_g^+,3_g^+,4_g^+,5_g^+\right) = F^{(2),[2]}\left(1_g^-,2_g^+,3_g^+,4_g^+,5_g^+\right) + \mathcal{O}(\epsilon), \tag{5.44c}$$

where

$$r_\Gamma = \frac{\Gamma^2(1-\epsilon)\Gamma(1+\epsilon)}{\Gamma(1-2\epsilon)}. \tag{5.45}$$

Note that, in (5.44b), the one-loop amplitude[2], $A^{(1),[1]}$, needs to be expanded up to $\mathcal{O}(\epsilon^2)$. In this section we will present a direct computation of the finite remainder $F^{(2),[i]}$.

The kinematic parts of the amplitude are written using a momentum twistor [40] parametrisation, as described in section 2.3. We decompose the amplitude into an integrand basis, using the method of integrand reduction via generalised unitarity. We then reduce the amplitude to master integrals by solving IBPs. The master integrals are in turn expressed as combinations of known pentagon functions, using the expressions computed in reference [98].

The algorithm is implemented numerically over finite fields. The Laurent expansion in ϵ of the results is obtained by performing a full reconstruction of its dependence on the dimensional regulator ϵ, for fixed numerical values of the kinematic variables. The Laurent expansion of the reconstructed function of ϵ thus provides a numerical evaluation of the ϵ-expansion of the final result. Finally, the full dependence of the expanded result on the kinematic variables is reconstructed from multiple numerical evaluations, using a modified version of the multi-variate reconstruction techniques presented in reference [119].

In the next sections, 5.2.1 - 5.2.4, we provide more details on the various steps of the calculation outlined above before presenting our results in section 5.2.5.

[2]Expressions for the one-loop amplitudes can be obtained from the authors on request.

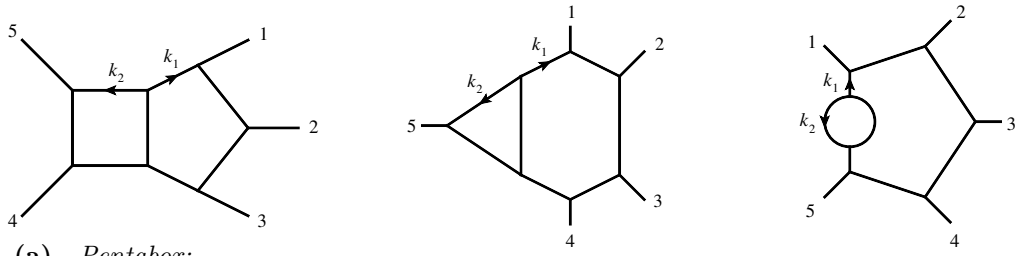

(a) *Pentabox:* $G_{11111111a_9a_{10}a_{11}}$

(b) *Hexatriangle:* $G_{111111a_711a_{10}a_{11}}$

(c) *Heptabubble:* $G_{21111a_6a_711a_{10}a_{11}}$

Figure 5.5 *Two-loop five-point master topologies. All external momenta are considered outgoing, arrows indicate loop momenta directions.*

5.2.1 Integration-by-parts compatible integrand reduction

We define an integral family by a complete, minimal set of propagators and irreducible scalar products (ISPs),

$$\begin{aligned} G_{a_1a_2a_3a_4a_5a_6a_7a_8a_9a_{10}a_{11}} = \int \frac{d^dk_1}{i\pi^{d/2}e^{-\epsilon\gamma_E}} \frac{d^dk_2}{i\pi^{d/2}e^{-\epsilon\gamma_E}} \\ \times \frac{1}{k_1^{2a_1}} \frac{1}{(k_1-p_1)^{2a_2}} \frac{1}{(k_1-p_1-p_2)^{2a_3}} \frac{1}{(k_1+p_4+p_5)^{2a_4}} \\ \times \frac{1}{k_2^{2a_5}} \frac{1}{(k_2-p_5)^{2a_6}} \frac{1}{(k_2-p_4-p_5)^{2a_7}} \frac{1}{(k_1+k_2)^{2a_8}} \\ \times \frac{1}{(k_1+p_5)^{2a_9}} \frac{1}{(k_2+p_1)^{2a_{10}}} \frac{1}{(k_2+p_1+p_2)^{2a_{11}}}, \end{aligned} \tag{5.46}$$

where the exponents, a_i, are integers and $d = 4-2\epsilon$. The three master topologies, shown in Figure 5.5, are,

$$\text{Pentabox:} \quad G_{11111111a_9a_{10}a_{11}}, \tag{5.47a}$$

$$\text{Hexatriangle:} \quad G_{111111a_711a_{10}a_{11}}, \tag{5.47b}$$

$$\text{Heptabubble:} \quad G_{21111a_6a_711a_{10}a_{11}}, \tag{5.47c}$$

while propagators with unspecified exponents, a_j, correspond to ISPs (i.e. $a_j \leq 0$).

All lower-point topologies are obtained by systematically pinching the propagators of the master topologies. Topologies with scaleless integrals are discarded since we work in dimensional regularisation. Pinching of propagators from different master topologies can lead to the same sub-topology. This happens in particular when all five cyclic permutations of the external momenta are included. In these cases the assignment to a master topology is not unique. The full set

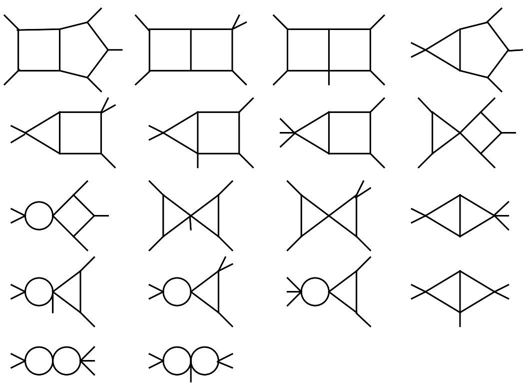

(a) *Topologies associated with the pentabox master topology (top left), see* (5.47a).

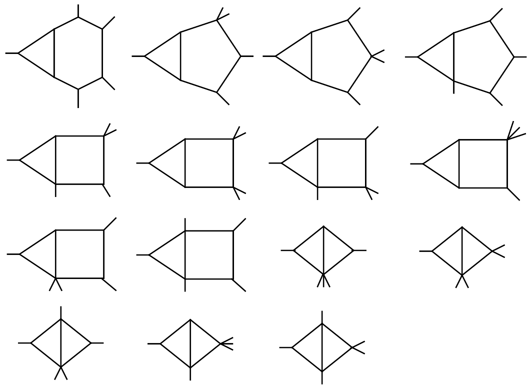

(b) *Topologies associated with the hexatriangle master topology (top left), see* (5.47b).

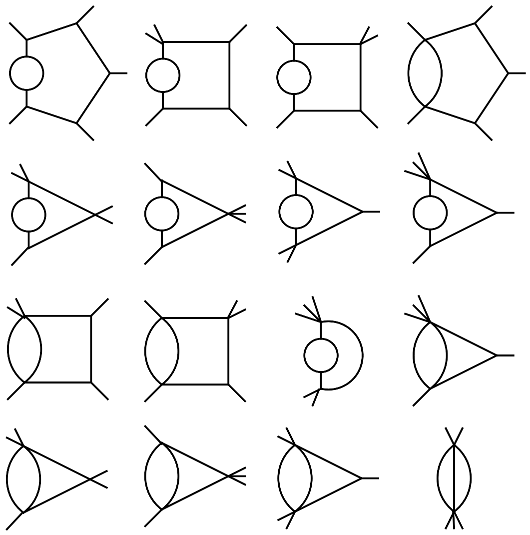

(c) *Topologies associated with the heptabubble master topology (top left), see* (5.47c).

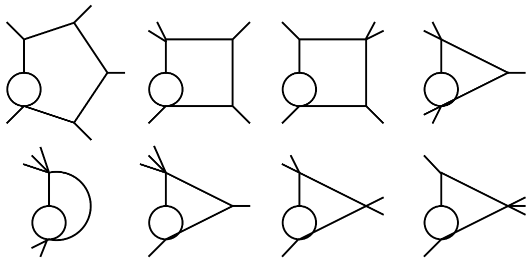

(d) *Topologies with divergent cuts that must be computed simultaneously with sub-topologies of the heptabubble master topology in Figure 5.6c.*

Figure 5.6 *All distinct two-loop five-point topologies.*

of 57 distinct topologies with a specific choice of master topology assignment is shown in Figure 5.6.

We parametrise the integrand numerators by writing the most general polynomials in the ISPs subject to a power counting constraint from renormalisability considerations. As an example, the pentabox of Figure 5.5a has the numerator parametrisation,

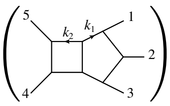

$$\Delta\left(\; \cdot \; \right) = \sum c_{11111111a_9a_{10}a_{11}}(k_1+p_5)^{-2a_9}(k_2+p_1)^{-2a_{10}}(k_2+p_1+p_2)^{-2a_{11}} \tag{5.48}$$

where the sum is truncated by the constraints on the exponents,

$$-5 \leq a_9 \leq 0, \tag{5.49a}$$

$$-4 \leq a_{10} + a_{11} \leq 0, \tag{5.49b}$$

$$-7 \leq a_9 + a_{10} + a_{10} \leq 0. \tag{5.49c}$$

Each topology has $11 - n$ ISPs where n is the number of distinct propagators. The five cyclic permutations of the external legs give a total of 425 irreducible numerators.

Integrand representations of the form (5.48) are less compact than representations making use of, for example, local integrands, spurious integrands, and extra-dimensional ISPs [2, 106–108, 162–164]. However, in our set-up the integrand is only sampled numerically and not analytically reconstructed. Simplification at the integrand level is therefore not a priority. Because our final integrated amplitude does not depend on the choice of integrand parametrisation, we have chosen a form which is directly compatible with IBPs, rather than one yielding a compact integrand representation. On the other hand there is potential for considerable improvements in the efficiency of the algorithm if a simpler integrand form could be identified.

We take a top down approach to solving the complete system of integrands which, apart from the basis choice described above, is identical to the approach taken in the previous section. The tree amplitudes used to compute the generalised unitarity cuts are evaluated by contracting Berends-Giele currents [26] as described in [119] and we use the six-dimensional spinor-helicity formalism [27]. Eight topologies, shown in Figure 5.6d, have divergent cuts and their integrand coefficients are determined simultaneously with sub-topologies in the heptabubble group, see Figure 5.6c. This follows the approach used previously in section 5.1.1 and references [2, 117].

The numerical sampling of the integrand can show quickly which coefficients vanish and hence what integrals require further reduction using IBPs. The number of non-vanishing coefficients at the integrand level split into the components of $d_s = 2, (d_s - 2), (d_s - 2)^2$ are $4387, 14565, 4420$ respectively. We find the maximum rank to be 5 for genuine two-loop topologies and rank 6 for a few integrals in the $(d_s - 2)^2$ component of the amplitude that can be written as (1-loop)^2 integrals, see Figure 5.6a.

At the end of the integrand reduction stage, the colour-ordered amplitude can be written as,

$$A^{(2)}\left(1,2,3,4,5\right) = \sum_{\mathbf{a}} c_{\mathbf{a}}^{[\partial \mathrm{A}]}\, G_{\mathbf{a}}, \tag{5.50}$$

where we sum over the tuples $\mathbf{a} = (a_1, a_2, a_3, a_4, a_5, a_6, a_7, a_8, a_9, a_{10}, a_{11})$. The coefficients $c_{\mathbf{a}}^{[\partial \mathrm{A}]}$ are rational functions in the momentum twistor variables only.

5.2.2 Integration-by-parts reduction

Each integral appearing in (5.50) is reduced to a set of master integrals J_k,

$$G_{\mathbf{a}} = \sum_{k} c_{\mathbf{a}k}^{[\mathrm{IBP}]} J_k, \tag{5.51}$$

where the sum runs over 155 master integrals (remembering that we include the 5 cyclic permutations of the integral family G). The reduction is obtained by solving a traditional Laporta system of IBP equations [138]. The system is generated in Mathematica with the help of LiteRed [93], and solved over finite fields, for numerical values of ϵ and the kinematic invariants, with a custom general-purpose linear solver for sparse systems of equations. The master integrals are chosen to be the uniform weight functions identified by Gehrmann, Henn and Lo Presti [98]. The $c_{\mathbf{a}k}^{[\mathrm{IBP}]}$ are rational functions in the momentum twistor variables and the dimensional regularisation parameter ϵ.

5.2.3 Map to pentagon functions

Our next step is to expand the master integrals into a basis of pentagon functions defined by Gehrmann, Henn and Lo Presti. These functions can be written in terms of Goncharov Polylogarithms. We take the results of expanding the master integrals in ϵ from reference [98],

$$J_k = \sum_{x=0}^{4} \sum_{l} c_{kl;x}^{[\mathrm{f}]}\, \epsilon^x\, m_{l;x}(f) + \mathcal{O}(\epsilon^5), \tag{5.52}$$

where $m_{l;x}(f)$ are monomials in the pentagon functions (note that the coefficients $c_{kl;x}^{[\mathrm{f}]}$ depend on the choice of the pentagon functions f).

The amplitude can thus be written as a combination of pentagon functions,

$$A^{(2)}\left(1,2,3,4,5\right) = \sum_{l,x} c_{l;x}^{[\mathrm{A}]}\, m_{l;x}(f) + \mathcal{O}(\epsilon), \tag{5.53}$$

where the coefficients are defined through matrix multiplication, from the three reduction steps,

$$c_{l;x}^{[\mathrm{A}]} = \sum_{\mathbf{a},k} c_{\mathbf{a}}^{[\partial \mathrm{A}]}\, c_{\mathbf{a}k}^{[\mathrm{IBP}]}\, c_{kl;x}^{[\mathrm{f}]}\, \epsilon^x. \tag{5.54}$$

We recall that, in the previous equation, there is also an implicit dependence on ϵ coming from the $c_{\mathbf{a}k}^{[\mathrm{IBP}]}$, which were defined in (5.51) to be the full coefficients of the IBP reduction. Hence, the coefficients $c_{l;x}^{[\mathrm{A}]}$ are rational functions of ϵ which need to be expanded, as we will explain in the next subsection.

The final step of the algorithm is to perform the same decomposition for the universal IR poles in (5.44b). For this we need the one-loop master integrals expanded up to weight four and written in the same alphabet as the two-loop integrals. These results were obtained directly from the differential equations in a canonical basis.[3] We then write the poles analytically as,

$$\left[-\frac{r_\Gamma}{\epsilon^2}\sum_{j=1}^{5}\left(\frac{\mu_R^2 e^{\gamma_E}}{-s_{j,j+1}}\right)^{\epsilon}\right] A^{(1),[i]}\left(1_g^-, 2_g^+, 3_g^+, 4_g^+, 5_g^+\right) = \sum_{l,x} c_{l;x}^{[\mathrm{IR}]} m_{l;x}(f) + \mathcal{O}(\epsilon). \tag{5.55}$$

Our numerical algorithm can then compute the difference,

$$c_{l;x}^{[\mathrm{F}]} = c_{l;x}^{[\mathrm{A}]} - c_{l;x}^{[\mathrm{IR}]}, \tag{5.56}$$

which we will expand in ϵ to find the finite remainder. At this point we have constructed a numerical algorithm which combines integrand reduction, IBP reduction and expansion of the master integrals into a basis of polylogarithms. This algorithm can be used to compute the finite remainder of the two-loop amplitude through evaluations of generalised unitarity cuts over finite fields.

[3] We are very grateful to Adriano Lo Presti for assistance in setting up the differential equations used in [109].

5.2.4 Laurent expansion

In the previous subsections we described a numerical calculation over finite fields of the coefficients $c^{[\mathrm{F}]}_{l;x}$. They are used in order to write the finite remainder, $F^{(2),[i]}$, of the amplitude in terms of known pentagon functions. The coefficients, computed as described above, are rational functions of ϵ. However, because the calculation uses the expansion in (5.52) for the master integrals in terms of pentagon functions, it is only valid up to $\mathcal{O}(\epsilon)$. Here we are interested in the finite part of the Laurent expansion in ϵ.

As mentioned before, in order to obtain this Laurent expansion, we first perform a full reconstruction of the functions $c^{[\mathrm{F}]}_{l;x}$ in ϵ, for numerical values over finite fields of the momentum twistor variables. The reconstructed function can thus be expanded in ϵ up to the desired order. This yields a decomposition of the form,

$$c^{[\mathrm{F}]}_{l;x} = \sum_{y=-4}^{0} c^{[\mathrm{F}]}_{l;x,y}\epsilon^y + \mathcal{O}(\epsilon), \tag{5.57}$$

where we are interested in the finite parts $c^{[\mathrm{F}]}_{l;x,0}$, while $c^{[\mathrm{F}]}_{l;x,y} = 0$ for $y < 0$. The finite remainder is therefore,

$$F^{(2),[1]}\left(1_g^-, 2_g^+, 3_g^+, 4_g^+, 5_g^+\right) = \sum_{l}\sum_{x=0}^{4} c^{[\mathrm{F}]}_{l;x,0}\, m_{l;x}(f) + \mathcal{O}(\epsilon), \tag{5.58}$$

with $c^{[\mathrm{F}]}_{l;x,0}$ defined by the Laurent expansion in (5.57).

The algorithm described above numerically computes the coefficients $c^{[\mathrm{F}]}_{l;x,0}$ of the finite remainder of the amplitude over finite fields, for any numerical value of the kinematic invariants represented by the momentum twistor variables. Full analytic formulas for the coefficients $c^{[\mathrm{F}]}_{l;x,0}$, as rational functions of the momentum twistor variables, are reconstructed from multiple numerical evaluations. The number of sample points for the three components $d_s = 2, (d_s-2), (d_s-2)^2$ are $3, 2214, 22886$ respectively and sampling over one finite field is sufficient. For this purpose, we use a slightly improved version of the multivariate reconstruction techniques presented in reference [119][4]. We note the large difference in the number of sample points needed for the different components in the $d_s = 2$ expansion. This happens since the coefficients of the pentagon function basis

[4]These improvements concern performance, memory usage, and parallelization, and will be described in a later publication.

used in the fit contains higher powers of spurious poles for $(d_s-2)^2$ than for (d_s-2) even though the integrals and topologies appearing are much simpler. Once these expressions are collected and written in terms of the finite integral functions described in the next section, both amplitudes take similarly compact forms. The difference in time to perform the fit was not prohibitive in this case so further optimisation of the basis before the fit was unnecessary.

In the next section we give a compact form of this result, obtained from the one in terms of momentum twistor variables, after converting it into spinor products and momentum invariants via some additional algebraic manipulations.

5.2.5 Analytic results

We present a compact form of the amplitude by making use of the symmetry $(1,2,3,4,5) \to (1,5,4,3,2)$ and extracting an overall phase written in terms of spinor products,

$$F^{(L),[i]}\left(1_g^-,2_g^+,3_g^+,4_g^+,5_g^+\right) = \frac{[25]^2}{[12]\langle 23\rangle\langle 34\rangle\langle 45\rangle[51]}\big(F^{(L),[i]}_{\rm sym}(1,2,3,4,5) + F^{(L),[i]}_{\rm sym}(1,5,4,3,2)\big), \quad (5.59)$$

where L labels the loop order and i labels the component in the expansion around $d_s = 2$. The known result at one loop can be written as,

$$F^{(1),[1]}_{\rm sym}(1,2,3,4,5) = \frac{{\rm tr}_+(2315)^2{\rm tr}_+(1243)}{3s_{25}^2 s_{23}s_{34}s_{15}} - \frac{{\rm tr}_+(2543)}{6s_{34}}, \quad (5.60)$$

where ${\rm tr}_+(ijkl) = \frac{1}{2}{\rm tr}\left((1+\gamma_5)\gamma_\mu\gamma_\nu\gamma_\sigma\gamma_\rho\right)p_i^\mu p_j^\nu p_k^\sigma p_l^\rho$ and $s_{ij} = (p_i+p_j)^2$.

The finite parts of the two-loop amplitude can be written compactly in terms of weight two functions, just as at one loop. We therefore follow the same strategy as at one loop to find a basis of integral functions free of large cancellations due to spurious singularities. We find that a convenient basis for the d_s-2 component

of the amplitude is,

$$\begin{aligned} F^{(2),[1]}_{\text{sym}}(1,2,3,4,5) = \quad & c^{(2)}_{51} F^{(2)}_{\text{box}}(s_{23}, s_{34}, s_{15}) + c^{(2)}_{34} F^{(2)}_{\text{box}}(s_{12}, s_{15}, s_{34}) \\ & + c^{(1)}_{51} F^{(1)}_{\text{box}}(s_{23}, s_{34}, s_{15}) + c^{(1)}_{34} F^{(1)}_{\text{box}}(s_{12}, s_{15}, s_{34}) \\ & + c^{(0)}_{51} F^{(0)}_{\text{box}}(s_{23}, s_{34}, s_{15}) + c^{(0)}_{34} F^{(0)}_{\text{box}}(s_{12}, s_{15}, s_{34}) \\ & + c_{45} F^{(0)}_{\text{box}}(s_{12}, s_{23}, s_{45}) + c_{34;51} \hat{L}_1(s_{34}, s_{15}) + c_{51;23} \hat{L}_1(s_{15}, s_{23}) \\ & + c_{\text{rat}}, \end{aligned} \tag{5.61}$$

and

$$\begin{aligned} F^{(2),[2]}_{\text{sym}}(1,2,3,4,5) = \quad & d^{(3)}_{34} F^{(3)}_{\text{box}}(s_{12}, s_{15}, s_{34}) + d^{(2)}_{34} F^{(2)}_{\text{box}}(s_{12}, s_{15}, s_{34}) \\ & + d^{(3)}_{34;51} \hat{L}_3(s_{34}, s_{15}) + d^{(2)}_{34;51} \hat{L}_2(s_{34}, s_{15}) \\ & + d^{(3)}_{51;23} \hat{L}_3(s_{15}, s_{23}) + d^{(2)}_{51;23} \hat{L}_2(s_{15}, s_{23}) + d_{\text{rat}}, \end{aligned} \tag{5.62}$$

for the $(d_s - 2)^2$ amplitude.

The integral functions are written in terms of simple logarithms and di-logarithms. All weight one functions appear as logarithms of ratios of kinematic invariants,

$$L_k(s,t) = \frac{\log(t/s)}{(s-t)^k}, \tag{5.63}$$

where the singular behaviour is removed by defining,

$$\hat{L}_0(s,t) = L_0(s,t), \tag{5.64a}$$

$$\hat{L}_1(s,t) = L_1(s,t), \tag{5.64b}$$

$$\hat{L}_2(s,t) = L_2(s,t) + \frac{1}{2(s-t)} \left(\frac{1}{s} + \frac{1}{t} \right), \tag{5.64c}$$

$$\hat{L}_3(s,t) = L_3(s,t) + \frac{1}{2(s-t)^2} \left(\frac{1}{s} + \frac{1}{t} \right). \tag{5.64d}$$

At weight two all functions can be written in terms of the six-dimensional box

function,

$$F_{\text{box}}^{(-1)}(s,t,m^2) = \text{Li}_2\left(1-\frac{s}{m^2}\right) + \text{Li}_2\left(1-\frac{t}{m^2}\right) + \log\left(\frac{s}{m^2}\right)\log\left(\frac{t}{m^2}\right) - \frac{\pi^2}{6}, \tag{5.65a}$$

$$F_{\text{box}}^{(0)}(s,t,m^2) = \frac{1}{u(s,t,m^2)} F_{\text{box}}^{(-1)}(s,t,m^2), \tag{5.65b}$$

$$F_{\text{box}}^{(1)}(s,t,m^2) = \frac{1}{u(s,t,m^2)}\left[F_{\text{box}}^{(0)}(s,t,m^2) + \hat{L}_1(s,m^2) + \hat{L}_1(m^2,t)\right], \tag{5.65c}$$

$$\begin{aligned} F_{\text{box}}^{(2)}(s,t,m^2) =& \frac{1}{u(s,t,m^2)}\left[F_{\text{box}}^{(1)}(s,t,m^2) + \frac{s-m^2}{2t}\hat{L}_2(s,m^2)\right. \\ &\left. + \frac{m^2-t}{2s}\hat{L}_2(m^2,t) - \left(\frac{1}{s}+\frac{1}{t}\right)\frac{1}{4m^2}\right], \end{aligned} \tag{5.65d}$$

$$\begin{aligned} F_{\text{box}}^{(3)}(s,t,m^2) =& \frac{1}{u(s,t,m^2)}\left[F_{\text{box}}^{(2)}(s,t,m^2) - \frac{(s-m^2)^2}{6t^2}\hat{L}_3(s,m^2)\right. \\ &\left. - \frac{(m^2-t)^2}{6s^2}\hat{L}_3(m^2,t) - \left(\frac{1}{s}+\frac{1}{t}\right)\frac{1}{6m^4}\right], \end{aligned} \tag{5.65e}$$

where $u(s,t,m^2) = m^2 - s - t$.

These functions serve the same purpose as the Ls and L functions introduced by Bern, Dixon, and Kosower in [84, 97]. The $\hat{L}_i(s,t)$ are finite as $s \to t$ and the $F_{\text{box}}^{(i)}(s,t,m^2)$ are finite as $s \to -t + m^2$. The definitions have been changed very slightly with respect to the Ls and L functions since the singularities from the box functions at $m^2 - s - t$ have been removed without introducing additional singularities in $s - m^2$ or $t - m^2$. For the $(d_s - 2)$ amplitude the coefficients are,

$$c_{51}^{(2)} = \frac{5 s_{23} s_{34} \text{tr}_+(1234)^2 \text{tr}_+(1542)^2}{s_{12} s_{15} \text{tr}_+(2543)^2}, \tag{5.66a}$$

$$c_{51}^{(1)} = -\frac{\text{tr}_+(1234)^2 \text{tr}_+(1534)\text{tr}_+(2453)^2}{6 s_{12} s_{34} s_{35} \text{tr}_+(2543)^2}, \tag{5.66b}$$

$$\begin{aligned} c_{51}^{(0)} =& \frac{s_{15}s_{45}\text{tr}_+(1234)}{3\text{tr}_+(2543)} - \frac{s_{15}s_{24}s_{45}\text{tr}_+(1234)^2}{6s_{12}\text{tr}_+(2543)^2} - \frac{\text{tr}_+(1234)^2\text{tr}_+(1542)}{6\text{tr}_+(2543)^2} \\ &- \frac{s_{23}s_{24}\text{tr}_+(1234)\text{tr}_+(1543)}{6\text{tr}_+(2543)^2} - \frac{s_{12}s_{23}s_{34}\text{tr}_+(1542)\text{tr}_+(1543)}{3s_{15}\text{tr}_+(2543)^2} \\ &+ \frac{2s_{23}\text{tr}_+(1234)\text{tr}_+(1543)^2}{3s_{15}\text{tr}_+(2543)^2} - \frac{s_{24}\text{tr}_+(1234)\text{tr}_+(1543)^2}{6s_{15}\text{tr}_+(2543)^2} \\ &- \frac{s_{24}\text{tr}_+(1234)^2\text{tr}_+(1543)^2}{6s_{12}s_{15}s_{34}\text{tr}_+(2543)^2} - \frac{s_{24}\text{tr}_+(1235)\text{tr}_+(1243)\text{tr}_+(1543)^2}{6s_{12}s_{15}s_{34}\text{tr}_+(2543)^2} \\ &- \frac{\text{tr}_+(1234)\text{tr}_+(1543)\text{tr}_+(2453)}{2\text{tr}_+(2543)^2}, \end{aligned} \tag{5.66c}$$

$$c_{34}^{(2)} = \frac{5}{2} s_{12}^2 s_{15}^2, \tag{5.67a}$$

$$c_{34}^{(1)} = \frac{\mathrm{tr}_+(1245)\mathrm{tr}_+(1534)\mathrm{tr}_+(1543)}{3 s_{15} s_{34} s_{45}} + \frac{1}{12} s_{12} s_{15} s_{34}, \tag{5.67b}$$

$$\begin{aligned} c_{34}^{(0)} = &- \frac{s_{15} s_{23} \mathrm{tr}_+(1234)}{12 \mathrm{tr}_+(2543)} - \frac{\mathrm{tr}_+(1234)^2 \mathrm{tr}_+(1532)}{12 s_{12} s_{34} \mathrm{tr}_+(2543)} + \frac{s_{25} \mathrm{tr}_+(1234)\mathrm{tr}_+(1543)}{12 s_{34} \mathrm{tr}_+(2543)} \\ &+ \frac{s_{12} \mathrm{tr}_+(1532)\mathrm{tr}_+(1543)}{12 s_{15} \mathrm{tr}_+(2543)} + \frac{s_{23} s_{25} \mathrm{tr}_+(1234)\mathrm{tr}_+(1543)^2}{12 s_{15} s_{34} \mathrm{tr}_+(2543)^2} \\ &+ \frac{s_{12} \mathrm{tr}_+(1543)^2 \mathrm{tr}_+(2354)}{12 s_{15} s_{34} s_{45} \mathrm{tr}_+(2543)} + \frac{s_{25} \mathrm{tr}_+(2543)}{12 s_{34}} - \frac{1}{3} s_{12} s_{15}, \end{aligned} \tag{5.67c}$$

$$c_{45} = -\frac{s_{13} s_{45} \mathrm{tr}_+(1234)^2 \mathrm{tr}_+(1534)}{6 s_{12} s_{34} \mathrm{tr}_+(2543)^2} + \frac{s_{23}^3 s_{34} \mathrm{tr}_+(1543)}{6 \mathrm{tr}_+(2543)^2} - \frac{s_{13} s_{23} \mathrm{tr}_+(1243)\mathrm{tr}_+(1543)^2}{6 s_{15} s_{34} \mathrm{tr}_+(2543)^2}, \tag{5.68}$$

$$\begin{aligned} c_{34;51} = &\frac{s_{12} s_{15} s_{34} s_{45}}{6 \mathrm{tr}_+(2543)} - \frac{11 \mathrm{tr}_+(1234)\mathrm{tr}_+(1543)}{6 \mathrm{tr}_+(2543)} + \frac{\mathrm{tr}_+(1234)^2 \mathrm{tr}_+(1542)\mathrm{tr}_+(1543)}{6 s_{12} s_{34} \mathrm{tr}_+(2543)^2} \\ &- \frac{s_{12} \mathrm{tr}_+(1324)\mathrm{tr}_+(1543)^2}{6 s_{13} \mathrm{tr}_+(2543)^2} - \frac{s_{45} \mathrm{tr}_+(1234)^2 \mathrm{tr}_+(1534)\mathrm{tr}_+(2453)}{6 s_{12} s_{34} s_{35} \mathrm{tr}_+(2543)^2}, \end{aligned} \tag{5.69}$$

$$\begin{aligned} c_{51;23} = &\frac{s_{23} s_{45} \mathrm{tr}_+(1234)^2 \mathrm{tr}_+(1534)}{6 s_{12} s_{34} \mathrm{tr}_+(2543)^2} + \frac{2 s_{12} s_{23} s_{34} s_{45} \mathrm{tr}_+(1543)}{3 \mathrm{tr}_+(2543)^2} \\ &- \frac{5 s_{23} s_{45} \mathrm{tr}_+(1234)\mathrm{tr}_+(1543)}{2 \mathrm{tr}_+(2543)^2}, \end{aligned} \tag{5.70}$$

$$c_{\mathrm{rat}} = -\frac{5 \mathrm{tr}_+(1234)\mathrm{tr}_+(1543)}{4 s_{34} \mathrm{tr}_+(2543)} + \frac{5 s_{23} \mathrm{tr}_+(1243)\mathrm{tr}_+(1543)^2}{2 s_{15} s_{34} \mathrm{tr}_+(2543)^2}. \tag{5.71}$$

While for the $(d_s - 2)^2$ amplitude the coefficients are:

$$d_{34}^{(3)} = -\frac{s_{12} s_{15} \mathrm{tr}_+(2543)^2}{12 s_{34}}, \tag{5.72a}$$

$$d_{34}^{(2)} = \frac{1}{6} s_{12} s_{15} \mathrm{tr}_+(2543), \tag{5.72b}$$

$$d_{34;51}^{(3)} = -\frac{1}{18} s_{15} s_{23} \mathrm{tr}_+(2543), \tag{5.72c}$$

$$d_{34;51}^{(2)} = -\frac{s_{15} \mathrm{tr}_+(2543)^2}{36 s_{12} s_{34}} - \frac{1}{6} s_{15} \mathrm{tr}_+(2543), \tag{5.72d}$$

$$d^{(3)}_{51;23} = \frac{s_{15}s_{23}s_{34}^2 s_{45}^2 \mathrm{tr}_+(1245)}{18\mathrm{tr}_+(2543)^2}, \tag{5.73a}$$

$$d^{(2)}_{51;23} = \frac{s_{12}s_{15}s_{23}s_{34}^2 s_{45}^2}{12\mathrm{tr}_+(2543)^2} - \frac{s_{15}s_{23}s_{34}s_{45}^2 \mathrm{tr}_+(1234)}{6\mathrm{tr}_+(2543)^2}, \tag{5.73b}$$

$$\begin{aligned} d_{\mathrm{rat}} = &\frac{s_{34}}{72} + \frac{5s_{45}}{36} - \frac{\mathrm{tr}_+(1234)\mathrm{tr}_+(1453)}{72s_{14}\mathrm{tr}_+(2543)} - \frac{s_{45}\mathrm{tr}_+(1543)}{72\mathrm{tr}_+(2543)} + \frac{\mathrm{tr}_+(2543)^2}{72s_{34}^3} \\ &- \frac{5\mathrm{tr}_+(1543)^2}{72s_{34}\mathrm{tr}_+(2543)} - \frac{s_{12}\mathrm{tr}_+(1543)^2}{72\mathrm{tr}_+(2543)^2} + \frac{s_{23}s_{34}s_{45}\mathrm{tr}_+(1543)}{18\mathrm{tr}_+(2543)^2}. \end{aligned} \tag{5.74}$$

These results can also be found in the ancillary file included with the arXiv version of our paper [4].

Chapter 6

Conclusions and outlook

In this thesis we have investigated a variety of modern methods used for the efficient calculation of scattering amplitudes. A common aim of these methods has been to use only physical degrees of freedom by making on-shell constraints manifest and avoiding gauge redundancies. Advances in calculational techniques are crucial to calculate the higher-order theoretical predictions necessary to keep the precision in line with experimental uncertainties.

In Chapter 2 and 3 we discussed techniques that are widely used in the calculation of both tree and one-loop level scattering amplitudes. Furthermore, working in six dimensions allowed for direct extraction of rational terms from integrand reduction via d-dimensional generalised unitarity cuts. These techniques were further developed in Chapter 4 and 5 for the study of present challenges in higher-order calculations. Of particular importance are the spinor-helicity formalism and momentum twistor coordinates which allow for a rational parametrisation of phase space as well as rational cut solutions. This enables us to employ efficient numerical sampling techniques to solve the large linear systems of equations appearing in integrand and integration-by-parts reductions. Numerical sampling and functional reconstruction over finite fields have proven especially powerful.

In Chapter 4 a new method to deal with massive fermions compatible with unitarity methods was presented. Embedding massive four-momenta in massless six-dimensional momenta allowed for a direct application of the six-dimensional spinor-helicity formalism. The coefficients of topologies with divergent generalised unitarity cuts were determined using universal pole structure in four and six dimensions. Using this approach we reproduced known analytic results for

$gg \to t\bar{t}$ at one-loop order using a purely on-shell approach.

New results for two-loop scattering amplitudes in Quantum Chromodynamics were presented in Chapter 5. Firstly, benchmark results for the five-parton helicity amplitudes were presented for the partonic channels $ggggg$, $qggg\bar{q}$, and $q\bar{q}gQ\bar{Q}$ in the Euclidean region of phase space. The pure gluon amplitudes were also evaluated in the physical region. The gluon results were obtained through integrand reduction while the fermionic channels used a Feynman diagrammatic approach. The evaluation of the integrals was done using both numerical and analytic results. Our results match those found by another group [165, 166].

Finally, in Chapter 5 we also presented the analytic five-gluon two-loop amplitude in the case where one gluon has negative helicity and the remaining gluons have positive helicities. This was achieved by employing finite field numerics to a combined system of integrand reduction, integration-by-parts identities, and an expansion of the master integrals into a basis of pentagon functions. Using the fact that the universal pole structure of two-loop amplitudes is known, it is only necessary to calculate the finite remainder. The compact result for the finite remainder of the amplitude was presented in terms of logarithms and dilogarithms. The rational coefficients are expressed directly in terms of generalised Mandelstam variables and Dirac traces of the external momenta.

More recently, several new important amplitude results have emerged. The remaining analytic helicity amplitudes were computed in [167] using a similar method to the one presented here. The symbol for non-planar corrections to five-point amplitudes in maximally super-symmetric theories have also recently been calculated [168–171]. This rapid increase in known amplitudes has partly been fuelled by the computation of the necessary master integrals. The calculation of the non-planar five-point integrals was completed recently [172]. This paves the way for calculating the remaining colour contributions to five-parton scattering at two loops.

The techniques of integrand reduction and d-dimensional cuts presented for simultaneously fitting of coefficients from two (or more) topologies in section 5.1.1 can readily be applied for determining the coefficients of non-planar topologies. This bypasses the challenge of finding rational solutions to the cut constraints in the non-planar case as the non-planar integrand coefficients can be determined from planar cut solutions. Alternatively, a change of basis for the momentum vectors solves this problem. This idea is pursued in Appendix F and general

representations of the six-dimensional spinors are derived. This construction is also useful for fermionic amplitudes and a similar approach was taken in [166].

While an increasing number of five-point QCD amplitudes are now known, other amplitudes of phenomenological relevance involving, for example, the Higgs and weak gauge bosons are still a big challenge due to the additional mass scales.

In order to obtain physical observables the recombination with the real radiation contributions remains to be done. While one should not underestimate these challenges for the real-virtual and double-real contributions, with the two-loop five-gluon contribution now known analytically one can hope to see phenomenological studies of leading-colour three-jet production in the near future.

Appendix A

Notation and conventions

We use the mostly minus metric in both four and six dimensions,

$$\eta^{\mu\nu} = \text{diag}\{1, -1, -1, -1\}, \tag{A.1a}$$

$$\eta^{MN} = \text{diag}\{1, -1, -1, -1, -1, -1\}, \tag{A.1b}$$

where lower case Greek letters are four-dimensional and upper case are six-dimensional. We define the the Pauli matrices in the Weyl representation,

$$\sigma^0_{\alpha\dot{\alpha}} = \begin{pmatrix} 1 & 0 \\ 0 & 1 \end{pmatrix}, \sigma^1_{\alpha\dot{\alpha}} = \begin{pmatrix} 0 & -1 \\ -1 & 0 \end{pmatrix}, \ \sigma^2_{\alpha\dot{\alpha}} = \begin{pmatrix} 0 & i \\ -i & 0 \end{pmatrix}, \ \sigma^3_{\alpha\dot{\alpha}} = \begin{pmatrix} -1 & 0 \\ 0 & 1 \end{pmatrix}, \tag{A.2}$$

and $(\tilde{\sigma}^\mu)^{\dot{\alpha}\alpha} = \epsilon^{\alpha\beta}\epsilon^{\dot{\alpha}\dot{\beta}}\sigma^\mu_{\beta\dot{\beta}}$ with $\epsilon^{12} = 1 = \epsilon_{21}$. We observe the properties,

$$\sigma^\mu_{a\dot{a}}\tilde{\sigma}^{\dot{b}b}_\mu = 2\delta^b_a\delta^{\dot{b}}_{\dot{a}}, \tag{A.3a}$$

$$\sigma^\mu_{a\dot{a}}\tilde{\sigma}^{\nu\dot{a}a} = 2\eta^{\mu\nu}. \tag{A.3b}$$

Using the Pauli matrices (A.2) we define the Σ-matrices,

$$\Sigma^0 = i\sigma^1 \times \sigma^2 \qquad \tilde{\Sigma}^0 = -i\sigma^1 \times \sigma^2 \tag{A.4a}$$

$$\Sigma^1 = i\sigma^2 \times \sigma^3 \qquad \tilde{\Sigma}^1 = i\sigma^2 \times \sigma^3 \tag{A.4b}$$

$$\Sigma^2 = \sigma^2 \times \sigma^0 \qquad \tilde{\Sigma}^2 = -\sigma^2 \times \sigma^0 \tag{A.4c}$$

$$\Sigma^3 = -i\sigma^2 \times \sigma^1 \qquad \tilde{\Sigma}^3 = -i\sigma^2 \times \sigma^1 \tag{A.4d}$$

$$\Sigma^4 = -\sigma^3 \times \sigma^2 \qquad \tilde{\Sigma}^4 = \sigma^3 \times \sigma^2 \tag{A.4e}$$

$$\Sigma^5 = -i\sigma^0 \times \sigma^2 \qquad \tilde{\Sigma}^5 = -i\sigma^0 \times \sigma^2, \tag{A.4f}$$

which obey the Clifford algebra,

$$\Sigma^M \tilde{\Sigma}^N + \Sigma^N \tilde{\Sigma}^M = 2\eta^{MN}, \tag{A.5}$$

as well as the identities,

$$\Sigma^M_{AB} \tilde{\Sigma}^{CD}_M = -2\left(\delta^C_A \delta^D_B - \delta^D_A \delta^C_B\right), \tag{A.6a}$$

$$\mathrm{tr}\left(\Sigma^M \tilde{\Sigma}^N\right) = 4\eta^{MN}. \tag{A.6b}$$

Appendix B

Trees and cuts in six dimensions

B.1 Three-point amplitudes

In this section we list the six-dimensional tree-level amplitudes used in this thesis.

$$A^{(0)}(1_q^a, 2_{\bar{q}}^b, 3_g^{c\dot{c}}) = \frac{i}{s_{r3}}\langle 1^a 2^b 3^c r^x\rangle\langle r_x|3^{\dot{c}}] \tag{B.1}$$

where r is a massless reference vector satisfying $s_{r3} \neq 0$.

$$\begin{aligned} A^{(0)}(1_{a\dot{a}}, 2_{b\dot{b}}, 3_{c\dot{c}}) &= i\Gamma_{abc}\tilde{\Gamma}_{\dot{a}\dot{b}\dot{c}} \\ \Gamma_{abc} &= u_{1a}u_{2b}w_{3c} + u_{1a}w_{2b}u_{3c} + w_{1a}u_{2b}u_{3c} \\ \tilde{\Gamma}_{\dot{a}\dot{b}\dot{c}} &= \tilde{u}_{1\dot{a}}\tilde{u}_{2\dot{a}}\tilde{w}_{3\dot{c}} + \tilde{u}_{1\dot{a}}\tilde{w}_{2\dot{a}}\tilde{u}_{3\dot{c}} + \tilde{w}_{1\dot{a}}\tilde{u}_{2\dot{a}}\tilde{u}_{3\dot{c}}, \end{aligned} \tag{B.2}$$

where the tensors Γ and $\tilde{\Gamma}$ are written in terms of the $SU(2)$ spinors $u, \tilde{u}$ satisfying the following properties, defined on a cyclic order $\{ijk\}$,

$$u_{ia}\tilde{u}_{j\dot{b}} = \langle i_a|j_{\dot{b}}], \qquad u_{ja}\tilde{u}_{i\dot{b}} = -\langle j_a|i_{\dot{b}}],$$

and $w, \tilde{w}$ are the inverse of the $u, \tilde{u}$

$$\epsilon_{ab} = u_a w_b - u_b w_a, \qquad \epsilon_{\dot{a}\dot{b}} = \tilde{u}_{\dot{a}}\tilde{w}_{\dot{b}} - \tilde{u}_{\dot{b}}\tilde{w}_{\dot{a}},$$

for which we impose momentum conservation

$$0 = \tilde{w}_{1\dot{a}}\tilde{\lambda}_{1A}^{\dot{a}} + \tilde{w}_{2\dot{a}}\tilde{\lambda}_{2A}^{\dot{a}} + \tilde{w}_{3\dot{a}}\tilde{\lambda}_{3A}^{\dot{a}}.$$

$$A^{(0)}(1_{\phi_{1,2}}, 2_{\phi_{1,2}}, 3_g^{a\dot{a}}) = \frac{-i}{2s_{r3}}\langle 3^a|(1-2)r|3^{\dot{a}}] \tag{B.3}$$

where r is a massless reference vector satisfying $s_{r3} \neq 0$.

$$A^{(0)}(1_{\phi_1}, 2_{\bar{q}}^a, 3_q^{\dot{b}}) = \frac{i}{\sqrt{2}}\langle 1^a|2^{\dot{b}}]. \tag{B.4}$$

$$A^{(0)}(1_{\phi_2}, 2_{\bar{q}}^a, 3_q^{\dot{b}}) = \frac{i}{\sqrt{2}}\langle 1^a|\gamma^5|2^{\dot{b}}]. \tag{B.5}$$

B.2 Four-point amplitudes

$$A^{(0)}(1_{a\dot{a}}, 2_{b\dot{b}}, 3_{c\dot{c}}, 4_{d\dot{d}}) = \frac{-i}{s_{12}s_{23}}\langle 1_a 2_b 3_c 4_d\rangle[1_{\dot{a}} 2_{\dot{b}} 3_{\dot{c}} 4_{\dot{d}}] \tag{B.6}$$

$$A^{(0)}(1_{q,a}, 2_{b\dot{b}}, 3_{c\dot{c}}, 4_{\bar{q},d}) = \frac{i}{2s_{12}s_{23}}\langle 1_a 2_b 3_c 4_d\rangle[1_{\dot{x}} 2_{\dot{b}} 3_{\dot{c}} 1^{\dot{x}}]. \tag{B.7}$$

$$A^{(0)}(1_{a\dot{a}}, 2_{b\dot{b}}, 3, 4) = \frac{i}{4s_{12}s_{23}}\langle 1_a 2_b 3_x 3^x\rangle[1_{\dot{a}} 2_{\dot{b}} 3_{\dot{x}} 3^{\dot{x}}] \tag{B.8}$$

B.3 Cut solutions in six dimensions

In this section we give details on the solutions for the triple and double cuts in six dimensions used in section 4.2. We will describe the parametrisation used to get the solutions without writing down any explicit expression for them. The implementation is given in the MATHEMATICA notebook attached to the arXiv version of our paper [1]. Notice that all the cut solutions are rational functions of the kinematics and the free parameters and contain no square roots.

For the triple cuts we write the six-dimensional loop momentum, ℓ_i^M, in the

following basis,

$$\beta = \left\{ v^M, w^M, \langle v^1 | \Sigma^M | w_1 \rangle, \langle v^1 | \Sigma^M | w_2 \rangle, \langle v^2 | \Sigma^M | w_1 \rangle, \langle v^2 | \Sigma^M | w_2 \rangle \right\}, \tag{B.9}$$

where v and w are six dimensional massless momenta and use the parametrisation,

$$\ell_i = \beta \cdot \{ y_1, y_2, y_3, y_4, \tau_1, \tau_2 \}. \tag{B.10}$$

We impose the cut conditions,

$$S_{ijk} = \begin{cases} \ell_i^2 = \ell_j^2 = \ell_k^2 = 0 \\ \ell_i^{(5)} = \begin{cases} 0 & \text{if } i \text{ is a gluon} \\ \pm m & \text{if } i \text{ is a fermion} \end{cases} \end{cases}, \tag{B.11}$$

where $\{ijk\}$ is the set of the three cut propagators and the sign of the mass component depends on the kinematic configuration. This system of equations for ℓ_i only constrains 4 parameters so solving for the y_i's, τ_1, τ_2 are left as free parameters.

For the double cut solutions we use the same basis, (B.9), and use the following parametrisation,

$$\ell_i = \beta \cdot \{ y_1, \tau_1, y_2, \tau_2, y_3, \tau_3 \}. \tag{B.12}$$

The y_i's are fixed by the double cut constraints,

$$S_{ij} = \begin{cases} \ell_i^2 = \ell_j^2 = 0 \\ \ell_i^{(5)} = \begin{cases} 0 & \text{if } i \text{ is a gluon} \\ \pm m & \text{if } i \text{ is a fermion} \end{cases} \end{cases}, \tag{B.13}$$

where $\{ij\}$ is the set of the two cut propagators and the sign of the mass component depends on the kinematic configuration. The parameters τ_1, τ_2, τ_3 are unconstrained.

B.4 Feynman rules for an effective Lagrangian

In this section we present selected Feynman rules for the six dimensional effective theory of interest to us, defined by the Lagrangian,

$$\mathcal{L}^6_{QCD} = \bar{\psi}(i\not{D} - m)\psi - \frac{1}{2}\mathrm{tr}\,(F_{\mu\nu}F^{\mu\nu}) + \frac{i}{2}\sigma_1\, g_s^3 m_t\, \bar{\psi}\gamma^\mu\gamma^\nu F_{\mu\nu}\psi \\ + i\sigma_2\, g_s^3\, \bar{\psi}F_{\mu\nu}\gamma^\mu D^\nu\psi + \frac{i}{6}\gamma\, g_s^3\, \mathrm{tr}\left(F^{\mu\nu}[F_{\mu\lambda}, F_\nu{}^\lambda]\right). \quad \text{(B.14)}$$

These rules were derived with the help of FeynCalc [173, 174] and FeynRules [175, 176]. The vertices are colour ordered and all momenta are considered to be outgoing. We include the coupling constants here for clarity though in the main text they are stripped off.

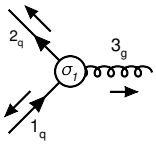

$$= -g_s^3\sigma_1\, m_t\sigma^{\mu_3\nu}p_{3\nu} \quad \text{(B.15)}$$

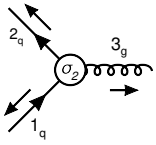

$$= -ig_s^3\sigma_2\, \left(p_2^{\mu_3}\not{p}_3 - p_2\cdot p_3\gamma^{\mu_3}\right) \quad \text{(B.16)}$$

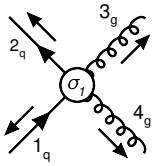

$$= g_s^4\sigma_1\, m_t\sigma^{\mu_3\mu_4} \quad \text{(B.17)}$$

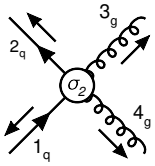

$$= -ig_s^4\sigma_2\, \left(g^{\mu_3\mu_4}\not{p}_3 - \gamma^{\mu_4}p_1^{\mu_3} + \gamma^{\mu_3}(p_1^{\mu_4} - p_3^{\mu_4})\right) \quad \text{(B.18)}$$

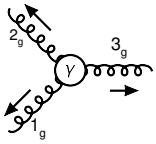

$$= -\frac{i}{2}g_s^3\gamma\, \Bigg(g^{\mu_1\mu_2}\,(p_1\cdot p_3\, p_2^{\mu_3} - p_2\cdot p_3\, p_1^{\mu_3}) \\ + g^{\mu_2\mu_3}\,(p_2\cdot p_1\, p_3^{\mu_1} - p_3\cdot p_1\, p_2^{\mu_1}) \\ + g^{\mu_3\mu_1}\,(p_3\cdot p_2\, p_1^{\mu_2} - p_1\cdot p_2\, p_3^{\mu_2}) \\ - p_3^{\mu_1}p_1^{\mu_2}p_2^{\mu_3} + p_2^{\mu_1}p_3^{\mu_2}p_1^{\mu_3} \Bigg). \quad \text{(B.19)}$$

where $\sigma^{\mu\nu} = \frac{i}{2}\,(\gamma^\mu\gamma^\nu - \gamma^\nu\gamma^\mu)$.

Appendix C

One-loop integral reduction

In this appendix we present the derivation of the integral reduction formulae presented in section 3.1.

It can be shown that all n-point integrals with $n > 4$ can be reduced to linear combinations of integrals with $n \leq 4$ [43]. Using the notation of section 3.1, we consider the massless pentagon integral in four dimensions,

$$I_{5;01234}[1] = \int \frac{d^4k}{(2\pi)^4} \frac{1}{D_0 D_1 D_2 D_3 D_4}. \tag{C.1}$$

For outgoing, cyclically ordered momenta the inverse propagators are,

$$D_0 = k^2, \tag{C.2a}$$
$$D_i = (k - q_i)^2, \qquad i = 1, 2, 3, 4, \tag{C.2b}$$
$$q_i = p_{1\ldots i}, \tag{C.2c}$$

where we have used the shorthand notation $p_{i_1 \ldots i_n} = \sum_{j=i_1}^{i_n} p_j$. With these definitions we have,

$$k \cdot q_i = -\frac{1}{2}\left(D_i - D_0 - q_i^2\right), \qquad i = 1, 2, 3, 4. \tag{C.3}$$

We will use the shorthand notation,

$$\mathrm{tr}_5\left(ijkl\right) = \mathrm{tr}_5\left(q_i q_j q_k q_l\right) = \mathrm{tr}\left(\gamma_5 \gamma_\mu \gamma_\nu \gamma_\rho \gamma_\sigma\right) q_i^\mu q_j^\nu q_k^\rho q_l^\sigma. \tag{C.4}$$

At five points, the four independent momenta sums in the propagators span the

four-dimensional space, and therefore the loop momentum can be written as a linear combination of them. This observation leads to a Schouten identity,

$$k^\mu \ \mathrm{tr}_5\,(1234) = \sum_{i=1}^{4} k\cdot q_i \ v_i^\mu, \tag{C.5}$$

where,

$$v_1^\mu = \mathrm{tr}_5\,(\gamma^\mu 234)\,,\ v_2^\mu = \mathrm{tr}_5\,(1\gamma^\mu 34)\,,\ v_3^\mu = \mathrm{tr}_5\,(12\gamma^\mu 4)\,,\ v_4^\mu = \mathrm{tr}_5\,(123\gamma^\mu)\,. \tag{C.6}$$

We contract (C.5) with k_μ to obtain,

$$\begin{aligned} k^2 \ \mathrm{tr}_5\,(1234) &= D_0 \ \mathrm{tr}_5\,(1234) \\ &= \sum_{i=1}^{4} k\cdot q_i \ v_i\cdot k \\ &= -\frac{1}{2}\sum_{i=1}^{4}(D_i - q_i^2) \ v_i\cdot k + \frac{1}{2}\sum_{i=1}^{4} D_0 \ v_i\cdot k. \end{aligned} \tag{C.7}$$

In the first sum, integrals with numerators $D_i \ v_i\cdot k$ vanish since they are spanned by $q_j,\ j\neq i$ and the right hand side in a Passarino-Veltman expansion like (3.5) will vanish upon contraction with v_i.

Considering now the second sum on the right hand side of (C.7), under the integral we can perform a shift, $k\to k+q_1$, to obtain,

$$\begin{aligned} \sum_{i=1}^{4} v_i\cdot k &\to \sum_{i=1}^{4}(v_i\cdot k + v_i\cdot q_1) \\ &= \mathrm{tr}_5\,[k(2-1)(3-1)(4-1)] + \mathrm{tr}_5\,(1234)\,. \end{aligned} \tag{C.8}$$

Using an expansion like (3.5), we see that the first term vanishes since the right hand side would become,

$$a(q_2-q_1)^\mu + b(q_3-q_1)^\mu + c(q_4-q_1)^\mu, \tag{C.9}$$

which vanishes upon contraction with $\mathrm{tr}_5\,[\gamma_\mu(2-1)(3-1)(4-1)]$. After these manipulations the relation (C.7) becomes:

$$D_0 \ \mathrm{tr}_5\,(1234) = \frac{1}{2}\sum_{i=1}^{4} q_i^2 \ v_i\cdot k + \frac{1}{2} D_0 \ \mathrm{tr}_5\,(1234) \tag{C.10}$$

Using the Schouten identity (C.5) in the sum,

$$\begin{aligned}\mathrm{tr}_5\left(1234\right) v_i \cdot k &= \sum_{j=1}^{4} k \cdot q_j \; v_i \cdot v_j \\ &= -\frac{1}{2}\sum_{j=1}^{4}\left(D_j - D_0 - q_j^2\right) \; v_i \cdot v_j, \end{aligned} \tag{C.11}$$

and rearranging (C.10) becomes,

$$\begin{aligned} 0 &= 2D_0 \mathrm{tr}_5\left(1234\right)^2 + \sum_{i=1}^{4}\sum_{j=1}^{4} q_i^2 \; \left(D_j - D_0 - q_j^2\right) \; v_i \cdot v_j \\ &= 2D_0 \mathrm{tr}_5\left(1234\right)^2 - w^2 + \sum_{i=1}^{4}\left(D_i - D_0\right) \; w \cdot v_i, \end{aligned} \tag{C.12}$$

where we introduced $w^\mu = \sum_{i=1}^{4} q_i^2 \; v_i^\mu$. Finally, the reduction formula for the pentagon integral is,

$$\begin{aligned} I_{5,01234}[1] = \frac{1}{w^2}\Big(&\left(2\mathrm{tr}_5\left(1234\right)^2 - \Sigma_{i=1}^{4} w \cdot v_i\right) I_{4;1234}\left[1\right] \\ &+ w \cdot v_1 I_{4;0234}\left[1\right] + w \cdot v_2 I_{4;0134}\left[1\right] + w \cdot v_3 I_{4;0124}\left[1\right] + w \cdot v_4 I_{4;0123}\left[1\right]\Big). \end{aligned} \tag{C.13}$$

The result with masses included can be found in the original reference [43].

For higher-point functions the additional vectors, $q_i, \; i > 4$, simplify the problem. For an n-point integral we choose, without loss of generality, to contract the Schouten identity (C.5) with an additional vector, $q_n, \; n > 4$, we have,

$$\begin{aligned} k \cdot q_n \; \mathrm{tr}_5\left(1234\right) &= \sum_{i=1}^{4} k \cdot q_i \; v_i \cdot q_n \\ &= -\frac{1}{2}\sum_{i=1}^{4}\left(D_i - D_0 - q_i^2\right) v_i \cdot q_n \\ &= -\frac{1}{2}\left(D_n - D_0 - q_n^2\right)\mathrm{tr}_5\left(1234\right), \end{aligned} \tag{C.14}$$

which leads to the reduction formula,

$$
\begin{aligned}
I_{n,0\ldots n-1}[1] = \frac{1}{w\cdot q_n - q_n^2\ \mathrm{tr}_5\,(1234)}\Big(\ & \left(\mathrm{tr}_5\,(1234) - \Sigma_{i=1}^{4} v_i\cdot q_n\right) I_{n-1;1\ldots n-1}\,[1] \\
& + v_1\cdot q_n I_{n-1;02\ldots n-1}\,[1] \\
& + v_2\cdot q_n I_{n-1;013\ldots n-1}\,[1] \\
& + v_3\cdot q_n I_{n-1;0124\ldots n-1}\,[1] \\
& + v_4\cdot q_n I_{n-1;01235\ldots n-1}\,[1] \\
& - \mathrm{tr}_5\,(1234)\, I_{n-1;0\ldots n-2}\,[1]\ \Big). \qquad \text{(C.15)}
\end{aligned}
$$

Appendix D

Functional reconstruction using finite field numerics

This appendix gives a short introduction to finite fields and the techniques described in [119]. A simple demonstration is given by reconstructing a univariate polynomial.

A finite field contains a finite number of elements. We will be interested in finite fields of integers,

$$\mathbb{Z}_n = \{0, 1, 2, .., n-1\}, \quad n \in \mathbb{Z}_+. \tag{D.1}$$

All arithmetic operations are therefore considered modulo n. In particular we can define an inverse given the element considered is co-prime with n. Co-prime numbers have 1 as greatest common divisor, therefore choosing n to be a prime is a simple way of ensuring this. In this situation we can define the inverse of $a \neq 0$ as,

$$a^{-1} \mod n = b \Leftrightarrow a \times b \mod n = 1, \quad b \in \mathbb{Z}_n. \tag{D.2}$$

The inverse can be computed using the extended Euclidean algorithm for finding greatest common divisors.

Greatest common divisor

For two integers $a, b \in \mathbb{Z}$ the extended Euclidean algorithm is used to calculate their greatest common divisor, $\gcd(a, b)$, and two integers s and t,

$$a \times s + b \times t = \gcd(a, b). \tag{D.3}$$

The algorithm starts with values,

$$\begin{aligned} r_0 &= a, \\ s_0 &= 1, \\ t_0 &= 0, \\ r_1 &= b, \\ s_1 &= 0, \\ t_1 &= 1. \end{aligned}$$

In each iteration of the algorithm the integer quotient,

$$q_i = \left\lfloor \frac{r_{i-2}}{r_{i-1}} \right\rfloor, \tag{D.4}$$

is used to compute the next step,

$$\begin{aligned} r_i &= r_{i-2} - q_i r_{i-1}, \\ s_i &= s_{i-2} - q_i s_{i-1}, \\ t_i &= t_{i-2} - q_i t_{i-1}, \end{aligned} \tag{D.5}$$

for $i \geq 2$. Each step in the algorithm satisfies,

$$a \times s_i + b \times t_i = r_i \tag{D.6}$$

and the algorithm terminates when $r_i = 1$ and we identify,

$$\{\gcd(a, b), s, t\} = \{r_{i-1}, s_{i-1}, t_{i-1}\}. \tag{D.7}$$

We continue by defining the multiplicative inverse by choosing a prime n and setting $b = n$ in (D.3). Taking the mod n on both sides yields,

$$a \times s \mod n = 1, \tag{D.8}$$

and hence,

$$a^{-1} \mod n = s. \tag{D.9}$$

We see that s is the multiplicative inverse of a. With the definition of an inverse we can consider $\mathbb{Z}_n$ to be a field.

The definition of an inverse implies that there is a map from rational numbers to integers in $\mathbb{Z}_n$. For $q = \frac{a}{b} \in \mathbb{Q}$ we define,

$$q \mod n = \left(a \times (b^{-1} \mod n)\right) \mod n. \tag{D.10}$$

This map is not invertible since $\mathbb{Q}$ is an infinite field and $\mathbb{Z}_n$ is a finite field. However, if $q \mod n = a \in \mathbb{Z}$ we notice that taking (D.6), setting $b = n$, and taking the modulo on both sides we arrive at a guess for q,

$$a \times s_i \mod n = r_i \Leftrightarrow a = \frac{r_i}{s_i} \mod n. \tag{D.11}$$

The ratio $\frac{r_i}{s_i}$ is a guess for q. Further discussion on the accuracy of this guess is given in the original reference [119].

Chinese remainder theorem

The Chinese remainder theorem allows us to reconstruct an integer, $a \in \mathbb{Z}_n$, from its images $a_i \in \mathbb{Z}_{n_i}$, where the moduli n_i are mutually co-prime and $n = \prod n_i$. Then,

$$a = \sum_i m_i a_i \mod n, \tag{D.12}$$

with

$$m_i = \left(\left(\frac{n}{n_i}\right)^{-1} \mod n_i\right) \frac{n}{n_i}. \tag{D.13}$$

Reconstructing a polynomial

For reconstruction of polynomials a common approach is based on Newton's polynomial representation. It is a recursive method and it is not necessary to

know the total degree of the polynomial a priori. A univariate polynomial $f(z)$ of degree N with a known set of function values $f(z_i)$ for points z_i with $i = 0, 1, 2, ...,$ can be written as,

$$f(z) = \sum_{n=0}^{N} c_n \prod_{i=0}^{n-1} (z - z_i). \tag{D.14}$$

The first coefficient c_0 is just the function value at the first point,

$$c_0 = f(z_0). \tag{D.15}$$

The factorisation in z of each term in the polynomial ensures that all subsequent coefficient a_n does not alter the reconstructed function for points z_i with $i < n$. The coefficients can therefore be constructed recursively,

$$\begin{aligned}
c_1 &= \frac{f(z_1) - c_0}{z_1 - z_0}, \\
c_2 &= \left(\frac{f(z_2) - c_0}{z_2 - z_0} - c_1 \right) \frac{1}{z_2 - z_1}, \\
&\dots \\
c_i &= \frac{f(z_i) - c_0}{\prod_{j=0}^{i-1} z_i - z_j} - \sum_{k=0}^{i-1} \frac{c_k}{\prod_{j=k}^{i-1} z_i - z_j}.
\end{aligned} \tag{D.16}$$

The recursion will terminate when all N coefficients have been reconstructed as any attempt at evaluating additional coefficients will give zero.

Reconstructing a polynomial with integer coefficients

We consider a simple univariate polynomial of second degree,

$$f(z) = z^2 - z. \tag{D.17}$$

We choose to evaluate it for,

z	11	12	13	14	15
$f(z)$	110	132	156	182	210

Using the reconstruction method from the previous section, we get the coefficients $(c_0, c_1, c_2) = (110, 22, 1)$ and arrive at the representation,

$$f(z) = 110 + 22(-11 + z) + (-12 + z)(-11 + z). \tag{D.18}$$

We now reconstruct the function using the finite fields $\mathbb{Z}_{17}$ and $\mathbb{Z}_{19}$ instead and list the reconstructed coefficients,

field	c_0	c_1	c_2
$\mathbb{Z}$	110	22	1
$\mathbb{Z}_{17}$	8	5	1
$\mathbb{Z}_{19}$	15	3	1

To reconstruct c_0 in $\mathbb{Z}_{17\cdot 19} = \mathbb{Z}_{323}$ we use the Chinese remainder theorem and calculate,

$$\begin{aligned} c_0 &= 8 \cdot m_1 + 15 \cdot m_2 \mod 323 \\ &= 8 \cdot \left[\left(19^{-1} \mod 17\right) \cdot 19\right] + 15 \cdot \left[\left(17^{-1} \mod 19\right) \cdot 17\right] \mod 323 \\ &= 8 \cdot [171] + 15 \cdot [153] \mod 323 \\ &= 3663 \mod 323 \\ &= 110. \end{aligned} \tag{D.19}$$

Note that the values of m_i in square brackets do not depend on the coefficient but only on the chosen finite fields. We can therefore immediately continue,

$$\begin{aligned} c_1 &= 5 \cdot [171] + 3 \cdot [153] \mod 323 \\ &= 1314 \mod 323 \\ &= 22, \end{aligned} \tag{D.20}$$

$$\begin{aligned} c_2 &= 1 \cdot [171] + 1 \cdot [153] \mod 323 \\ &= 324 \mod 323 \\ &= 1, \end{aligned} \tag{D.21}$$

and we have reconstructed the polynomial.

The generalisations necessary for reconstruction of multivariate rational functions can be found in the original reference [119].

Appendix E

Some two-loop integrand parametrisations

In this appendix we give some examples of the two-loop integrand parametrisations used in Chapter 5. The spurious directions, ω_i, are orthogonal to the independent external legs, q_j, of the topology, $\omega_i \cdot q_j = 0$. An n-point topology has $n-1$ independent external legs, so $j = 1, ..., n-1$ while $i = 1, ..., 5-n$. The extra-dimensional irreducible scalar products are defined by $\mu_{ij} = -k_{\perp,i}^{[-2\epsilon]} \cdot k_{\perp,j}^{[-2\epsilon]}$, see also equation (5.6). The momentum twistor coordinates, x_i, can be written in terms of generalised Mandelstam variables using (2.74).

Δ 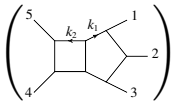

$$
\begin{aligned}
&= c_0 + c_1(k_1 \cdot p_5) + c_2(k_2 \cdot p_1) + c_3(k_2 \cdot p_2) \\
&\quad + c_4\mu_{11} + c_5(k_1 \cdot p_5)\mu_{11} + c_6(k_2 \cdot p_1)\mu_{11} \\
&\quad + c_7(k_1 \cdot p_5)(k_2 \cdot p_1)\mu_{11} + c_8(k_2 \cdot p_1)^2\mu_{11} + c_9(k_2 \cdot p_1)^3\mu_{11} \\
&\quad + c_{10}(k_2 \cdot p_1)^4\mu_{11} + c_{11}(k_2 \cdot p_2)\mu_{11} + c_{12}(k_2 \cdot p_1)(k_2 \cdot p_2)\mu_{11} \\
&\quad + c_{13}(k_2 \cdot p_1)^2(k_2 \cdot p_2)\mu_{11} + c_{14}(k_2 \cdot p_1)^3(k_2 \cdot p_2)\mu_{11} + c_{15}\mu_{11}^2 \\
&\quad + c_{16}(k_1 \cdot p_5)\mu_{11}^2 + c_{17}(k_2 \cdot p_1)\mu_{11}^2 + c_{18}(k_1 \cdot p_5)(k_2 \cdot p_1)\mu_{11}^2 \\
&\quad + c_{19}\mu_{12} + c_{20}(k_1 \cdot p_5)\mu_{12} + c_{21}(k_2 \cdot p_1)\mu_{12} \\
&\quad + c_{22}(k_1 \cdot p_5)(k_2 \cdot p_1)\mu_{12} + c_{23}(k_2 \cdot p_1)^2\mu_{12} + c_{24}(k_2 \cdot p_1)^3\mu_{12} \\
&\quad + c_{25}(k_2 \cdot p_2)\mu_{12} + c_{26}(k_2 \cdot p_1)(k_2 \cdot p_2)\mu_{12} \\
&\quad + c_{27}(k_2 \cdot p_1)^2(k_2 \cdot p_2)\mu_{12} + c_{28}\mu_{11}\mu_{12}
\end{aligned}
$$

$$
\begin{aligned}
&+ c_{29}(k_1\cdot p_5)\mu_{11}\mu_{12} + c_{30}(k_2\cdot p_1)\mu_{11}\mu_{12}\\
&+ c_{31}(k_1\cdot p_5)(k_2\cdot p_1)\mu_{11}\mu_{12} + c_{32}(k_2\cdot p_1)^2\mu_{11}\mu_{12}\\
&+ c_{33}(k_2\cdot p_1)^3\mu_{11}\mu_{12} + c_{34}(k_2\cdot p_2)\mu_{11}\mu_{12}\\
&+ c_{35}(k_2\cdot p_1)(k_2\cdot p_2)\mu_{11}\mu_{12} + c_{36}(k_2\cdot p_1)^2(k_2\cdot p_2)\mu_{11}\mu_{12}\\
&+ c_{37}\mu_{11}^2\mu_{12} + c_{38}(k_2\cdot p_1)\mu_{12}\mu_{11}^2 + c_{39}(k_2\cdot p_2)\mu_{12}\mu_{11}^2\\
&+ c_{40}\mu_{12}^2 + c_{41}(k_2\cdot p_1)\mu_{12}^2 + c_{42}(k_2\cdot p_1)^2\mu_{12}^2\\
&+ c_{43}(k_2\cdot p_2)\mu_{12}^2 + c_{44}(k_2\cdot p_1)(k_2\cdot p_2)\mu_{12}^2 + c_{45}\mu_{11}\mu_{12}^2\\
&+ c_{46}(k_2\cdot p_1)\mu_{11}\mu_{12}^2 + c_{47}(k_2\cdot p_2)\mu_{11}\mu_{12}^2 + c_{48}\mu_{22}\\
&+ c_{49}(k_1\cdot p_5)\mu_{22} + c_{50}(k_2\cdot p_1)\mu_{22} + c_{51}(k_1\cdot p_5)(k_2\cdot p_1)\mu_{22}\\
&+ c_{52}(k_2\cdot p_1)^2\mu_{22} + c_{53}(k_2\cdot p_2)\mu_{22} + c_{54}(k_2\cdot p_1)(k_2\cdot p_2)\mu_{22}\\
&+ c_{55}\mu_{11}\mu_{22} + c_{56}(k_1\cdot p_5)\mu_{11}\mu_{22} + c_{57}(k_2\cdot p_1)\mu_{11}\mu_{22}\\
&+ c_{58}(k_1\cdot p_5)(k_2\cdot p_1)\mu_{11}\mu_{22} + c_{59}(k_2\cdot p_1)^2\mu_{11}\mu_{22}\\
&+ c_{60}(k_2\cdot p_2)\mu_{11}\mu_{22} + c_{61}(k_2\cdot p_1)(k_2\cdot p_2)\mu_{11}\mu_{22}\\
&+ c_{62}\mu_{11}^2\mu_{22} + c_{63}(k_1\cdot p_5)\mu_{22}\mu_{11}^2\\
&+ c_{64}(k_2\cdot p_1)\mu_{22}\mu_{11}^2 + c_{65}(k_2\cdot p_2)\mu_{22}\mu_{11}^2 + c_{66}\mu_{12}\mu_{22}\\
&+ c_{67}(k_2\cdot p_1)\mu_{12}\mu_{22} + c_{68}(k_2\cdot p_2)\mu_{12}\mu_{22} + c_{69}\mu_{11}\mu_{12}\mu_{22}\\
&+ c_{70}(k_2\cdot p_1)\mu_{11}\mu_{12}\mu_{22} + c_{71}(k_2\cdot p_2)\mu_{11}\mu_{12}\mu_{22} + c_{72}\mu_{22}^2\\
&+ c_{73}(k_1\cdot p_5)\mu_{22}^2 + c_{74}\mu_{11}\mu_{22}^2 + c_{75}(k_1\cdot p_5)\mu_{11}\mu_{22}^2. \qquad \text{(E.1)}
\end{aligned}
$$

$\Delta\left(\right.$ 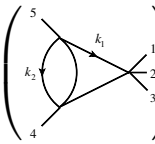 $\left.\right) = c_0 + c_1(k_1\cdot p_4) + c_2(k_1\cdot p_4)(k_2\cdot p_4) + c_3(k_1\cdot p_4)^2(k_2\cdot p_4)$

$$
\begin{aligned}
&+ c_4(k_2\cdot p_4)^2 + c_5(k_1\cdot p_4)(k_2\cdot p_4)^2 + c_6(k_2\cdot p_4)(k_2\cdot p_5)\\
&+ c_7(k_1\cdot p_4)(k_2\cdot p_4)(k_2\cdot p_5) + c_8(k_2\cdot p_5)^2 + c_9(k_1\cdot p_4)(k_2\cdot p_5)^2\\
&+ c_{10}\mu_{12} + c_{11}(k_1\cdot p_4)\mu_{12} + c_{12}(k_2\cdot p_4)\mu_{12}\\
&+ c_{13}(k_2\cdot p_5)\mu_{12} + c_{14}\mu_{22} + c_{15}(k_1\cdot p_4)\mu_{22}\\
&+ c_{16}(k_1\cdot w_1) + c_{17}(k_1\cdot p_4)(k_1\cdot w_1) + c_{18}(k_1\cdot p_4)^2(k_1\cdot w_1)\\
&+ c_{19}(k_1\cdot w_1)^3 + c_{20}(k_1\cdot w_2) + c_{21}(k_1\cdot p_4)(k_1\cdot w_2)\\
&+ c_{22}(k_1\cdot p_4)^2(k_1\cdot w_2) + c_{23}(k_1\cdot w_1)(k_1\cdot w_2)\\
&+ c_{24}(k_1\cdot p_4)(k_1\cdot w_1)(k_1\cdot w_2) + c_{25}(k_1\cdot w_1)^2(k_1\cdot w_2)\\
&+ c_{26}\left(\tfrac{1}{2}(k_1\cdot w_1)^2 + \tfrac{1}{2}(k_1\cdot w_2)^2\right)
\end{aligned}
$$

$$
\begin{aligned}
&+ c_{27}\big(\tfrac{1}{2}(k_1\cdot p_4)(k_1\cdot w_1)^2 + \tfrac{1}{2}(k_1\cdot p_4)(k_1\cdot w_2)^2\big)\\
&+ c_{28}(k_1\cdot w_1)(k_2\cdot p_4) + c_{29}(k_1\cdot p_4)(k_1\cdot w_1)(k_2\cdot p_4)\\
&+ c_{30}(k_1\cdot w_2)(k_2\cdot p_4) + c_{31}(k_1\cdot p_4)(k_1\cdot w_2)(k_2\cdot p_4)\\
&+ c_{32}(k_1\cdot w_1)(k_1\cdot w_2)(k_2\cdot p_4) + c_{33}(k_1\cdot w_1)(k_2\cdot p_4)^2\\
&+ c_{34}(k_1\cdot w_2)(k_2\cdot p_4)^2\\
&+ c_{35}\big(\tfrac{1}{2}(k_1\cdot w_1)^2(k_2\cdot p_4) + \tfrac{1}{2}(k_1\cdot w_2)^2(k_2\cdot p_4)\big)\\
&+ c_{36}(k_1\cdot w_1)(k_2\cdot p_5) + c_{37}(k_1\cdot p_4)(k_1\cdot w_1)(k_2\cdot p_5)\\
&+ c_{38}(k_1\cdot w_2)(k_2\cdot p_5) + c_{39}(k_1\cdot p_4)(k_1\cdot w_2)(k_2\cdot p_5)\\
&+ c_{40}(k_1\cdot w_1)(k_1\cdot w_2)(k_2\cdot p_5) + c_{41}(k_1\cdot w_1)(k_2\cdot p_4)(k_2\cdot p_5)\\
&+ c_{42}(k_1\cdot w_2)(k_2\cdot p_4)(k_2\cdot p_5) + c_{43}(k_1\cdot w_1)(k_2\cdot p_5)^2\\
&+ c_{44}(k_1\cdot w_2)(k_2\cdot p_5)^2\\
&+ c_{45}\big(\tfrac{1}{2}(k_1\cdot w_1)^2(k_2\cdot p_5) + \tfrac{1}{2}(k_1\cdot w_2)^2(k_2\cdot p_5)\big)\\
&+ c_{46}(k_2\cdot w_1) + c_{47}(k_1\cdot p_4)(k_2\cdot w_1) + c_{48}(k_1\cdot p_4)^2(k_2\cdot w_1)\\
&+ c_{49}(k_1\cdot w_1)^2(k_2\cdot w_1) + c_{50}(k_1\cdot w_2)(k_2\cdot w_1)\\
&+ c_{51}(k_1\cdot p_4)(k_1\cdot w_2)(k_2\cdot w_1) + c_{52}(k_2\cdot p_4)(k_2\cdot w_1)\\
&+ c_{53}(k_1\cdot p_4)(k_2\cdot p_4)(k_2\cdot w_1) + c_{54}(k_1\cdot w_2)(k_2\cdot p_4)(k_2\cdot w_1)\\
&+ c_{55}(k_2\cdot p_5)(k_2\cdot w_1) + c_{56}(k_1\cdot p_4)(k_2\cdot p_5)(k_2\cdot w_1)\\
&+ c_{57}(k_1\cdot w_2)(k_2\cdot p_5)(k_2\cdot w_1) + c_{58}(k_1\cdot w_1)(k_2\cdot w_1)^2\\
&+ c_{59}(k_2\cdot w_2) + c_{60}(k_1\cdot p_4)(k_2\cdot w_2) + c_{61}(k_1\cdot p_4)^2(k_2\cdot w_2)\\
&+ c_{62}(k_1\cdot w_1)(k_2\cdot w_2) + c_{63}(k_1\cdot p_4)(k_1\cdot w_1)(k_2\cdot w_2)\\
&+ c_{64}(k_1\cdot w_1)^2(k_2\cdot w_2) + c_{65}(k_2\cdot p_4)(k_2\cdot w_2)\\
&+ c_{66}(k_1\cdot p_4)(k_2\cdot p_4)(k_2\cdot w_2) + c_{67}(k_1\cdot w_1)(k_2\cdot p_4)(k_2\cdot w_2)\\
&+ c_{68}(k_2\cdot p_5)(k_2\cdot w_2) + c_{69}(k_1\cdot p_4)(k_2\cdot p_5)(k_2\cdot w_2)\\
&+ c_{70}(k_1\cdot w_1)(k_2\cdot p_5)(k_2\cdot w_2) + c_{71}(k_2\cdot w_1)(k_2\cdot w_2)\\
&+ c_{72}(k_1\cdot p_4)(k_2\cdot w_1)(k_2\cdot w_2) + c_{73}(k_1\cdot w_1)(k_2\cdot w_1)(k_2\cdot w_2)\\
&+ c_{74}\big(\tfrac{1}{2}(k_1\cdot w_1)(k_2\cdot w_1) + \tfrac{1}{2}(k_1\cdot w_2)(k_2\cdot w_2)\big)\\
&+ c_{75}\big(\tfrac{1}{2}(k_1\cdot p_4)(k_1\cdot w_1)(k_2\cdot w_1) + \tfrac{1}{2}(k_1\cdot p_4)(k_1\cdot w_2)(k_2\cdot w_2)\big)\\
&+ c_{76}\big(\tfrac{1}{2}(k_1\cdot w_1)(k_2\cdot p_4)(k_2\cdot w_1) + \tfrac{1}{2}(k_1\cdot w_2)(k_2\cdot p_4)(k_2\cdot w_2)\big)\\
&+ c_{77}\big(\tfrac{1}{2}(k_1\cdot w_1)(k_2\cdot p_5)(k_2\cdot w_1) + \tfrac{1}{2}(k_1\cdot w_2)(k_2\cdot p_5)(k_2\cdot w_2)\big)\\
&+ c_{78}\big(\tfrac{1}{2}(k_2\cdot w_1)^2 + \tfrac{1}{2}(k_2\cdot w_2)^2\big)\\
&+ c_{79}\big(\tfrac{1}{2}(k_1\cdot p_4)(k_2\cdot w_1)^2 + \tfrac{1}{2}(k_1\cdot p_4)(k_2\cdot w_2)^2\big)\\
&+ c_{80}\big(-\tfrac{1}{2}x_5 + (k_1\cdot p_4) + 2(k_2\cdot p_4)\big)
\end{aligned}
$$

$$
\begin{aligned}
&+ c_{81}\big(-\tfrac{1}{2}(k_1\cdot p_4)x_5 + (k_1\cdot p_4)^2 + 2(k_1\cdot p_4)(k_2\cdot p_4)\big)\\
&+ c_{82}\big(-\tfrac{1}{2}(k_1\cdot p_4)^2x_5 + 2(k_1\cdot p_4)^2(k_2\cdot p_4) + (k_1\cdot p_4)^3\big)\\
&+ c_{83}(k_1\cdot w_1)\mu_{11} + c_{84}(k_1\cdot w_2)\mu_{11} + c_{85}(k_2\cdot w_1)\mu_{11}\\
&+ c_{86}(k_2\cdot w_2)\mu_{11} + c_{87}\big(-\tfrac{1}{2}\mu_{11}x_5 + (k_1\cdot p_4)\mu_{11} + 2(k_2\cdot p_4)\mu_{11}\big)\\
&+ c_{88}(k_1\cdot w_1)\mu_{12} + c_{89}(k_1\cdot w_2)\mu_{12} + c_{90}(k_2\cdot w_1)\mu_{12}\\
&+ c_{91}(k_2\cdot w_2)\mu_{12} + c_{92}\big(\mu_{11} + 2\mu_{12}\big)\\
&+ c_{93}\big((k_1\cdot p_4)\mu_{11} + 2(k_1\cdot p_4)\mu_{12}\big)\\
&+ c_{94}(k_1\cdot w_1)\mu_{22} + c_{95}(k_1\cdot w_2)\mu_{22}\\
&+ c_{96}\big(-\tfrac{1}{2}k_1^2 + \tfrac{1}{2}(k_1-p_1-p_2-p_3)^2 + \tfrac{1}{2}x_5 - (k_1\cdot p_4)\\
&\qquad + 2(k_2\cdot p_5)\big)\\
&+ c_{97}\big(-\tfrac{1}{2}(k_1)^2(k_1\cdot p_4) + \tfrac{1}{2}(k_1\cdot p_4)(k_1-p_1-p_2-p_3)^2\\
&\qquad + \tfrac{1}{2}(k_1\cdot p_4)x_5 - (k_1\cdot p_4)^2 + 2(k_1\cdot p_4)(k_2\cdot p_5)\big)\\
&+ c_{98}\big(-\tfrac{1}{2}(k_1)^2(k_1\cdot p_4)^2 + \tfrac{1}{2}(k_1\cdot p_4)^2(k_1-p_1-p_2-p_3)^2\\
&\qquad + \tfrac{1}{2}(k_1\cdot p_4)^2x_5 + 2(k_1\cdot p_4)^2(k_2\cdot p_5) - (k_1\cdot p_4)^3\big)\\
&+ c_{99}\big(-\tfrac{1}{2}k_1^2\mu_{11} + \tfrac{1}{2}(k_1-p_1-p_2-p_3)^2\mu_{11} + \tfrac{1}{2}\mu_{11}x_5\\
&\qquad - (k_1\cdot p_4)\mu_{11} + 2(k_2\cdot p_5)\mu_{11}\big). \qquad \text{(E.2)}
\end{aligned}
$$

$\Delta \Big($ 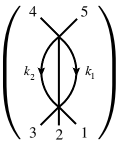 $\Big)$

$$
\begin{aligned}
&= c_0 + c_1(k_1\cdot p_{123}) + c_2(k_1\cdot p_{123})(k_2\cdot p_{123}) + c_3\mu_{12}\\
&+ c_4(k_1\cdot w_1) + c_5(k_1\cdot p_{123})(k_1\cdot w_1) + c_6(k_1\cdot w_2)\\
&+ c_7(k_1\cdot p_{123})(k_1\cdot w_2) + c_8(k_1\cdot w_1)(k_1\cdot w_2) + c_9(k_1\cdot w_3)\\
&+ c_{10}(k_1\cdot p_{123})(k_1\cdot w_3) + c_{11}(k_1\cdot w_1)(k_1\cdot w_3) + c_{12}(k_1\cdot w_2)(k_1\cdot w_3)\\
&+ c_{13}\big((k_1\cdot p_{123}) - (k_2\cdot p_{123})\big) + c_{14}(k_1\cdot w_1)(k_2\cdot p_{123})\\
&+ c_{15}(k_1\cdot w_2)(k_2\cdot p_{123}) + c_{16}(k_1\cdot w_3)(k_2\cdot p_{123})\\
&+ c_{17}\big(-(k_1\cdot p_{123})^2 + (k_2\cdot p_{123})^2\big) + c_{18}(k_2\cdot w_1)\\
&+ c_{19}(k_1\cdot p_{123})(k_2\cdot w_1) + c_{20}(k_1\cdot w_2)(k_2\cdot w_1) + c_{21}(k_1\cdot w_3)(k_2\cdot w_1)\\
&+ c_{22}(k_2\cdot p_{123})(k_2\cdot w_1) + c_{23}(k_2\cdot w_2) + c_{24}(k_1\cdot p_{123})(k_2\cdot w_2)\\
&+ c_{25}(k_1\cdot w_1)(k_2\cdot w_2) + c_{26}(k_1\cdot w_3)(k_2\cdot w_2) + c_{27}(k_2\cdot p_{123})(k_2\cdot w_2)\\
&+ c_{28}(k_2\cdot w_1)(k_2\cdot w_2) + c_{29}(k_2\cdot w_3) + c_{30}(k_1\cdot p_{123})(k_2\cdot w_3)\\
&+ c_{31}(k_1\cdot w_1)(k_2\cdot w_3) + c_{32}(k_1\cdot w_2)(k_2\cdot w_3) + c_{33}(k_2\cdot p_{123})(k_2\cdot w_3)
\end{aligned}
$$

$$
\begin{aligned}
&+ c_{34}(k_2 \cdot w_1)(k_2 \cdot w_3) + c_{35}(k_2 \cdot w_2)(k_2 \cdot w_3) \\
&+ c_{36}\big(\tfrac{1}{3}(k_1 \cdot w_1)^2 - \tfrac{1}{3x_5}(k_1 \cdot w_3)^2(x_4 - x_5)^2 + \tfrac{2}{3}(k_1 \cdot w_2)^2\big) \\
&+ c_{37}\big(\tfrac{1}{3}(k_1 \cdot w_2)^2 + \tfrac{1}{3x_5}(k_1 \cdot w_3)^2(x_4 - x_5)^2 + \tfrac{2}{3}(k_1 \cdot w_1)^2\big) \\
&+ c_{38}\big(\tfrac{1}{3}(k_1 \cdot w_1)(k_2 \cdot w_1) - \tfrac{1}{3x_5}(k_1 \cdot w_3)(k_2 \cdot w_3)(x_4 - x_5)^2 \\
&\qquad\qquad + \tfrac{2}{3}(k_1 \cdot w_2)(k_2 \cdot w_2)\big) \\
&+ c_{39}\big(\tfrac{1}{3}(k_1 \cdot w_2)(k_2 \cdot w_2) + \tfrac{1}{3x_5}(k_1 \cdot w_3)(k_2 \cdot w_3)(x_4 - x_5)^2 \\
&\qquad\qquad + \tfrac{2}{3}(k_1 \cdot w_1)(k_2 \cdot w_1)\big) \\
&+ c_{40}\big(\tfrac{1}{3}(k_2 \cdot w_1)^2 - \tfrac{1}{3x_5}(k_2 \cdot w_3)^2(x_4 - x_5)^2 + \frac{2}{3}(k_2 \cdot w_2)^2\big) \\
&+ c_{41}\big(\tfrac{1}{3}(k_2 \cdot w_2)^2 + \tfrac{1}{3x_5}(k_2 \cdot w_3)^2(x_4 - x_5)^2 + \tfrac{2}{3}(k_2 \cdot w_1)^2\big) \\
&+ c_{42}\big((k_1 \cdot p_{123})^2 + 2(k_1 \cdot p_{123})(k_2 \cdot p_{123}) + (k_1 \cdot p_{123})x_5\big) \\
&+ c_{43}\big(\mu_{11} + 2\mu_{12}\big) + c_{44}\big(-\mu_{11} + \mu_{22}\big)
\end{aligned}
\tag{E.3}
$$

Appendix F

Rational spinors for six-dimensional loop momenta

In [165] a redefinition of the scalar product between two vectors is used to ensure rational on-shell loop momentum representations. In this appendix we will extend this discussion to six-dimensional spinors. The new scalar product between two six-dimensional vectors will depend on the cut topology through dependence on the extra-dimensional ISPs, $\mu_{ij} = -k_{\perp,i}^{[-2\epsilon]} \cdot k_{\perp,j}^{[-2\epsilon]}$. We define,

$$\begin{aligned} k_i \cdot k_j &= k_i^{[4d]} \cdot k_j^{[4d]} + g_{44} k_i^4 k_j^4 + g_{55} k_i^5 k_j^5 \\ &= k_i^{[4d]} \cdot k_j^{[4d]} + \mu_{11} k_i^4 k_j^4 + \left(\frac{\mu_{22}\mu_{11} - \mu_{12}^2}{\mu_{11}} \right) k_i^5 k_j^5. \end{aligned} \tag{F.1}$$

Reading off the metric we have,

$$\begin{aligned} g_{MN} &= \text{diag}\left(1, -1, -1, -1, \mu_{11}, \frac{\mu_{22}\mu_{11} - \mu_{12}^2}{\mu_{11}}\right), \\ g^{MN} &= \text{diag}\left(1, -1, -1, -1, \frac{1}{\mu_{11}}, \frac{\mu_{11}}{\mu_{22}\mu_{11} - \mu_{12}^2}\right), \end{aligned} \tag{F.2}$$

such that $g_{MN} g^{NO} = \delta_M^O$. The loop momenta are,

$$\begin{aligned} k_1^M &= (k_1^\mu, 1, 0), \\ k_2^M &= \left(k_2^\mu, \frac{\mu_{12}}{\mu_{11}}, 1\right). \end{aligned} \tag{F.3}$$

To satisfy the Clifford algebra,

$$\left\{\Sigma^M, \tilde{\Sigma}^N\right\} = 2g^{MN}, \tag{F.4}$$

the first four Σ-matrices, (A.4a)-(A.4d), are left unchanged but the extra-dimensional ones become,

$$\Sigma^4 = \begin{pmatrix} 0 & -\frac{1}{c\mu_{11}} & 0 & 0 \\ \frac{1}{c\mu_{11}} & 0 & 0 & 0 \\ 0 & 0 & 0 & c \\ 0 & 0 & -c & 0 \end{pmatrix}, \qquad \tilde{\Sigma}^4 = \begin{pmatrix} 0 & c & 0 & 0 \\ -c & 0 & 0 & 0 \\ 0 & 0 & 0 & -\frac{1}{c\mu_{11}} \\ 0 & 0 & \frac{1}{c\mu_{11}} & 0 \end{pmatrix}, \tag{F.5a}$$

$$\Sigma^5 = \begin{pmatrix} 0 & -\frac{1}{c\sqrt{\mu_{12}^2-\mu_{11}\mu_{22}}} & 0 & 0 \\ \frac{1}{c\sqrt{\mu_{12}^2-\mu_{11}\mu_{22}}} & 0 & 0 & 0 \\ 0 & 0 & 0 & -\frac{c\mu_{11}}{\sqrt{\mu_{12}^2-\mu_{11}\mu_{22}}} \\ 0 & 0 & \frac{c\mu_{11}}{\sqrt{\mu_{12}^2-\mu_{11}\mu_{22}}} & 0 \end{pmatrix}, \tag{F.5b}$$

$$\tilde{\Sigma}^5 = \begin{pmatrix} 0 & -\frac{c\mu_{11}}{\sqrt{\mu_{12}^2-\mu_{11}\mu_{22}}} & 0 & 0 \\ \frac{c\mu_{11}}{\sqrt{\mu_{12}^2-\mu_{11}\mu_{22}}} & 0 & 0 & 0 \\ 0 & 0 & 0 & -\frac{1}{c\sqrt{\mu_{12}^2-\mu_{11}\mu_{22}}} \\ 0 & 0 & \frac{1}{c\sqrt{\mu_{12}^2-\mu_{11}\mu_{22}}} & 0 \end{pmatrix}, \tag{F.5c}$$

where c is a free parameter. A tempting choice is to set $c = 1/\sqrt{\mu_{11}}$ to obtain uniform mass dimension in the matrix entries. However, in an implementation relying on rational parametrisations we will need to define an algebra that keeps separate track of every square root. It is therefore more convenient to choose $c = 1$ and the only square-root is then,

$$F \equiv \sqrt{\mu_{12}^2 - \mu_{11}\mu_{22}}. \tag{F.6}$$

With this definition the last Σ-matrices can be written,

$$\Sigma^5 = \frac{1}{F}\begin{pmatrix} 0 & -1 & 0 & 0 \\ 1 & 0 & 0 & 0 \\ 0 & 0 & 0 & -\mu_{11} \\ 0 & 0 & \mu_{11} & 0 \end{pmatrix}, \qquad \tilde{\Sigma}^5 = \frac{1}{F}\begin{pmatrix} 0 & -\mu_{11} & 0 & 0 \\ \mu_{11} & 0 & 0 & 0 \\ 0 & 0 & 0 & -1 \\ 0 & 0 & 1 & 0 \end{pmatrix}. \tag{F.7}$$

Six-dimensional Feynman slashed momenta can then be written in terms of two matrices, a, b, which are free of square roots,

$$\not{p}_{AB} = p_M \Sigma^M_{AB} = a_p + F b_p. \tag{F.8}$$

Matrix multiplication of two slashed momenta is done through,

$$\not{p}\not{q} = \underbrace{(a_p.a_q + F^2 b_p.q_p)}_{\text{rational}} + F \underbrace{(a_p.b_q + b_p.a_q)}_{\text{rational}}. \tag{F.9}$$

The loop momenta (F.3) in Feynman slash notation are,

$$\not{k}_1 = k_1^{[4d]} \cdot \Sigma^{[4d]} + \mu_{11}\Sigma^4, \tag{F.10a}$$

$$\not{k}_2 = k_2^{[4d]} \cdot \Sigma^{[4d]} + \mu_{12}\Sigma^4 - \frac{F^2}{\mu_{11}}\Sigma^5, \tag{F.10b}$$

and we read off the matrices,

$$a_1 = k_1^{[4d]} \cdot \Sigma^{[4d]} + \mu_{11}\Sigma^4, \qquad b_1 = 0, \tag{F.11a}$$

$$a_2 = k_2^{[4d]} \cdot \Sigma^{[4d]} + \mu_{12}\Sigma^4, \qquad b_2 = \begin{pmatrix} 0 & \frac{1}{\mu_{11}} & 0 & 0 \\ -\frac{1}{\mu_{11}} & 0 & 0 & 0 \\ 0 & 0 & 0 & 1 \\ 0 & 0 & -1 & 0 \end{pmatrix}. \tag{F.11b}$$

Note that numerically $b_2 = -\Sigma^4$. For the $\tilde{\Sigma}$-matrices we get similar relations,

$$\not{k}_i^{AB} = k_{iM}\tilde{\Sigma}^{M,AB} = \tilde{a}_i + F\tilde{b}_i, \tag{F.12}$$

$$\tilde{a}_1 = k_1^{[4d]} \cdot \tilde{\Sigma}^{[4d]} + \mu_{11}\tilde{\Sigma}^4 \qquad \tilde{b}_1 = 0 \tag{F.13a}$$

$$\tilde{a}_2 = k_2^{[4d]} \cdot \tilde{\Sigma}^{[4d]} + \mu_{12}\tilde{\Sigma}^4 \qquad \tilde{b}_2 = \begin{pmatrix} 0 & 1 & 0 & 0 \\ -1 & 0 & 0 & 0 \\ 0 & 0 & 0 & \frac{1}{\mu_{11}} \\ 0 & 0 & -\frac{1}{\mu_{11}} & 0 \end{pmatrix}, \tag{F.13b}$$

where numerically $\tilde{b}_2 = \tilde{\Sigma}^4$. Note that because $b_1 = 0$ and $\tilde{b}_1 = 0$ the one-loop case is automatically square-root free.

We can now construct spinors by requiring that they solve the Dirac equation and satisfy the completeness relation,

$$\not{k}_{i,AB}\lambda^B = 0, \qquad \not{k}_i^{AB} = \lambda_{ia}^A \epsilon^{ab} \lambda_{ib}^B. \tag{F.14}$$

The general solution when $k_-^\perp = k^1 - ik^2 \neq 0$ can be written,

$$\lambda^A(k) = \begin{pmatrix} 0 & -1 \\ \Lambda\mu_{11}^2 k^4 & \frac{k_+}{k_-^\perp} \\ k_-^\perp & 0 \\ k_- & \frac{k^4}{k_-^\perp} \end{pmatrix} + F \begin{pmatrix} 0 & 0 \\ \Lambda\mu_{11} k^5 & 0 \\ 0 & 0 \\ 0 & \frac{-k^5}{k_-^\perp}\frac{1}{\mu_{11}} \end{pmatrix}, \tag{F.15a}$$

$$\tilde{\lambda}_A(k) = \begin{pmatrix} \Lambda\mu_{11} k^4 & \frac{k_+}{k_-^\perp} \\ 0 & 1 \\ k_- & \frac{k^4\mu_{11}}{k_-^\perp} \\ -k_-^\perp & 0 \end{pmatrix} + F \begin{pmatrix} -\Lambda k^5 & 0 \\ 0 & 0 \\ 0 & \frac{k^5}{k_-^\perp} \\ 0 & 0 \end{pmatrix}, \tag{F.15b}$$

where,

$$\Lambda(k) = \frac{k_+k_- - k_+^\perp k_-^\perp}{(k^4)^2\mu_{11}^2 - (k^5)^2F^2}. \tag{F.16}$$

Notice that the term linear in F vanishes for k_1 since $k_1^5 = 0$. It is also worth noting that in spinor products the coefficient of F^2 always vanishes. It should be emphasised that the μ_{ij}'s come from the topology specific loop momenta, while we have kept the components of k^M general. In practical applications the loop

momenta is given by (4.46) and $\Lambda(k)$ simplifies and becomes identical for k_1 and k_2,

$$\Lambda(k_1) = -\frac{1}{\mu_{11}}, \qquad \Lambda(k_2) = -\frac{1}{\mu_{11}}. \tag{F.17}$$

$\Lambda(k)$ is therefore divergent for four-dimensional momenta, but since the Σ-matrices are unchanged in the four-dimensional subspace we can use the simple solutions in (2.22).

When calculating two-loop fermion cuts with these spinors it turns out that the result for the chiral and anti-chiral spinors only differ by the sign of the term linear in F. Calculation for one of the fermions is therefore sufficient to determine the cut, thereby lowering the computational expense related to the handling of the square root.

The six-dimensional spinor product between the two loop momenta become,

$$\begin{aligned}\lambda_a^A(k_1)\lambda_{A\dot{a}}(k_2) = &\begin{pmatrix} -k_{1-}k_2^{\perp}{}_{-} + k_1^{\perp}{}_{-}k_{2-} & \frac{k_1^{\perp}{}_{-}}{k_2^{\perp}{}_{-}}\mu_{12} - \mu_{11} \\ -\frac{k_2^{\perp}{}_{-}}{k_1^{\perp}{}_{-}}\mu_{11} + \mu_{12} & \frac{k_{1+}}{k_1^{\perp}{}_{-}} - \frac{k_{2+}}{k_2^{\perp}{}_{-}} \end{pmatrix} \\ &+ F\begin{pmatrix} 0 & \frac{k_1^{\perp}{}_{-}}{k_2^{\perp}{}_{-}} \\ -\frac{1}{\mu_{11}} & 0 \end{pmatrix}.\end{aligned} \tag{F.18}$$

We end this appendix by giving an alternative solution to (F.15). In the case when $k_-^{\perp} = 0$ we instead use,

$$\lambda^A(k) = \begin{pmatrix} \Lambda\mu_{11}^2 k^4 & \frac{k_-}{k_+^{\perp}} \\ 0 & -1 \\ k_+ & \frac{k^4}{k_+^{\perp}} \\ k_{\perp} & 0 \end{pmatrix} + F\begin{pmatrix} \Lambda\mu_{11}k^5 & 0 \\ 0 & 0 \\ 0 & \frac{-k^5}{k_+^{\perp}}\frac{1}{\mu_{11}} \\ 0 & 0 \end{pmatrix}, \tag{F.19a}$$

$$\tilde{\lambda}_A(k) = \begin{pmatrix} 0 & -1 \\ -\Lambda\mu_{11}k^4 & \frac{-k_-}{k_+^{\perp}} \\ k_+^{\perp} & 0 \\ -k_+ & \frac{-k^4\mu_{11}}{k_+^{\perp}} \end{pmatrix} + F\begin{pmatrix} 0 & 0 \\ \Lambda k^5 & 0 \\ 0 & 0 \\ 0 & \frac{-k^5}{k_+^{\perp}} \end{pmatrix}. \tag{F.19b}$$

Bibliography

[1] S. Badger, C. Brønnum-Hansen, F. Buciuni and D. O'Connell, *A unitarity compatible approach to one-loop amplitudes with massive fermions*, *JHEP* **06** (2017) 141, [1703.05734].

[2] S. Badger, C. Brønnum-Hansen, H. B. Hartanto and T. Peraro, *First look at two-loop five-gluon scattering in QCD*, *Phys. Rev. Lett.* **120** (2018) 092001, [1712.02229].

[3] S. Badger, C. Brønnum-Hansen, T. Gehrmann, H. B. Hartanto, J. Henn, N. A. Lo Presti et al., *Applications of integrand reduction to two-loop five-point scattering amplitudes in QCD*, in *14th DESY Workshop on Elementary Particle Physics: Loops and Legs in Quantum Field Theory 2018 (LL2018) St Goar, Germany, April 29-May 4, 2018*, 2018. 1807.09709.

[4] S. Badger, C. Brønnum-Hansen, H. B. Hartanto and T. Peraro, *Analytic helicity amplitudes for two-loop five-gluon scattering: the single-minus case*, *JHEP* **01** (2019) 186, [1811.11699].

[5] M. Peskin and D. Schroeder, *An introduction to quantum field theory*. Addison-Wesley, Reading, Mass., 1995.

[6] R. K. Ellis, W. J. Stirling and B. R. Webber, *QCD and Collider Physics*. Cambridge Monographs on Particle Physics, Nuclear Physics and Cosmology ; no. 8. Cambridge University Press, Cambridge, 1996.

[7] M. L. Mangano and S. J. Parke, *Multi-parton amplitudes in gauge theories*, *Phys.Rept.* **200** (1991) 301–367, [hep-th/0509223].

[8] L. J. Dixon, *Calculating scattering amplitudes efficiently*, in *QCD and beyond. Proceedings, Theoretical Advanced Study Institute in Elementary*

Particle Physics, TASI-95, Boulder, USA, June 4-30, 1995, pp. 539–584, 1996. hep-ph/9601359.

[9] L. H. Ryder, *Quantum field theory*. Cambridge University Press, Cambridge, second ed., 1996.

[10] M. A. Srednicki, *Quantum field theory*. Cambridge University Press, Cambridge, 2007.

[11] F. A. Berends and W. Giele, *The Six Gluon Process as an Example of Weyl-Van Der Waerden Spinor Calculus*, *Nucl. Phys.* **B294** (1987) 700–732.

[12] M. L. Mangano, S. J. Parke and Z. Xu, *Duality and Multi - Gluon Scattering*, *Nucl. Phys.* **B298** (1988) 653–672.

[13] R. K. Ellis and G. Zanderighi, *Scalar one-loop integrals for QCD*, *JHEP* **02** (2008) 002, [0712.1851].

[14] F. Bloch and A. Nordsieck, *Note on the radiation field of the electron*, *Phys. Rev.* **52** (Jul, 1937) 54–59.

[15] T. Kinoshita, *Mass singularities of Feynman amplitudes*, *J. Math. Phys.* **3** (1962) 650–677.

[16] T. D. Lee and M. Nauenberg, *Degenerate systems and mass singularities*, *Phys. Rev.* **133** (Mar, 1964) B1549–B1562.

[17] Particle Data Group collaboration, M. Tanabashi, K. Hagiwara, K. Hikasa, K. Nakamura, Y. Sumino, F. Takahashi et al., *Review of particle physics*, *Phys. Rev. D* **98** (Aug, 2018) 030001.

[18] P. A. Baikov, K. G. Chetyrkin and J. H. Kühn, *Five-Loop Running of the QCD coupling constant*, *Phys. Rev. Lett.* **118** (2017) 082002, [1606.08659].

[19] F. Herzog, B. Ruijl, T. Ueda, J. A. M. Vermaseren and A. Vogt, *The five-loop beta function of Yang-Mills theory with fermions*, *JHEP* **02** (2017) 090, [1701.01404].

[20] J. C. Collins, D. E. Soper and G. Sterman, *Factorization of Hard Processes in QCD*, *Adv.Ser.Direct.High Energy Phys.* **5** (1988) 1–91, [hep-ph/0409313].

[21] W. T. Giele and E. W. N. Glover, *Higher order corrections to jet cross-sections in e+ e- annihilation*, *Phys. Rev.* **D46** (1992) 1980–2010.

[22] S. Catani and M. H. Seymour, *A General Algorithm for Calculating Jet Cross Sections in NLO QCD*, *Nucl.Phys. B485 (1997) 291-419; Erratum-ibid.* **B510** (1998) 503–504, [hep-ph/9605323].

[23] J. R. Andersen et al., *Les Houches 2017: Physics at TeV Colliders Standard Model Working Group Report*, in *10th Les Houches Workshop on Physics at TeV Colliders (PhysTeV 2017) Les Houches, France, June 5-23, 2017*, 2018. 1803.07977.

[24] H. Elvang and Y.-t. Huang, *Scattering Amplitudes in Gauge Theory and Gravity*. Cambridge University Press, 2015.

[25] S. J. Parke and T. R. Taylor, *An Amplitude for n Gluon Scattering*, *Phys. Rev. Lett.* **56** (1986) 2459.

[26] F. Berends and W. Giele, *Recursive calculations for processes with n gluons*, *Nuclear Physics B* **306** (1988) 759 – 808.

[27] C. Cheung and D. O'Connell, *Amplitudes and Spinor-Helicity in Six Dimensions*, *JHEP* **07** (2009) 075, [0902.0981].

[28] R. Boels, *Covariant representation theory of the Poincare algebra and some of its extensions*, *JHEP* **01** (2010) 010, [0908.0738].

[29] T. Dennen, Y.-t. Huang and W. Siegel, *Supertwistor space for 6D maximal super Yang-Mills*, *JHEP* **04** (2010) 127, [0910.2688].

[30] Z. Bern, J. J. Carrasco, T. Dennen, Y.-t. Huang and H. Ita, *Generalized Unitarity and Six-Dimensional Helicity*, *Phys. Rev.* **D83** (2011) 085022, [1010.0494].

[31] S. Caron-Huot and D. O'Connell, *Spinor Helicity and Dual Conformal Symmetry in Ten Dimensions*, *JHEP* **08** (2011) 014, [1010.5487].

[32] T. Dennen and Y.-t. Huang, *Dual Conformal Properties of Six-Dimensional Maximal Super Yang-Mills Amplitudes*, *JHEP* **01** (2011) 140, [1010.5874].

[33] S. Davies, *One-Loop QCD and Higgs to Partons Processes Using Six-Dimensional Helicity and Generalized Unitarity*, *Phys. Rev.* **D84** (2011) 094016, [1108.0398].

[34] R. H. Boels and D. O'Connell, *Simple superamplitudes in higher dimensions*, *JHEP* **06** (2012) 163, [1201.2653].

[35] S. Badger, F. Buciuni and T. Peraro, *One-loop triple collinear splitting amplitudes in QCD*, *JHEP* **09** (2015) 188, [1507.05070].

[36] R. Britto, F. Cachazo and B. Feng, *New recursion relations for tree amplitudes of gluons*, *Nucl. Phys.* **B715** (2005) 499–522, [hep-th/0412308].

[37] R. Britto, F. Cachazo, B. Feng and E. Witten, *Direct proof of tree-level recursion relation in Yang-Mills theory*, *Phys. Rev. Lett.* **94** (2005) 181602, [hep-th/0501052].

[38] L. J. Dixon, *A brief introduction to modern amplitude methods*, in *Proceedings, 2012 European School of High-Energy Physics (ESHEP 2012): La Pommeraye, Anjou, France, June 06-19, 2012*, pp. 31–67, 2014. 1310.5353. DOI.

[39] N. Arkani-Hamed and J. Kaplan, *On tree amplitudes in gauge theory and gravity*, *JHEP* **0804** (2008) 076, [0801.2385].

[40] A. Hodges, *Eliminating spurious poles from gauge-theoretic amplitudes*, *JHEP* **05** (2013) 135, [0905.1473].

[41] S. Badger, *Automating QCD amplitudes with on-shell methods*, 1605.02172.

[42] G. Passarino and M. J. G. Veltman, *One Loop Corrections for e+ e- Annihilation Into mu+ mu- in the Weinberg Model*, *Nucl. Phys.* **B160** (1979) 151–207.

[43] W. L. van Neerven and J. A. M. Vermaseren, *Large Loop Integrals*, *Phys. Lett.* **B137** (1984) 241–244.

[44] Z. Bern, L. J. Dixon and D. A. Kosower, *Dimensionally regulated one loop integrals*, *Phys. Lett.* **B302** (1993) 299–308, [hep-ph/9212308].

[45] G. 't Hooft and M. J. G. Veltman, *Scalar One Loop Integrals*, *Nucl. Phys.* **B153** (1979) 365–401.

[46] A. Denner, U. Nierste and R. Scharf, *A Compact expression for the scalar one loop four point function*, *Nucl. Phys.* **B367** (1991) 637–656.

[47] G. Ossola, C. G. Papadopoulos and R. Pittau, *Reducing full one-loop amplitudes to scalar integrals at the integrand level*, *Nucl. Phys.* **B763** (2007) 147–169, [hep-ph/0609007].

[48] R. K. Ellis, W. T. Giele and Z. Kunszt, *A Numerical Unitarity Formalism for Evaluating One-Loop Amplitudes*, *JHEP* **03** (2008) 003, [0708.2398].

[49] W. T. Giele, Z. Kunszt and K. Melnikov, *Full one-loop amplitudes from tree amplitudes*, *JHEP* **04** (2008) 049, [0801.2237].

[50] Z. Bern, L. J. Dixon, D. C. Dunbar and D. A. Kosower, *One loop n point gauge theory amplitudes, unitarity and collinear limits*, *Nucl. Phys.* **B425** (1994) 217–260, [hep-ph/9403226].

[51] Z. Bern, L. J. Dixon, D. C. Dunbar and D. A. Kosower, *Fusing gauge theory tree amplitudes into loop amplitudes*, *Nucl. Phys.* **B435** (1995) 59–101, [hep-ph/9409265].

[52] R. E. Cutkosky, *Singularities and discontinuities of Feynman amplitudes*, *J. Math. Phys.* **1** (1960) 429–433.

[53] R. Britto, F. Cachazo and B. Feng, *Generalized unitarity and one-loop amplitudes in N=4 super-Yang-Mills*, *Nucl. Phys.* **B725** (2005) 275–305, [hep-th/0412103].

[54] D. Forde, *Direct extraction of one-loop integral coefficients*, *Phys. Rev.* **D75** (2007) 125019, [0704.1835].

[55] Z. Bern and D. A. Kosower, *The computation of loop amplitudes in gauge theories*, *Nuclear Physics B* **379** (1992) 451 – 561.

[56] Z. Bern, A. De Freitas, L. J. Dixon and H. L. Wong, *Supersymmetric regularization, two loop QCD amplitudes and coupling shifts*, *Phys. Rev.* **D66** (2002) 085002, [hep-ph/0202271].

[57] Z. Bern, L. J. Dixon and D. A. Kosower, *On-Shell Recurrence Relations for One-Loop QCD Amplitudes*, *Phys.Rev.D* **71** (2005) 105013, [hep-th/0501240].

[58] Z. Bern, L. J. Dixon and D. A. Kosower, *The Last of the Finite Loop Amplitudes in QCD*, *Phys.Rev.D* **72** (2005) 125003, [hep-ph/0505055].

[59] Z. Bern, L. J. Dixon and D. A. Kosower, *Bootstrapping Multi-Parton Loop Amplitudes in QCD*, *Phys.Rev.D* **73** (2006) 065013, [hep-ph/0507005].

[60] G. Ossola, C. G. Papadopoulos and R. Pittau, *On the rational terms of the one-loop amplitudes*, *JHEP* **0805** (2008) 004, [0802.1876].

[61] Z. Bern and A. G. Morgan, *Massive loop amplitudes from unitarity*, *Nucl. Phys.* **B467** (1996) 479–509, [hep-ph/9511336].

[62] Z. Bern, L. Dixon, D. Dunbar and D. Kosower, *One-Loop Self-Dual and N=4 Super Yang-Mills*, *Phys.Lett.B* **394** (1997) 105–115, [hep-th/9611127].

[63] S. D. Badger, *Direct extraction of one loop rational terms*, *JHEP* **0901** (2009) 049, [0806.4600].

[64] G. 't Hooft and M. J. G. Veltman, *Regularization and Renormalization of Gauge Fields*, *Nucl. Phys.* **B44** (1972) 189–213.

[65] M. Czakon, P. Fiedler and A. Mitov, *Total Top-Quark Pair-Production Cross Section at Hadron Colliders Through $O(\alpha_S^4)$*, *Phys. Rev. Lett.* **110** (2013) 252004, [1303.6254].

[66] M. Czakon, D. Heymes and A. Mitov, *High-precision differential predictions for top-quark pairs at the LHC*, *Phys. Rev. Lett.* **116** (2016) 082003, [1511.00549].

[67] G. Bevilacqua, H. B. Hartanto, M. Kraus and M. Worek, *Top Quark Pair Production in Association with a Jet with Next-to-Leading-Order QCD Off-Shell Effects at the Large Hadron Collider*, *Phys. Rev. Lett.* **116** (2016) 052003, [1509.09242].

[68] S. Höche, P. Maierhoefer, N. Moretti, S. Pozzorini and F. Siegert, *Next-to-leading order QCD predictions for top-quark pair production with up to three jets*, 1607.06934.

[69] H. van Deurzen, G. Luisoni, P. Mastrolia, E. Mirabella, G. Ossola and T. Peraro, *Next-to-Leading-Order QCD Corrections to Higgs Boson Production in Association with a Top Quark Pair and a Jet*, *Phys. Rev. Lett.* **111** (2013) 171801, [1307.8437].

[70] J. R. Andersen et al., *Les Houches 2015: Physics at TeV Colliders Standard Model Working Group Report*, in *9th Les Houches Workshop on*

Physics at TeV Colliders (PhysTeV 2015) Les Houches, France, June 1-19, 2015, 2016. 1605.04692.

[71] R. Britto and B. Feng, *Unitarity cuts with massive propagators and algebraic expressions for coefficients*, *Phys. Rev.* **D75** (2007) 105006, [hep-ph/0612089].

[72] R. Britto, B. Feng and P. Mastrolia, *Closed-Form Decomposition of One-Loop Massive Amplitudes*, *Phys. Rev.* **D78** (2008) 025031, [0803.1989].

[73] J. S. Rozowsky, *Feynman diagrams and cutting rules*, hep-ph/9709423.

[74] S. Badger, J. M. Campbell and R. K. Ellis, *QCD corrections to the hadronic production of a heavy quark pair and a W-boson including decay correlations*, *JHEP* **03** (2011) 027, [1011.6647].

[75] S. Badger, R. Sattler and V. Yundin, *One-Loop Helicity Amplitudes for $t\bar{t}$ Production at Hadron Colliders*, *Phys. Rev.* **D83** (2011) 074020, [1101.5947].

[76] J. M. Campbell and R. K. Ellis, *Top-quark processes at NLO in production and decay*, *J. Phys.* **G42** (2015) 015005, [1204.1513].

[77] R. K. Ellis, W. T. Giele, Z. Kunszt and K. Melnikov, *Masses, fermions and generalized D-dimensional unitarity*, *Nucl. Phys.* **B822** (2009) 270–282, [0806.3467].

[78] R. Britto and E. Mirabella, *External leg corrections in the unitarity method*, *JHEP* **01** (2012) 045, [1109.5106].

[79] R. Kleiss and W. J. Stirling, *Spinor Techniques for Calculating p anti-p $\to W^{\pm}/Z^0$ + Jets*, *Nucl. Phys.* **B262** (1985) 235–262.

[80] K. Hagiwara and D. Zeppenfeld, *Helicity Amplitudes for Heavy Lepton Production in e+ e- Annihilation*, *Nucl. Phys.* **B274** (1986) 1–32.

[81] C. Schwinn and S. Weinzierl, *Scalar diagrammatic rules for Born amplitudes in QCD*, *JHEP* **05** (2005) 006, [hep-th/0503015].

[82] G. Rodrigo, *Multigluonic scattering amplitudes of heavy quarks*, *JHEP* **09** (2005) 079, [hep-ph/0508138].

[83] D. Maitre and P. Mastrolia, *S@M, a Mathematica Implementation of the Spinor-Helicity Formalism*, *Comput. Phys. Commun.* **179** (2008) 501–574, [0710.5559].

[84] Z. Bern, L. J. Dixon and D. A. Kosower, *One loop corrections to two quark three gluon amplitudes*, *Nucl. Phys.* **B437** (1995) 259–304, [hep-ph/9409393].

[85] K. Risager Larsen, *Unitarity and On-Shell Recursion Methods for Scattering Amplitudes*. PhD thesis, Bohr Inst., 2007. 0804.3310.

[86] C. F. Berger, Z. Bern, L. J. Dixon, F. Febres Cordero, D. Forde, H. Ita et al., *An Automated Implementation of On-Shell Methods for One-Loop Amplitudes*, *Phys. Rev.* **D78** (2008) 036003, [0803.4180].

[87] S. Catani, S. Dittmaier and Z. Trocsanyi, *One loop singular behavior of QCD and SUSY QCD amplitudes with massive partons*, *Phys. Lett.* **B500** (2001) 149–160, [hep-ph/0011222].

[88] M. B. Wise and E. Witten, *A Diagrammatic Analysis of Some Contributions to the $\Delta I = 1/2$ Rule*, *Phys. Rev.* **D20** (1979) 1216.

[89] H. D. Politzer, *Power Corrections at Short Distances*, *Nucl. Phys.* **B172** (1980) 349–382.

[90] C. Arzt, *Reduced effective Lagrangians*, *Phys. Lett.* **B342** (1995) 189–195, [hep-ph/9304230].

[91] C. Grosse-Knetter, *Effective Lagrangians with higher derivatives and equations of motion*, *Phys. Rev.* **D49** (1994) 6709–6719, [hep-ph/9306321].

[92] H. Simma, *Equations of motion for effective Lagrangians and penguins in rare B decays*, *Z. Phys.* **C61** (1994) 67–82, [hep-ph/9307274].

[93] R. N. Lee, *Presenting LiteRed: a tool for the Loop InTEgrals REDuction*, 1212.2685.

[94] B. Grinstein, R. P. Springer and M. B. Wise, *Effective Hamiltonian for Weak Radiative B Meson Decay*, *Phys. Lett.* **B202** (1988) 138–144.

[95] E. W. N. Glover, C. Oleari and M. E. Tejeda-Yeomans, *Two loop QCD corrections to gluon-gluon scattering*, *Nucl. Phys.* **B605** (2001) 467–485, [hep-ph/0102201].

[96] Z. Bern, A. De Freitas and L. J. Dixon, *Two loop helicity amplitudes for gluon-gluon scattering in QCD and supersymmetric Yang-Mills theory*, *JHEP* **03** (2002) 018, [hep-ph/0201161].

[97] Z. Bern, L. J. Dixon and D. A. Kosower, *One loop corrections to five gluon amplitudes*, *Phys. Rev. Lett.* **70** (1993) 2677–2680, [hep-ph/9302280].

[98] T. Gehrmann, J. M. Henn and N. A. Lo Presti, *Pentagon functions for massless planar scattering amplitudes*, *JHEP* **10** (2018) 103, [1807.09812].

[99] Z. Bern, L. J. Dixon and D. A. Kosower, *One loop amplitudes for e+ e- to four partons*, *Nucl. Phys.* **B513** (1998) 3–86, [hep-ph/9708239].

[100] P. Mastrolia and G. Ossola, *On the Integrand-Reduction Method for Two-Loop Scattering Amplitudes*, *JHEP* **11** (2011) 014, [1107.6041].

[101] P. Mastrolia, E. Mirabella, G. Ossola and T. Peraro, *Scattering Amplitudes from Multivariate Polynomial Division*, *Phys. Lett.* **B718** (2012) 173–177, [1205.7087].

[102] P. Mastrolia, E. Mirabella, G. Ossola and T. Peraro, *Integrand-Reduction for Two-Loop Scattering Amplitudes through Multivariate Polynomial Division*, *Phys. Rev.* **D87** (2013) 085026, [1209.4319].

[103] P. Mastrolia, E. Mirabella, G. Ossola and T. Peraro, *Multiloop Integrand Reduction for Dimensionally Regulated Amplitudes*, *Phys. Lett.* **B727** (2013) 532–535, [1307.5832].

[104] S. Badger, H. Frellesvig and Y. Zhang, *Hepta-Cuts of Two-Loop Scattering Amplitudes*, *JHEP* **04** (2012) 055, [1202.2019].

[105] Y. Zhang, *Integrand-Level Reduction of Loop Amplitudes by Computational Algebraic Geometry Methods*, *JHEP* **09** (2012) 042, [1205.5707].

[106] S. Badger, H. Frellesvig and Y. Zhang, *A Two-Loop Five-Gluon Helicity Amplitude in QCD*, *JHEP* **12** (2013) 045, [1310.1051].

[107] S. Badger, G. Mogull, A. Ochirov and D. O'Connell, *A Complete Two-Loop, Five-Gluon Helicity Amplitude in Yang-Mills Theory*, *JHEP* **10** (2015) 064, [1507.08797].

[108] S. Badger, G. Mogull and T. Peraro, *Local integrands for two-loop all-plus Yang-Mills amplitudes*, *JHEP* **08** (2016) 063, [1606.02244].

[109] T. Gehrmann, J. M. Henn and N. A. Lo Presti, *Analytic form of the two-loop planar five-gluon all-plus-helicity amplitude in QCD*, *Phys. Rev. Lett.* **116** (2016) 062001, [1511.05409].

[110] D. C. Dunbar and W. B. Perkins, *Two-loop five-point all plus helicity Yang-Mills amplitude*, *Phys. Rev.* **D93** (2016) 085029, [1603.07514].

[111] D. C. Dunbar, G. R. Jehu and W. B. Perkins, *The two-loop n-point all-plus helicity amplitude*, *Phys. Rev.* **D93** (2016) 125006, [1604.06631].

[112] D. C. Dunbar, G. R. Jehu and W. B. Perkins, *Two-loop six gluon all plus helicity amplitude*, *Phys. Rev. Lett.* **117** (2016) 061602, [1605.06351].

[113] D. C. Dunbar, J. H. Godwin, G. R. Jehu and W. B. Perkins, *Analytic all-plus gluon amplitudes in QCD*, 1710.10071.

[114] D. A. Kosower and K. J. Larsen, *Maximal Unitarity at Two Loops*, *Phys. Rev.* **D85** (2012) 045017, [1108.1180].

[115] S. Caron-Huot and K. J. Larsen, *Uniqueness of two-loop master contours*, *JHEP* **10** (2012) 026, [1205.0801].

[116] S. Abreu, F. Febres Cordero, H. Ita, M. Jaquier, B. Page and M. Zeng, *Two-Loop Four-Gluon Amplitudes from Numerical Unitarity*, *Phys. Rev. Lett.* **119** (2017) 142001, [1703.05273].

[117] S. Abreu, F. Febres Cordero, H. Ita, M. Jaquier and B. Page, *Subleading Poles in the Numerical Unitarity Method at Two Loops*, *Phys. Rev.* **D95** (2017) 096011, [1703.05255].

[118] H. Ita, *Two-loop Integrand Decomposition into Master Integrals and Surface Terms*, *Phys. Rev.* **D94** (2016) 116015, [1510.05626].

[119] T. Peraro, *Scattering amplitudes over finite fields and multivariate functional reconstruction*, *JHEP* **12** (2016) 030, [1608.01902].

[120] P. Mastrolia, T. Peraro and A. Primo, *Adaptive Integrand Decomposition in parallel and orthogonal space*, *JHEP* **08** (2016) 164, [1605.03157].

[121] P. S. Wang, *A p-adic algorithm for univariate partial fractions*, in *Proceedings of the Fourth ACM Symposium on Symbolic and Algebraic Computation*, SYMSAC '81, (New York, NY, USA), pp. 212–217, ACM, 1981. DOI.

[122] P. S. Wang, M. J. T. Guy and J. H. Davenport, *P-adic reconstruction of rational numbers*, *SIGSAM Bull.* **16** (May, 1982) 2–3.

[123] *ISSAC '06: Proceedings of the 2006 International Symposium on Symbolic and Algebraic Computation*, (New York, NY, USA), ACM, 2006.

[124] M. Kauers, *Fast Solvers for Dense Linear Systems*, *Nuclear Physics B (Proc. Suppl.)* **183** (2008) 245–250.

[125] P. Nogueira, *Automatic Feynman graph generation*, *J. Comput. Phys.* **105** (1993) 279–289.

[126] J. Kuipers, T. Ueda, J. A. M. Vermaseren and J. Vollinga, *FORM version 4.0*, *Comput. Phys. Commun.* **184** (2013) 1453–1467, [1203.6543].

[127] B. Ruijl, T. Ueda and J. Vermaseren, *FORM version 4.2*, 1707.06453.

[128] Z. Bern, M. Czakon, D. A. Kosower, R. Roiban and V. A. Smirnov, *Two-loop iteration of five-point N=4 super-Yang-Mills amplitudes*, *Phys. Rev. Lett.* **97** (2006) 181601, [hep-th/0604074].

[129] O. V. Tarasov, *Connection between Feynman integrals having different values of the space-time dimension*, *Phys. Rev.* **D54** (1996) 6479–6490, [hep-th/9606018].

[130] R. N. Lee, *Space-time dimensionality D as complex variable: Calculating loop integrals using dimensional recurrence relation and analytical properties with respect to D*, *Nucl. Phys.* **B830** (2010) 474–492, [0911.0252].

[131] A. V. Smirnov, *FIESTA4: Optimized Feynman integral calculations with GPU support*, *Comput. Phys. Commun.* **204** (2016) 189–199, [1511.03614].

[132] S. Borowka, G. Heinrich, S. Jahn, S. P. Jones, M. Kerner, J. Schlenk et al., *pySecDec: a toolbox for the numerical evaluation of multi-scale integrals*, 1703.09692.

[133] T. Gehrmann and E. Remiddi, *Two loop master integrals for gamma* —¿ 3 jets: The Planar topologies*, *Nucl. Phys.* **B601** (2001) 248–286, [hep-ph/0008287].

[134] A. V. Smirnov, *FIRE5: a C++ implementation of Feynman Integral REduction*, *Comput. Phys. Commun.* **189** (2015) 182–191, [1408.2372].

[135] A. von Manteuffel and C. Studerus, *Reduze 2 - Distributed Feynman Integral Reduction*, 1201.4330.

[136] F. V. Tkachov, *A Theorem on Analytical Calculability of Four Loop Renormalization Group Functions*, *Phys. Lett.* **100B** (1981) 65–68.

[137] K. G. Chetyrkin and F. V. Tkachov, *Integration by Parts: The Algorithm to Calculate beta Functions in 4 Loops*, *Nucl. Phys.* **B192** (1981) 159–204.

[138] S. Laporta, *High precision calculation of multiloop Feynman integrals by difference equations*, *Int. J. Mod. Phys.* **A15** (2000) 5087–5159, [hep-ph/0102033].

[139] K. J. Larsen and Y. Zhang, *Integration-by-parts reductions from unitarity cuts and algebraic geometry*, *Phys. Rev.* **D93** (2016) 041701, [1511.01071].

[140] D. A. Kosower, *Direct Solution of Integration-by-Parts Systems*, 1804.00131.

[141] C. Anastasiou and A. Lazopoulos, *Automatic integral reduction for higher order perturbative calculations*, *JHEP* **0407** (2004) 046, [hep-ph/0404258].

[142] A. Smirnov, *Algorithm fire – feynman integral reduction*, *JHEP* **0810** (2008) 107, [0807.3243].

[143] A. V. Smirnov and F. S. Chukharev, *FIRE6: Feynman Integral REduction with Modular Arithmetic*, 1901.07808.

[144] C. Studerus, *Reduze - Feynman Integral Reduction in C++*, *Comput.Phys.Commun.* **181** (2010) 1293–1300, [0912.2546].

[145] A. von Manteuffel and C. Studerus, *Reduze 2 - Distributed Feynman Integral Reduction*, *ZU-TH 01/12, MZ-TH/12-03, BI-TP 2012/02* (01, 2012) , [1201.4330].

[146] P. Maierhoefer, J. Usovitsch and P. Uwer, *Kira - A Feynman Integral Reduction Program*, 1705.05610.

[147] P. Maierhöfer and J. Usovitsch, *Kira 1.2 Release Notes*, 1812.01491.

[148] J. M. Henn, *Multiloop integrals in dimensional regularization made simple*, *Phys. Rev. Lett.* **110** (2013) 251601, [1304.1806].

[149] R. Lee, *Calculating multiloop integrals using dimensional recurrence relation and d-analyticity*, *Nucl.Phys.Proc.Suppl.205-* **206** (2010) 135–140, [1007.2256].

[150] S. Catani, *The Singular behavior of QCD amplitudes at two loop order*, *Phys. Lett.* **B427** (1998) 161–171, [hep-ph/9802439].

[151] T. Becher and M. Neubert, *On the Structure of Infrared Singularities of Gauge-Theory Amplitudes*, *JHEP* **06** (2009) 081, [0903.1126].

[152] T. Becher and M. Neubert, *Infrared singularities of scattering amplitudes in perturbative QCD*, *Phys. Rev. Lett.* **102** (2009) 162001, [0901.0722].

[153] E. Gardi and L. Magnea, *Factorization constraints for soft anomalous dimensions in QCD scattering amplitudes*, *JHEP* **03** (2009) 079, [0901.1091].

[154] C. Gnendiger, A. Signer and D. Stöckinger, *The infrared structure of QCD amplitudes and $H \to gg$ in FDH and DRED*, *Phys. Lett.* **B733** (2014) 296–304, [1404.2171].

[155] S. Caron-Huot and J. M. Henn, *Iterative structure of finite loop integrals*, *JHEP* **06** (2014) 114, [1404.2922].

[156] C. G. Papadopoulos, D. Tommasini and C. Wever, *The Pentabox Master Integrals with the Simplified Differential Equations approach*, *JHEP* **04** (2016) 078, [1511.09404].

[157] S. Caron-Huot, L. J. Dixon, M. von Hippel, A. J. McLeod and G. Papathanasiou, *The Double Pentaladder Integral to All Orders*, 1806.01361.

[158] L. J. Dixon, J. Drummond, T. Harrington, A. J. McLeod, G. Papathanasiou and M. Spradlin, *Heptagons from the Steinmann Cluster Bootstrap*, *JHEP* **02** (2017) 137, [1612.08976].

[159] S. Caron-Huot, L. J. Dixon, A. McLeod and M. von Hippel, *Bootstrapping a Five-Loop Amplitude Using Steinmann Relations*, *Phys. Rev. Lett.* **117** (2016) 241601, [1609.00669].

[160] L. J. Dixon, M. von Hippel and A. J. McLeod, *The four-loop six-gluon NMHV ratio function*, *JHEP* **01** (2016) 053, [1509.08127].

[161] Almelid, Øyvind and Duhr, Claude and Gardi, Einan and McLeod, Andrew and White, Chris D., *Bootstrapping the QCD soft anomalous dimension*, *JHEP* **09** (2017) 073, [1706.10162].

[162] N. Arkani-Hamed, J. L. Bourjaily, F. Cachazo, S. Caron-Huot and J. Trnka, *The All-Loop Integrand For Scattering Amplitudes in Planar N=4 SYM*, *JHEP* **01** (2011) 041, [1008.2958].

[163] N. Arkani-Hamed, J. L. Bourjaily, F. Cachazo and J. Trnka, *Local Integrals for Planar Scattering Amplitudes*, *JHEP* **06** (2012) 125, [1012.6032].

[164] J. L. Bourjaily, E. Herrmann and J. Trnka, *Prescriptive Unitarity*, *JHEP* **06** (2017) 059, [1704.05460].

[165] S. Abreu, F. Febres Cordero, H. Ita, B. Page and M. Zeng, *Planar Two-Loop Five-Gluon Amplitudes from Numerical Unitarity*, 1712.03946.

[166] S. Abreu, F. Febres Cordero, H. Ita, B. Page and V. Sotnikov, *Planar Two-Loop Five-Parton Amplitudes from Numerical Unitarity*, *JHEP* **11** (2018) 116, [1809.09067].

[167] S. Abreu, J. Dormans, F. Febres Cordero, H. Ita and B. Page, *Analytic Form of the Planar Two-Loop Five-Gluon Scattering Amplitudes in QCD*, 1812.04586.

[168] S. Abreu, L. J. Dixon, E. Herrmann, B. Page and M. Zeng, *The two-loop five-point amplitude in $\mathcal{N} = 4$ super-Yang-Mills theory*, 1812.08941.

[169] D. Chicherin, J. M. Henn, P. Wasser, T. Gehrmann, Y. Zhang and S. Zoia, *Analytic result for a two-loop five-particle amplitude*, 1812.11057.

[170] S. Abreu, L. J. Dixon, E. Herrmann, B. Page and M. Zeng, *The two-loop five-point amplitude in $\mathcal{N} = 8$ supergravity*, 1901.08563.

[171] D. Chicherin, T. Gehrmann, J. M. Henn, P. Wasser, Y. Zhang and S. Zoia, *The two-loop five-particle amplitude in $\mathcal{N} = 8$ supergravity*, 1901.05932.

[172] D. Chicherin, T. Gehrmann, J. M. Henn, P. Wasser, Y. Zhang and S. Zoia, *All master integrals for three-jet production at NNLO*, 1812.11160.

[173] R. Mertig, M. Bohm and A. Denner, *FEYN CALC: Computer algebraic calculation of Feynman amplitudes*, *Comput. Phys. Commun.* **64** (1991) 345–359.

[174] V. Shtabovenko, R. Mertig and F. Orellana, *New Developments in FeynCalc 9.0*, *Comput. Phys. Commun.* **207** (2016) 432–444, [1601.01167].

[175] N. D. Christensen and C. Duhr, *FeynRules - Feynman rules made easy*, *Comput. Phys. Commun.* **180** (2009) 1614–1641, [0806.4194].

[176] A. Alloul, N. D. Christensen, C. Degrande, C. Duhr and B. Fuks, *FeynRules 2.0 - A complete toolbox for tree-level phenomenology*, *Comput. Phys. Commun.* **185** (2014) 2250–2300, [1310.1921].